AD NUMBER
AD874843
LIMITATION CHANGES
TO: **Approved for public release; distribution is unlimited. Document partially illegible.**
FROM: **Distribution authorized to U.S. Gov't. agencies and their contractors; Critical Technology; JUN 1970. Other requests shall be referred to Air Force Technical Applications Center, VSC, Alexandria, VA 22313. This document contains export-controlled technical data.**
AUTHORITY
usaf, ltr, 25 jan 1972

ANALYSIS OF LONG PERIOD SEISMIC SIGNALS AND NOISE RECORDED AT LASA, TFO AND UBO

19 June 1970

Prepared For
AIR FORCE TECHNICAL APPLICATIONS CENTER
Washington, D. C.

BY
Robert P. Massé
Don M. Clark
Herman J. Mecklenburg
SEISMIC DATA LABORATORY

Under
Project VELA UNIFORM

Sponsored By
ADVANCED RESEARCH PROJECTS AGENCY
Nuclear Monitoring Research Office
ARPA Order No. 624

119

DISCLAIMER NOTICE

THIS DOCUMENT IS THE BEST QUALITY AVAILABLE.

COPY FURNISHED CONTAINED A SIGNIFICANT NUMBER OF PAGES WHICH DO NOT REPRODUCE LEGIBLY.

ANALYSIS OF LONG PERIOD SEISMIC SIGNALS AND NOISE RECORDED AT LASA, TFO AND UBO

SEISMIC DATA LABORATORY REPORT NO. 254

AFTAC Project No.:	VELA T/0706
Project Title:	Seismic Data Laboratory
ARPA Order No.:	624
ARPA Program Code No.:	9F10
Name of Contractor:	TELEDYNE GEOTECH
Contract No.:	F33657-70-C-0941
Date of Contract:	01 April 1970
Amount of Contract:	$ 1,785,000
Contract Expiration Date:	30 June 1971
Project Manager:	Royal A. Hartenberger (703) 836-7647

P. O. Box 334, Alexandria, Virginia

This document is subject to special export controls and each transmittal to foreign governments or foreign nationals may be made only with prior approval of Chief, AFTAC.

This research was supported by the Advanced Research Projects Agency, Nuclear Monitoring Research Office, under Project VELA-UNIFORM and accomplished under technical direction of the Air Force Technical Applications Center under Contract F33657-70-C-0941.

Neither the Advanced Research Projects Agency nor the Air Force Technical Applications Center will be responsible for information contained herein which may have been supplied by other organizations or contractors, and this document is subject to later revision as may be necessary.

ABSTRACT

Long period signals recorded at the seismic arrays UBO, TFO and LASA were analyzed to determine the fundamental mode Rayleigh wave dispersion curves for paths from different source areas to each of the arrays. These paths are mixed continental and oceanic, and the dispersion curves calculated fall within the range between the average dispersion for a pure continental path and that for a pure oceanic path. Analysis of the long period noise (15 to 50 seconds) recorded at each array shows the rms value to be in the 8 to 20 mμ range. Simple beamforming gives approximately $N^{\frac{1}{2}}$db reduction in noise at all arrays. Using a group velocity of 3.5 km/sec results in signal loss for some events in the LASA beams.

TABLE OF CONTENTS

LIST OF FIGURES

LIST OF FIGURES (Cont'd.)

LIST OF FIGURES (Cont'd.)

LIST OF FIGURES (Cont'd.)

LIST OF FIGURES (Cont'd.)

LIST OF FIGURES (Cont'd.)

LIST OF FIGURES (Cont'd.)

LIST OF FIGURES (Cont'd.)

LIST OF TABLES

INTRODUCTION

Long period signals and noise recorded at the seismic arrays UBO, TFO and LASA were analyzed to provide information useful to signal detection efforts and to evaluate the performance of simple long-period beams formed with these arrays. The analysis included the computation of group velocity dispersion for fundamental mode Rayleigh waves generated by seismic events recorded at these arrays, and the calculation of noise reducing properties of beamforming each of the three arrays for a set of twenty five events. All data analyzed in this report were recorded by the arrays UBO, TFO and LASA within the time period June 1, 1969 to December 31, 1969.

RAYLEIGH WAVE GROUP VELOCITY DISPERSION

Knowledge of the Rayleigh group velocity as a function of period for a path, from a specific source area to an array makes it possible to predict accurately the Rayleigh wave arrival time at the array given an event origin time. Alternately it is possible to determine the epicenter location and origin time of an event by using surface wave arrival times at several recording stations and employing the known Rayleigh group velocity dispersion from the source area to each of these stations. The dispersion of Rayleigh wave group velocities is important, therefore, in signal detection, epicenter location, and, used together with other data, in the determination of crustal and upper mantle properties along the path travelled by the surface wave.

The group velocity dispersion for the fundamental mode Rayleigh wave was computed for a set of events. The computations were made by Fourier analysis of the digital data using a moving window technique (Cohen, 1970, and Dziewonski et al, 1969). The source parameters of the events for which dispersion to the arrays was calculated are given in Table I. The actual array instruments which recorded the digital data used in the dispersion calculations are also listed in Table I. No correction was made for the small group delay of the seismograph system.

The calculated Rayleigh fundamental mode dispersion curves are shown in Figures 1 through 20 along with the actual seismograms analyzed. In many cases, these seismograms are of sufficient quality (good signal to noise ratio) to consider them for use as matched filters for other events from the same source areas.

The paths from the source areas to each of the arrays are mixed continental and oceanic for all the events processed. The summary of observed surface wave dispersion presented by Oliver (1962) verifies that the calculated dispersion curves given in Figures 1 through 20 are consistent with previous work in that they do indeed fall within the range bounded by the dispersion curves for pure continental and pure oceanic paths.

ANALYSIS OF ARRAY BEAMS

In forming beams using the long period sensors of the seismic arrays UBO, TFO and LASA, N traces were shifted in time corresponding to a signal group velocity of 3.5 km/sec and then summed. The averages of signal and of noise values for all traces used in forming the beams were computed along with the signal and noise values for the beams. The signal values were calculated by taking one half of the absolute value of the largest peak-to-peak amplitude in the signals. Noise values were determined by calculating the rms amplitude value over a time interval of length ranging from 600 to 800 seconds and selected so that the entire time interval preceded the arrival time of the P phase for the event being processed. The ratio of signal to noise (S/N) in db was then computed for each trace used to make the beam and also for the beam. The S/N improvement in db of the beam over the mean trace S/N was then determined by

$$20 \log \left(\frac{\text{S/N for the beam}}{\text{Mean S/N for all traces in the beam}} \right)$$

For the case of uncorrelated noise, the theoretical improvement is $N^{\frac{1}{2}}$ db.

Beams were formed using the vertical long period instruments of the arrays UBO, TFO and LASA for twenty five different events. The source parameters of these events are listed in TableII. All traces used in forming these beams for UBO, TFO and LASA were first processed through the 15 to 50 second band-pass filter shown in Figure 21.

Signal, noise and signal-to-noise values were then determined for each of the events by the methods previously described. The results are tabulated in Table III. Mean signal values and S/N values are indicated by the word Mean under the appropriate column headings. The average noise values are listed under the letters rms. For the beams, the signal, noise and S/N values are all listed under the Σ headings. The signal and noise reduction are both given by 20 log $\left(\frac{\Sigma}{\text{Mean}}\right)$, with Σ and Mean representing signal values in the first case and noise values in the second case.

Each of the events for which UBO, TFO, or LASA beams were formed are presented in Figures 22 through 70. These figures show the actual traces used in formation of the beam and the unphased and phased (beam) traces. The noise traces shown for each event are the entire noise samples used to compute the rms noise values. So that the character of the noise might be more obvious, the noise traces for each event are shown at two magnifications. The trace labeled only with the instrument is at the same gain as the signal trace for that instrument. The trace labeled with the instrument followed by the word NOISE is at an arbitrarily higher gain to show better the noise character.

The mean rms noise levels for UBO, TFO and LASA determined for each event processed are presented in Figure 71. Most noise values for all three of the arrays can be seen to fall within the range of 8 to 20 mμ. The mean noise values higher than 20 mμ can generally be found to have a clearly detectable signal from an event (other than the event being processed) within the noise time sample. Examples of this situation are the Costa Rica, Fox Island, Kermadec Island, Kurile Island, Ryukyu Island, and Sinkiang events.

The reduction of the noise levels at UBO, TFO and LASA by beam formation is shown in Figure 72, and the S/N improvement of the beams for each of the arrays is presented in Figure 73.

In Figures 72 and 73, only those events are included for which 6 or 7 traces were used in the UBO and TFO beams, and 16 or 17 traces were used in the LASA beams.

From Figure 72, it can be seen that the noise reducing properties of UBO and TFO are approximately the same for all the signals processed. The noise reduction of all three arrays for most events processed seems to be within 2 db of the theoretical $N^{\frac{1}{2}}$ for uncorrelated noise. For the Costa Rica and Fox Island events which have a signal in the noise sample, greater noise reduction than the expected $N^{\frac{1}{2}}$ is attained. A fairly large signal in the noise sample can either increase or decrease the noise reducing properties of an array beam, depending on the relative location of the event in the noise sample and the event being processed. For some of the events processed, a slight improvement (less than one db) in the LASA noise reduction properties may be obtained by adjusting the calibration used to convert the digital counts to millimicrons for data from the C1Z and C2Z instruments. These instruments have very low gains and were not calibrated for these gains in forming some of the beams. In these cases C1Z and C2Z are of low amplitude and contribute very little in reducing the noise.

The S/N improvement of the beams of each of the arrays is shown in Figures 73 and 74. From Figure 73, it can be seen that UBO beams using 6 or 7 traces give about the same S/N improvement as LASA beams using 16 or 17 traces for the events presented. In Figure 74, the S/N improvement compared to $N^{\frac{1}{2}}$ for all events processed (having any number of traces) is presented. This figure shows that the UBO and TFO beams perform equally well and that the S/N improvement is usually within 4 db of the $N^{\frac{1}{2}}$ values, while the LASA beams are often more than 3 db below the theoretical $N^{\frac{1}{2}}$ values.

Loss of signal amplitude in the process of forming beams using a group velocity of 3.5 km/sec seems to be one factor making the LASA beams relatively less effective than the UBO and TFO beams. This observation is confirmed by forming beams using only the AOZ instrument and either the C-ring or the F-ring instruments for group velocities of 3.0 km/sec and 3.8 km/sec (Table IV). Using the C-ring instruments, the diameter of the array is not large enough to show much difference in S/N for the two group velocities. However, there is 3 db difference in the S/N for group velocities of 3.0 and 3.8 km/sec using AOZ and the F-ring instruments. It is apparent, therefore, that care should be taken in the selection of the group velocity with which to beam a large aperture long period array.

Long period beams were formed using a low-pass filter (Figure 21) on the vertical components for events recorded at UBO and TFO. The results are presented in Table V. Comparing the data in Table V with that in Table III, it can be seen that the band-pass filter eliminated approximately the same amount of noise as did the low-pass filter.

Beams formed using band-passed horizontal traces for UBO and TFO (Table VI) show that these horizontal beams are as efficient as the vertical component beams. The noise reduction for any one event recorded at any array are approximately the same for both the horizontal components.

CONCLUSIONS

Utilization of the long period signals assembled and the fundamental Rayleigh mode dispersion curves calculated in this study should increase the effectiveness of the arrays UBO, TFO and LASA as detectors of energy from seismic events.

The rms noise level seems to be in the 8 to 20 mμ range for each of the arrays UBO, TFO and LASA. The reduction of noise through simple beamforming approaches the value of $N^{\frac{1}{2}}$ db for each of the three arrays. Signal loss is incurred, however, in beaming LASA with a group velocity of 3.5 km/sec for all events.

REFERENCES

Cohen, T.J., 1969, Seismoprints, Teledyne Geotech, Seismic Data Laboratory Report No. 238, Alexandria, Virginia.

Dziewonski, A., S. Bloch, and M. Landisman, 1969, A technique for the analysis of transient seismic signals, Bull. Seism. Soc. Am., v. 59, pp. 427-444.

Oliver, J., 1962, A summary of observed seismic surface wave dispersion, Bull. Seism. Soc. Am., v. 52, pp 81-86.

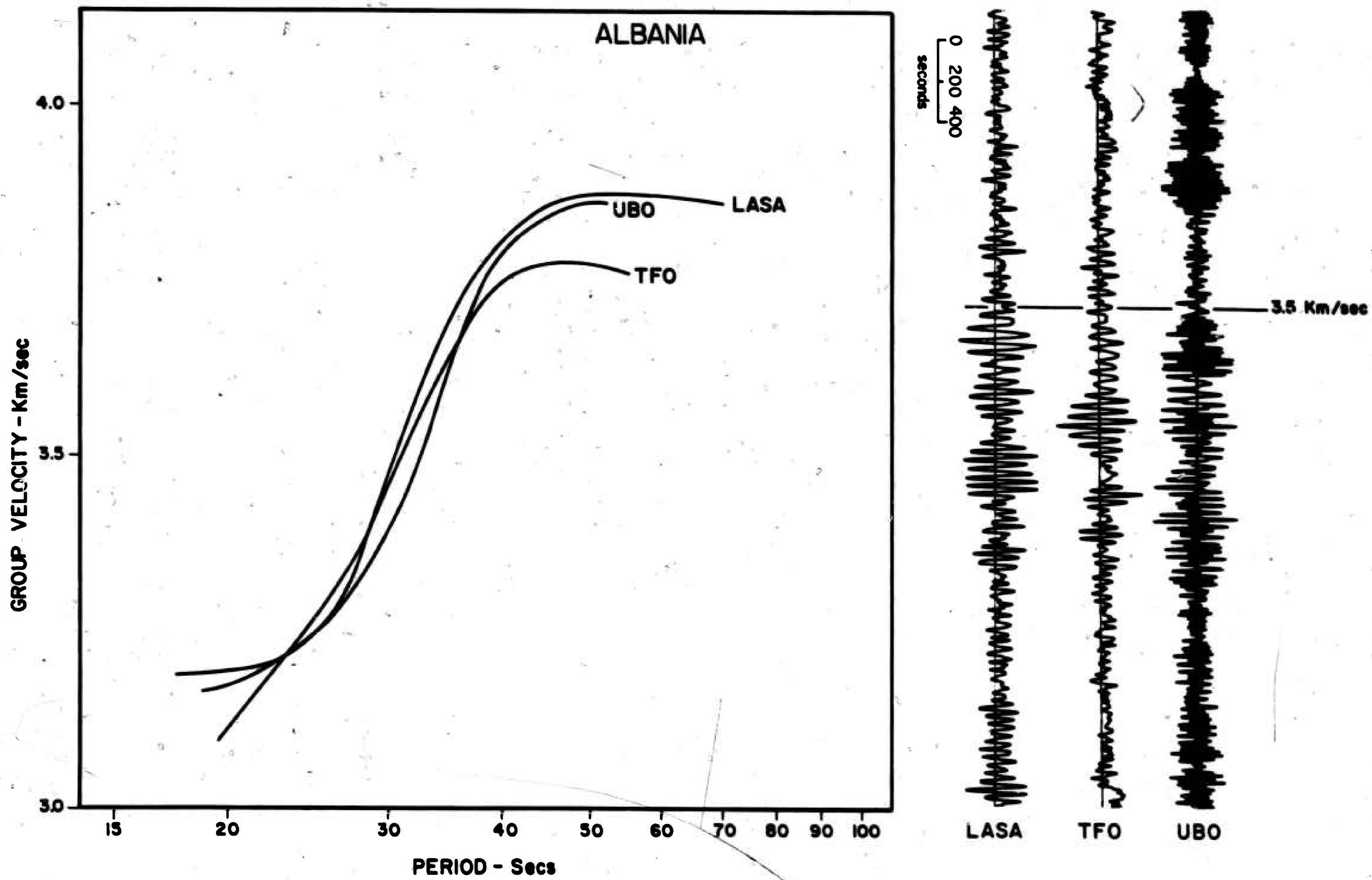

Figure 1. Dispersion of fundamental mode Rayleigh waves from an event in Albania.

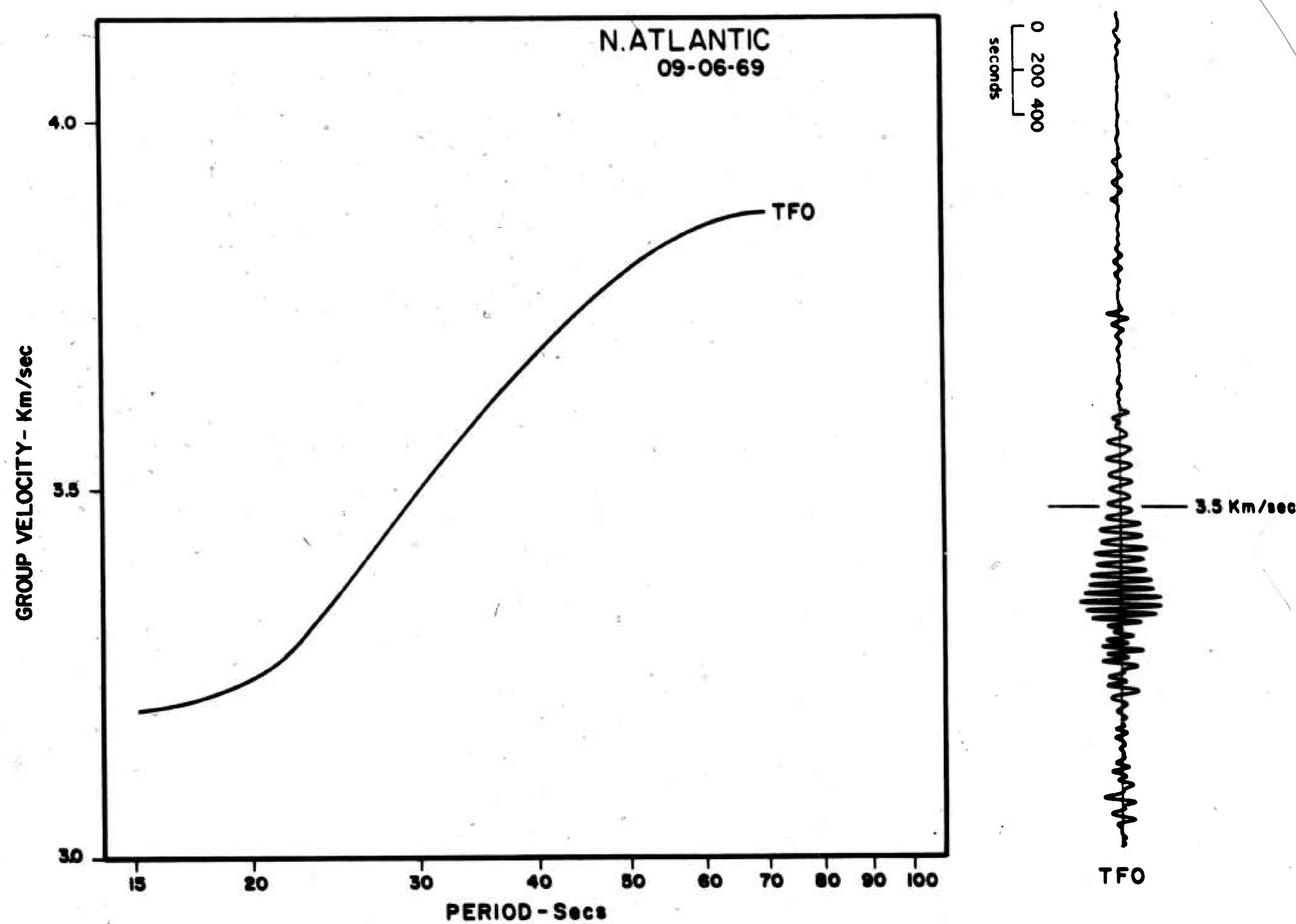

Figure 2. Dispersion of fundamental mode Rayleigh waves from an event in the North Atlantic.

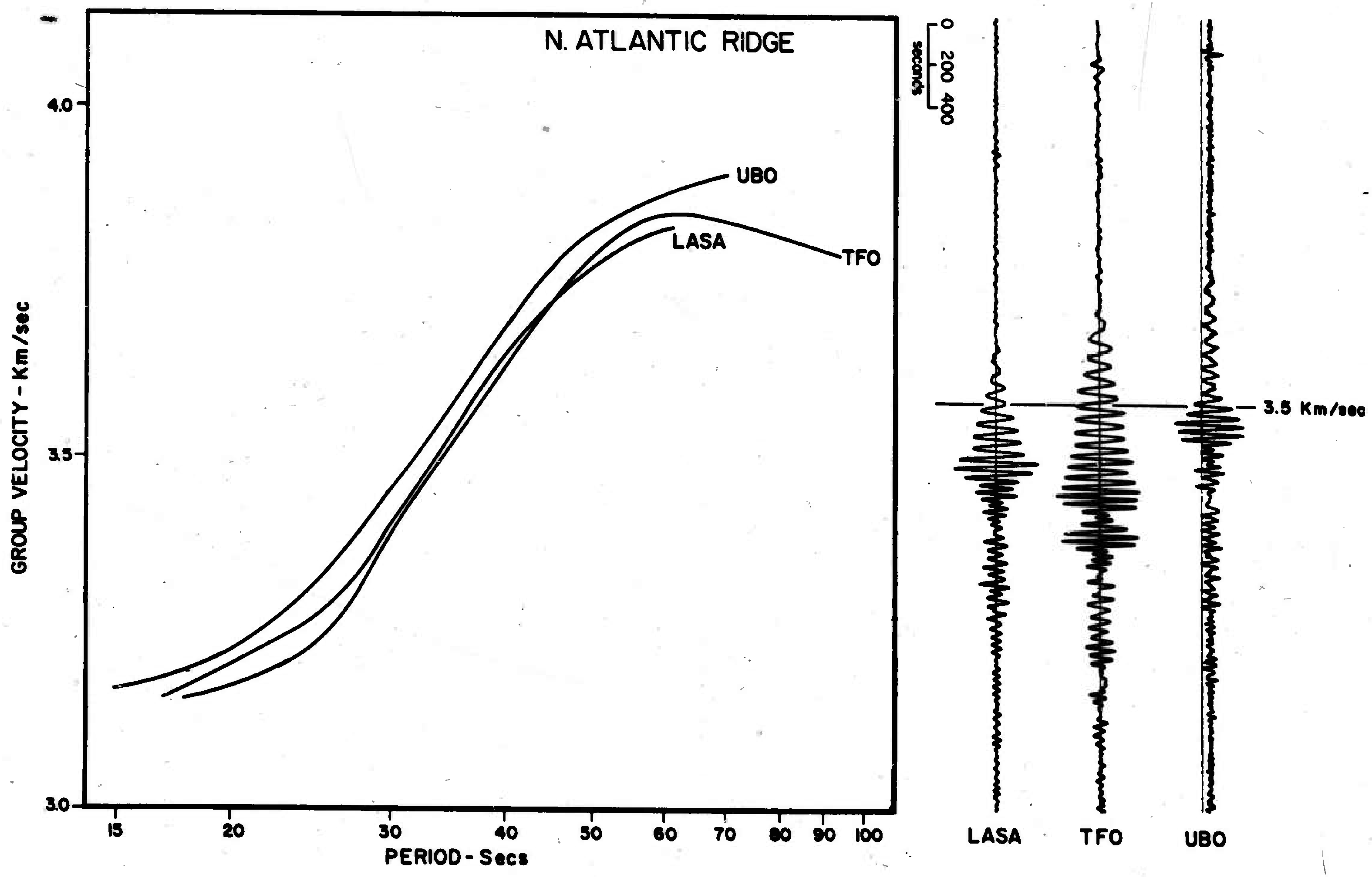

Figure 3. Dispersion of fundamental mode Rayleigh waves from an event in the North Atlantic Ridge.

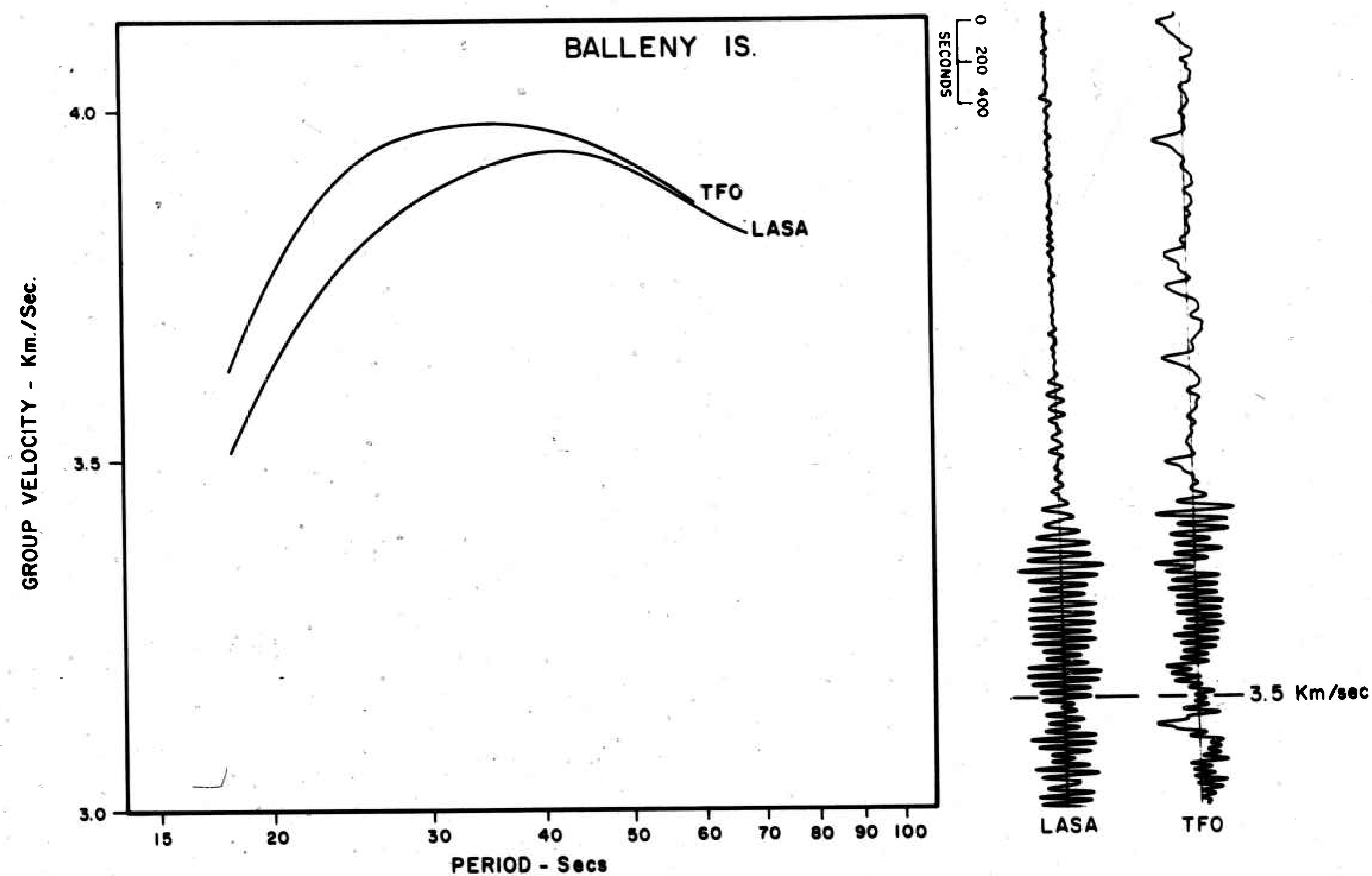

Figure 4. Dispersion of fundamental mode Rayleigh waves from an event in the Balleny Islands.

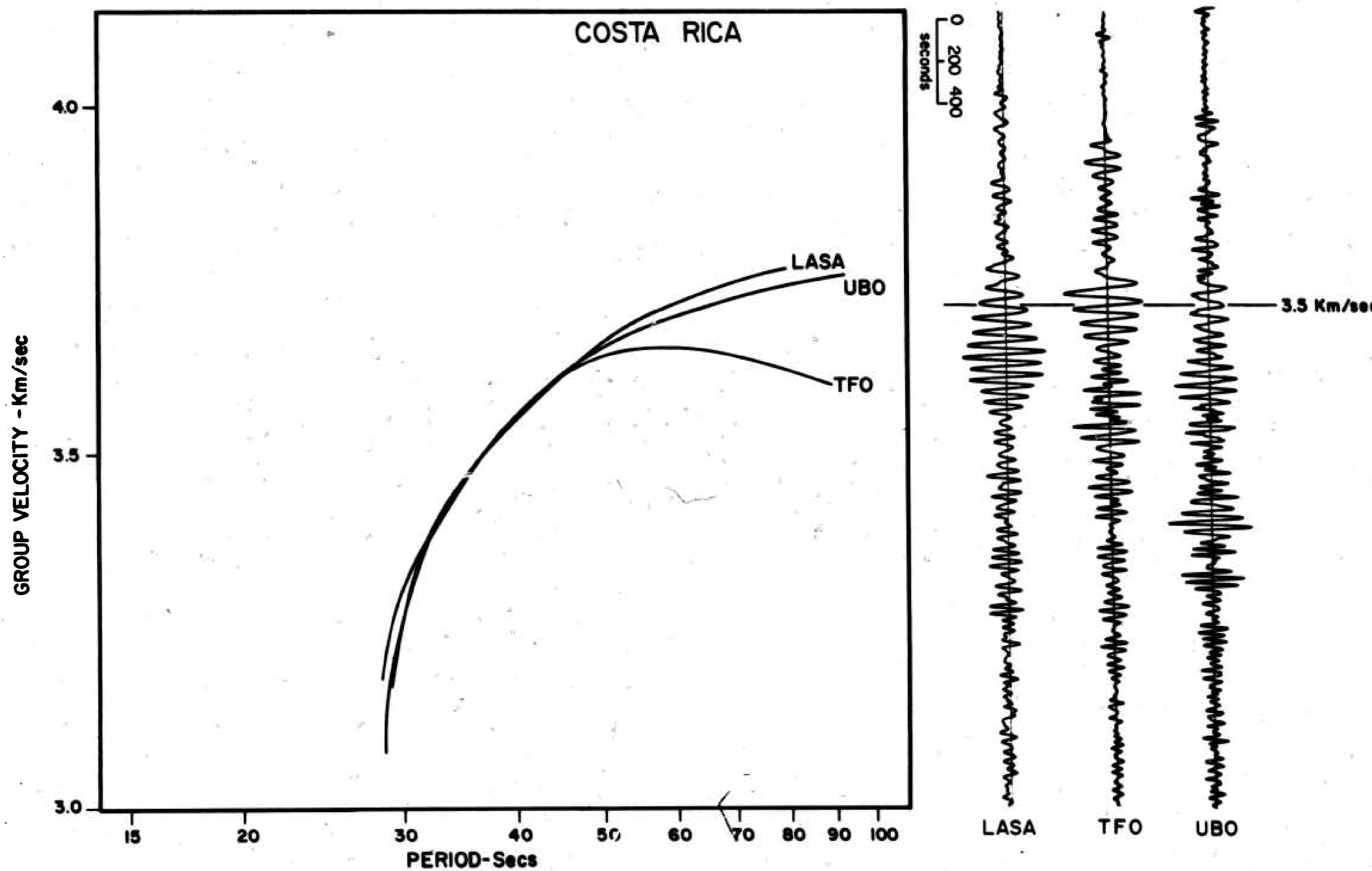

Figure 5. Dispersion of fundamental mode Rayleigh waves from an event in Costa Rica.

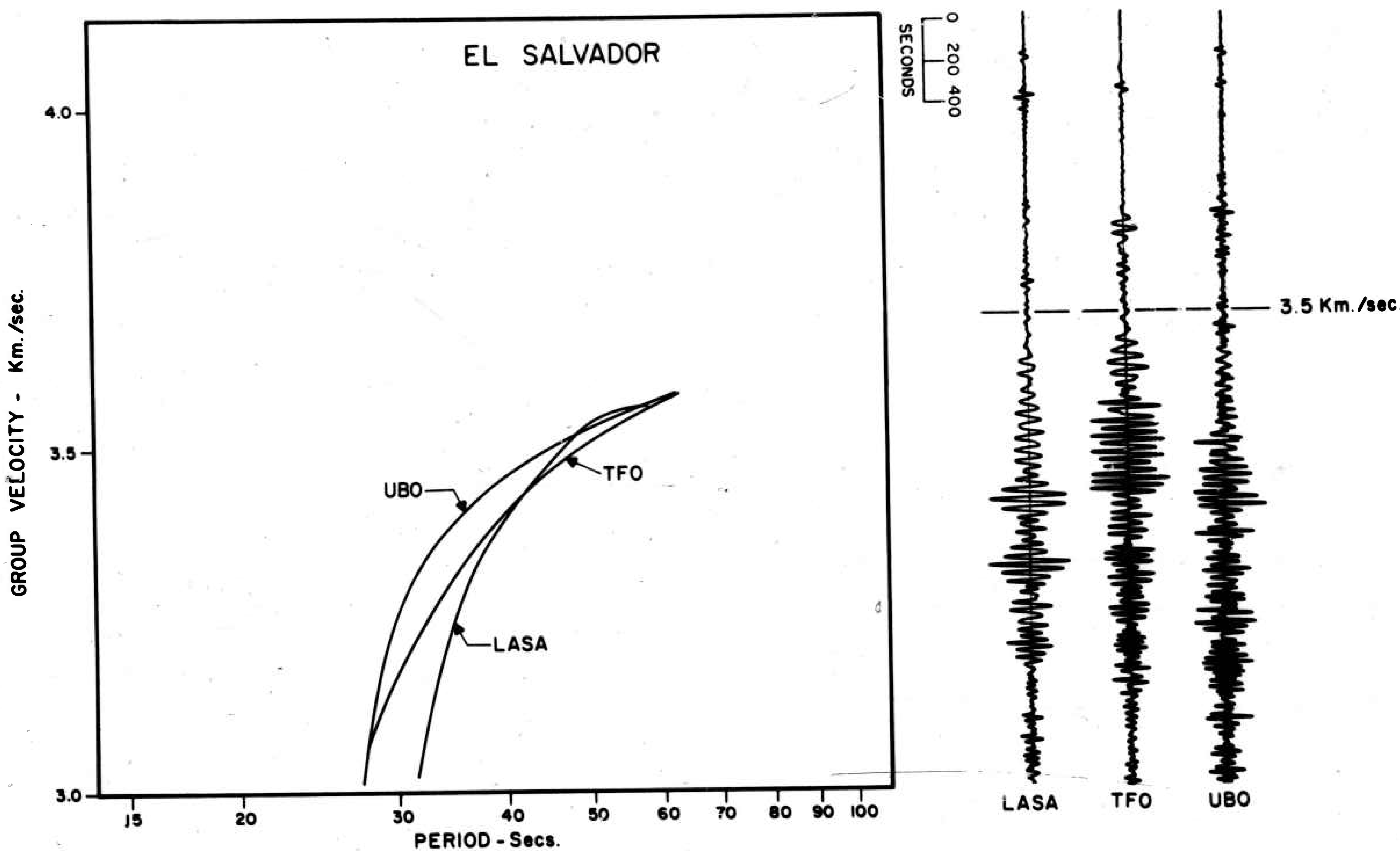

Figure 6. Dispersion of fundamental mode Rayleigh waves from an event in El Salvador.

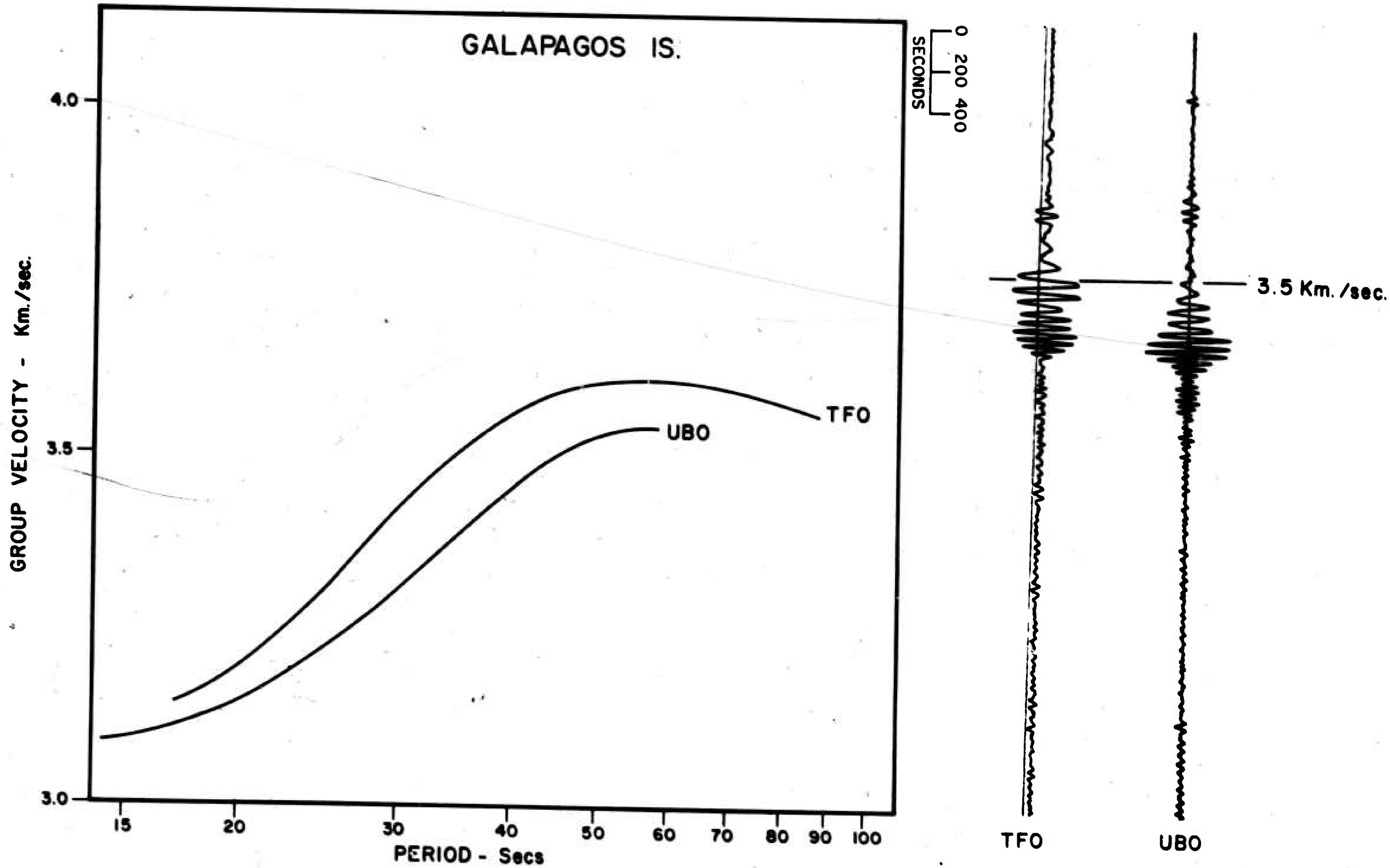

Figure 7. Dispersion of fundamental mode Rayleigh waves from an event in the Galapagos.

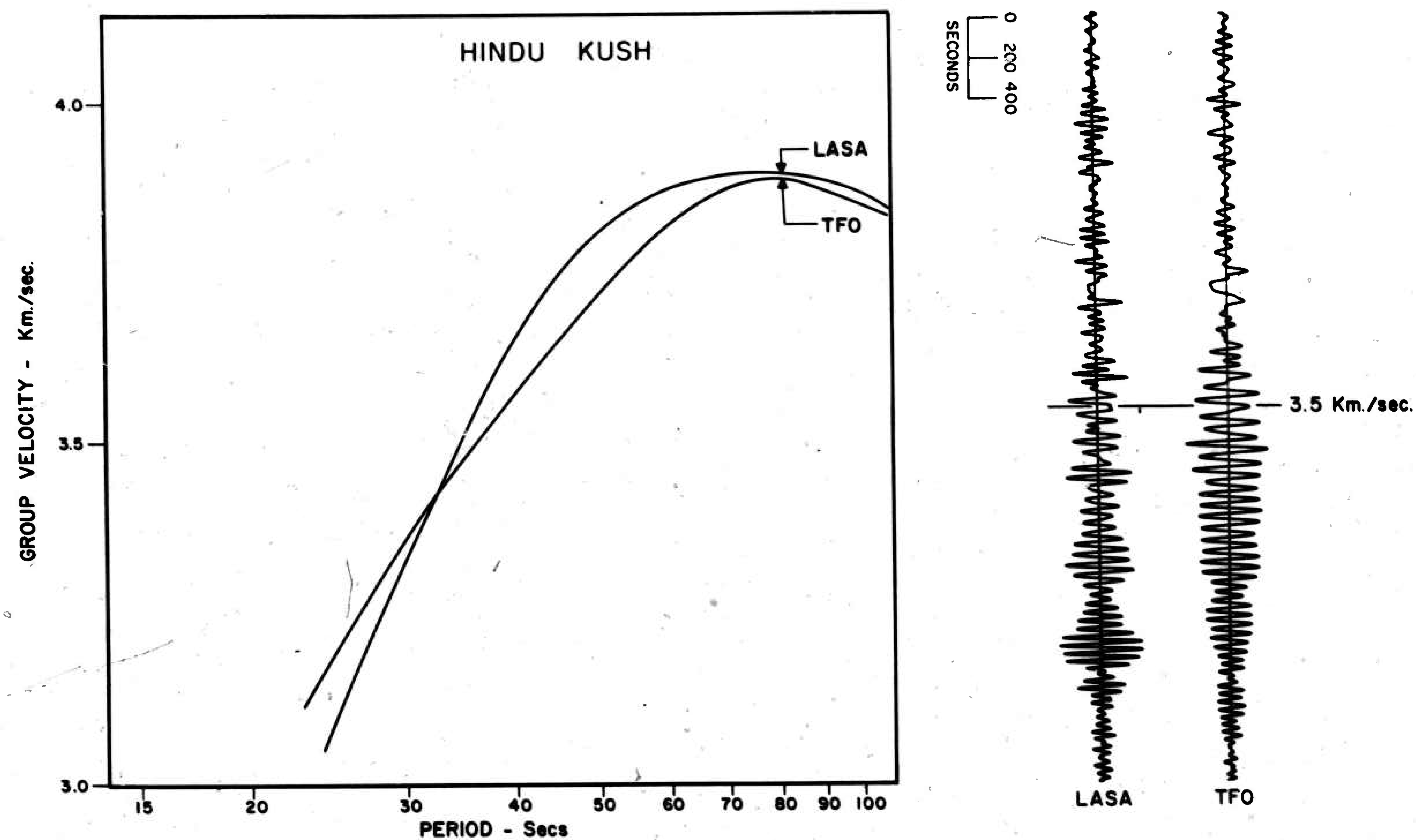

Figure 8. Dispersion of fundamental mode Rayleigh waves from an event in Hindu Kush.

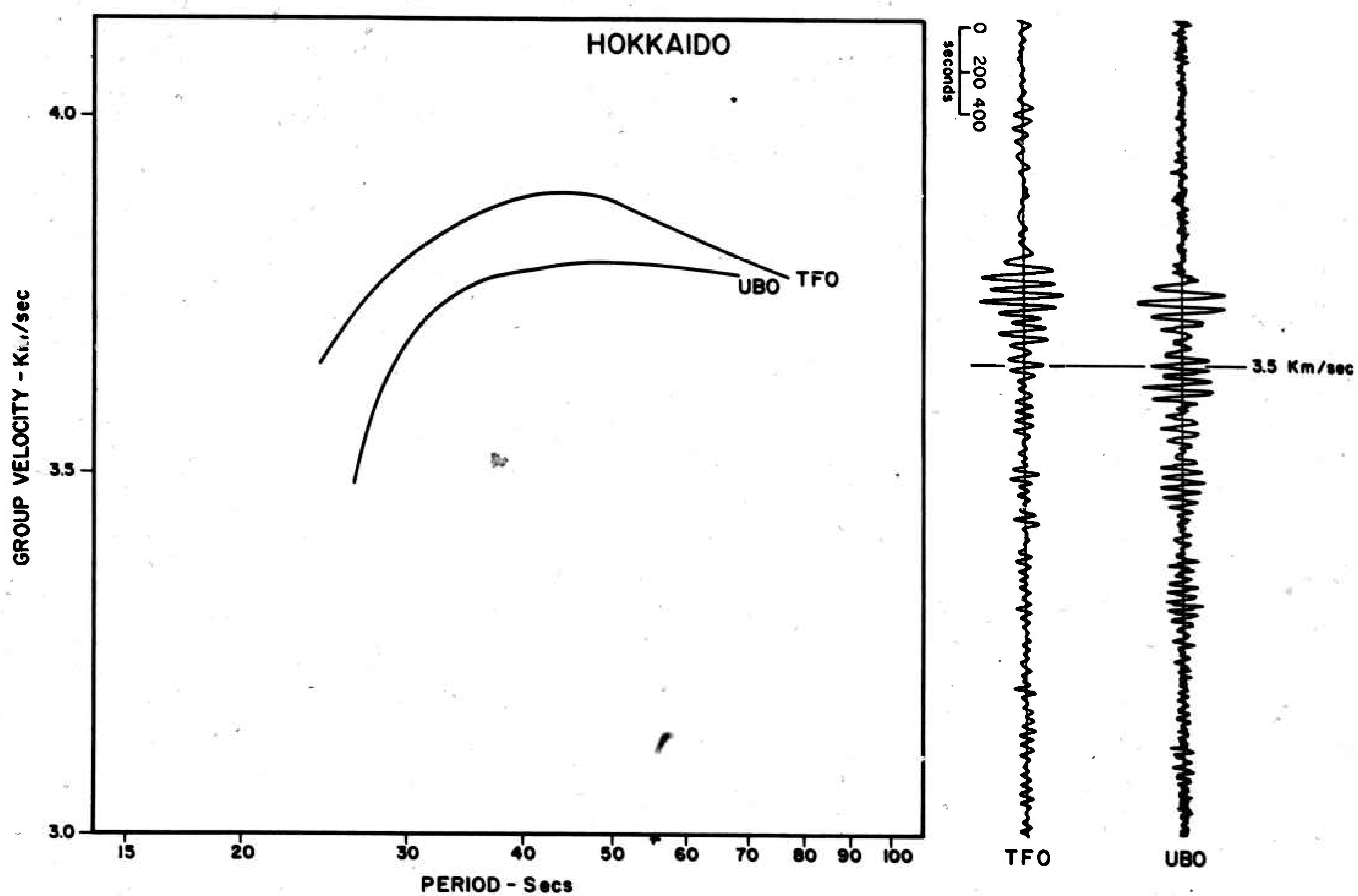

Figure 9. Dispersion of fundamental mode Rayleigh waves from an event in Hokkaido.

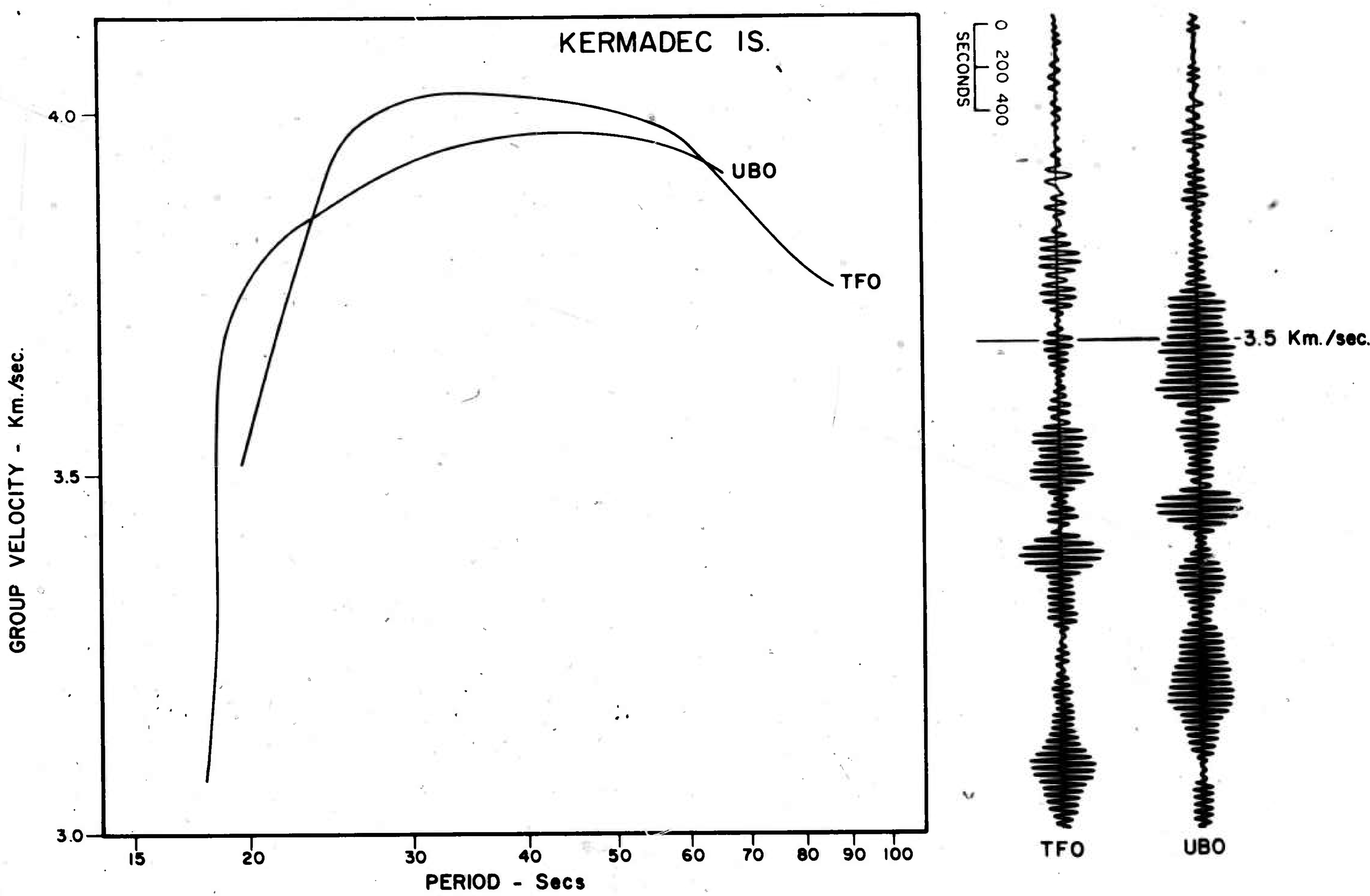

Figure 10. Dispersion of fundamental mode Rayleigh waves from an event in the Kermadec Islands.

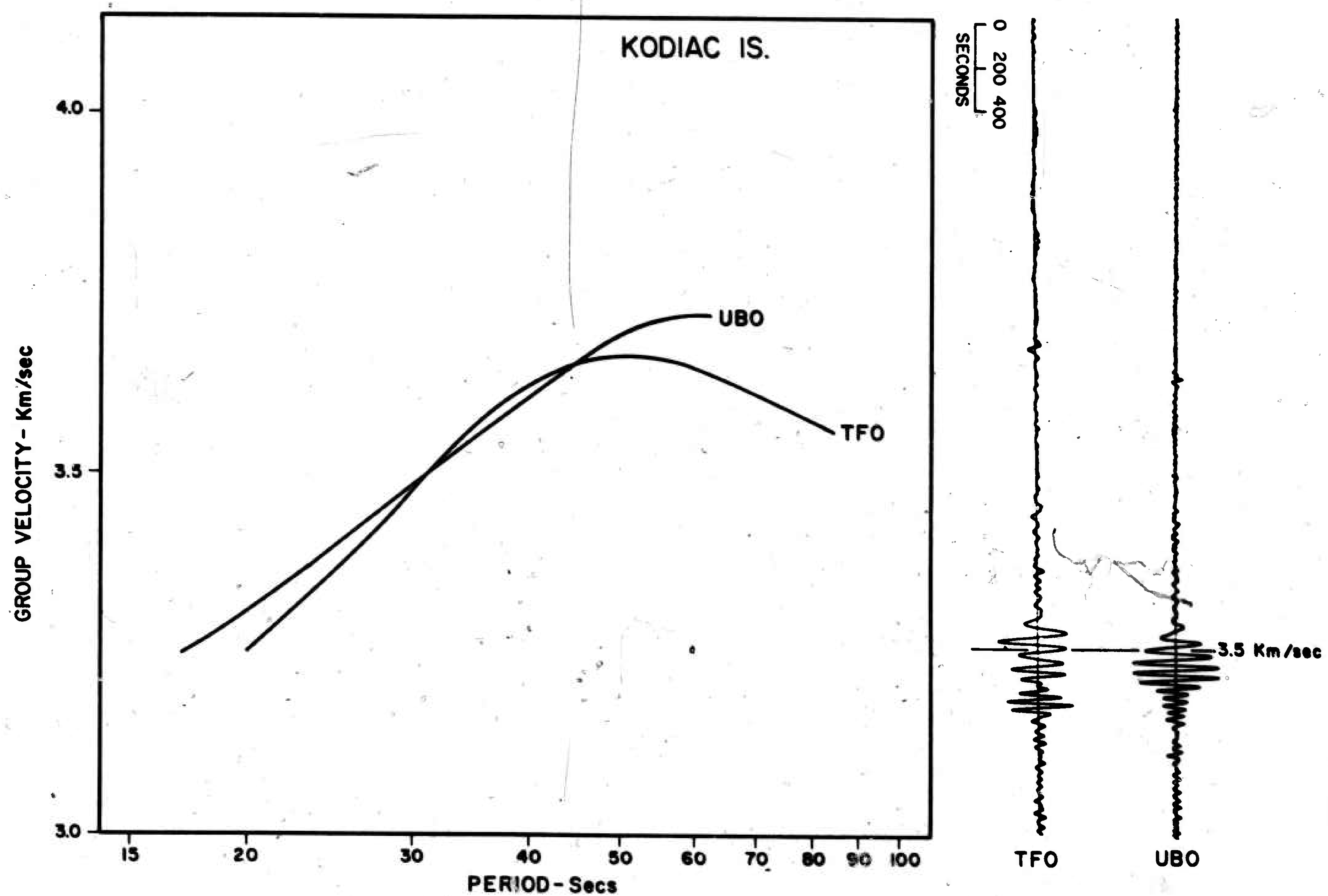

Figure 11. Dispersion of fundamental mode Rayleigh waves from an event in the Kodiac Islands.

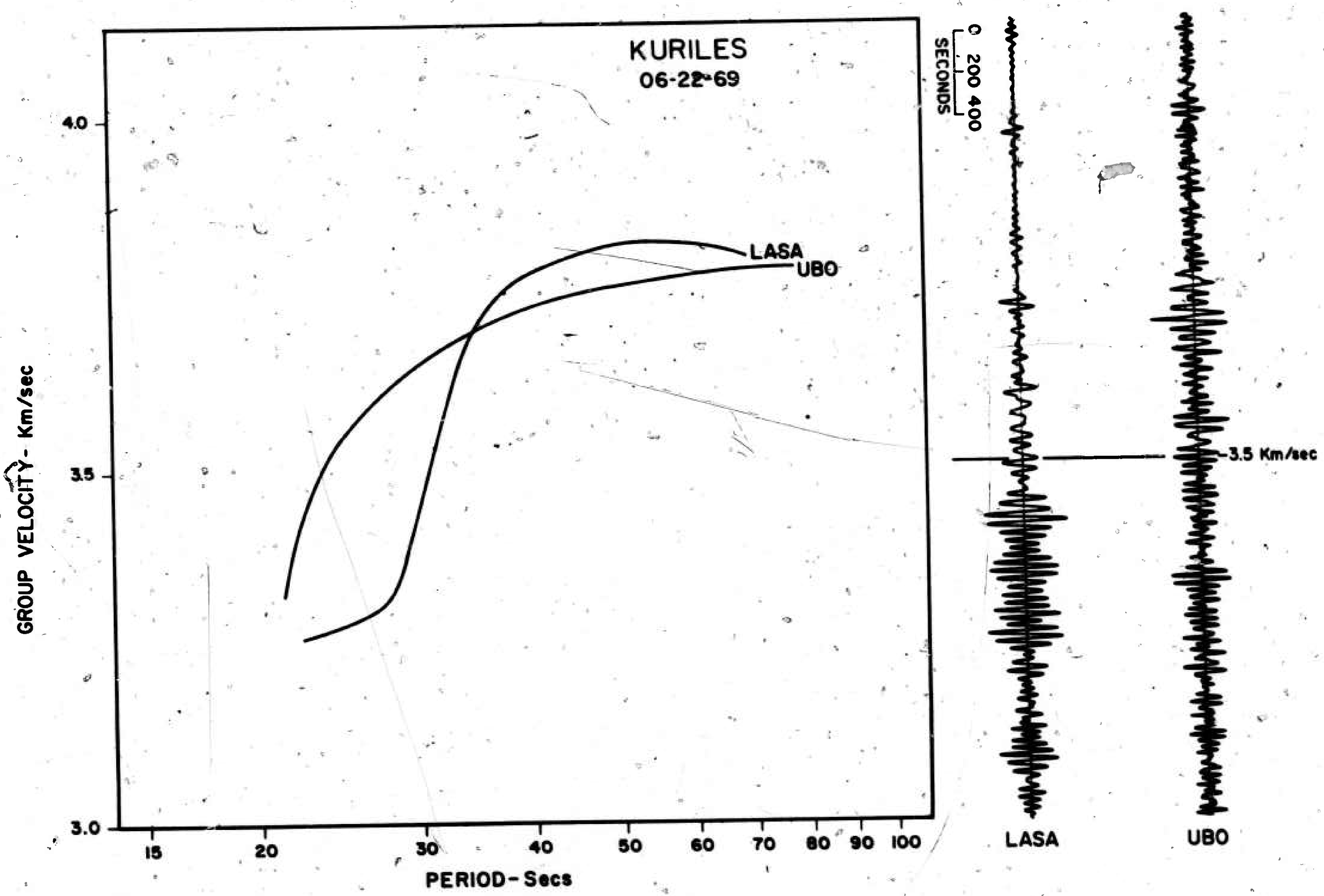

Figure 12. Dispersion of fundamental mode Rayleigh waves from an event in the Kurile Islands.

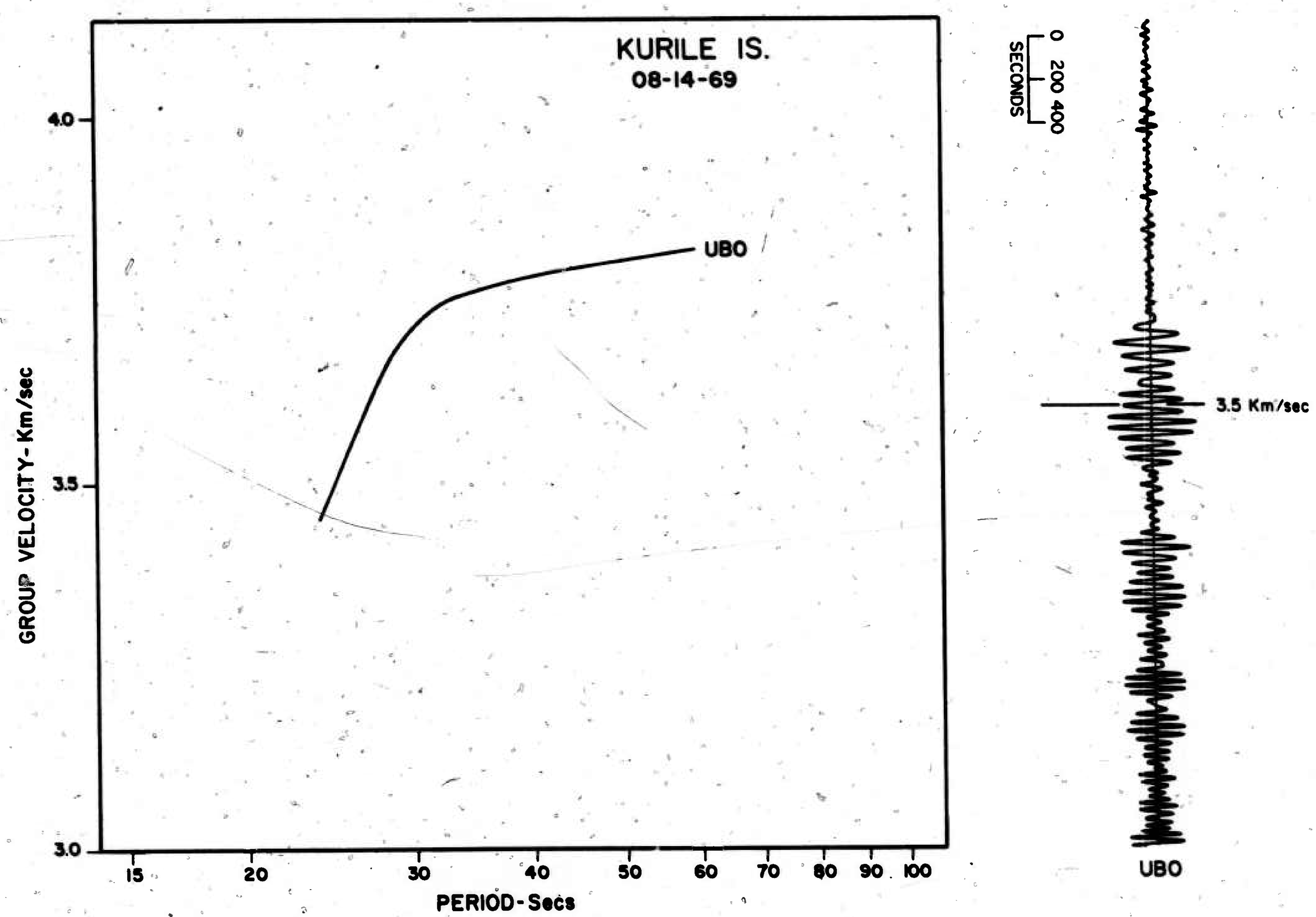

Figure 13. Dispersion of fundamental mode Rayleigh waves from an event in the Kurile Islands.

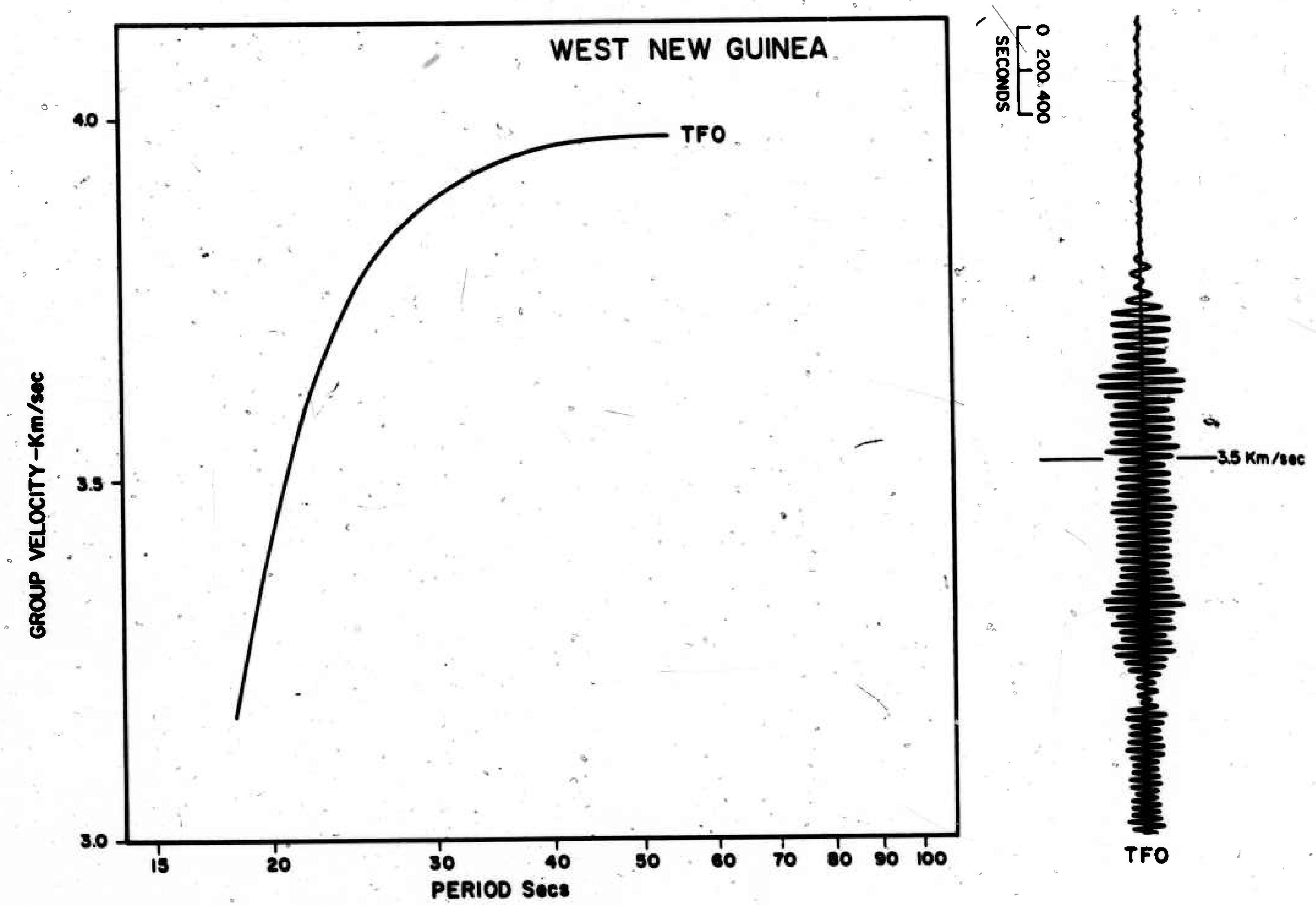

Figure 14. Dispersion of fundamental mode Rayleigh waves from an event in West New Guinea.

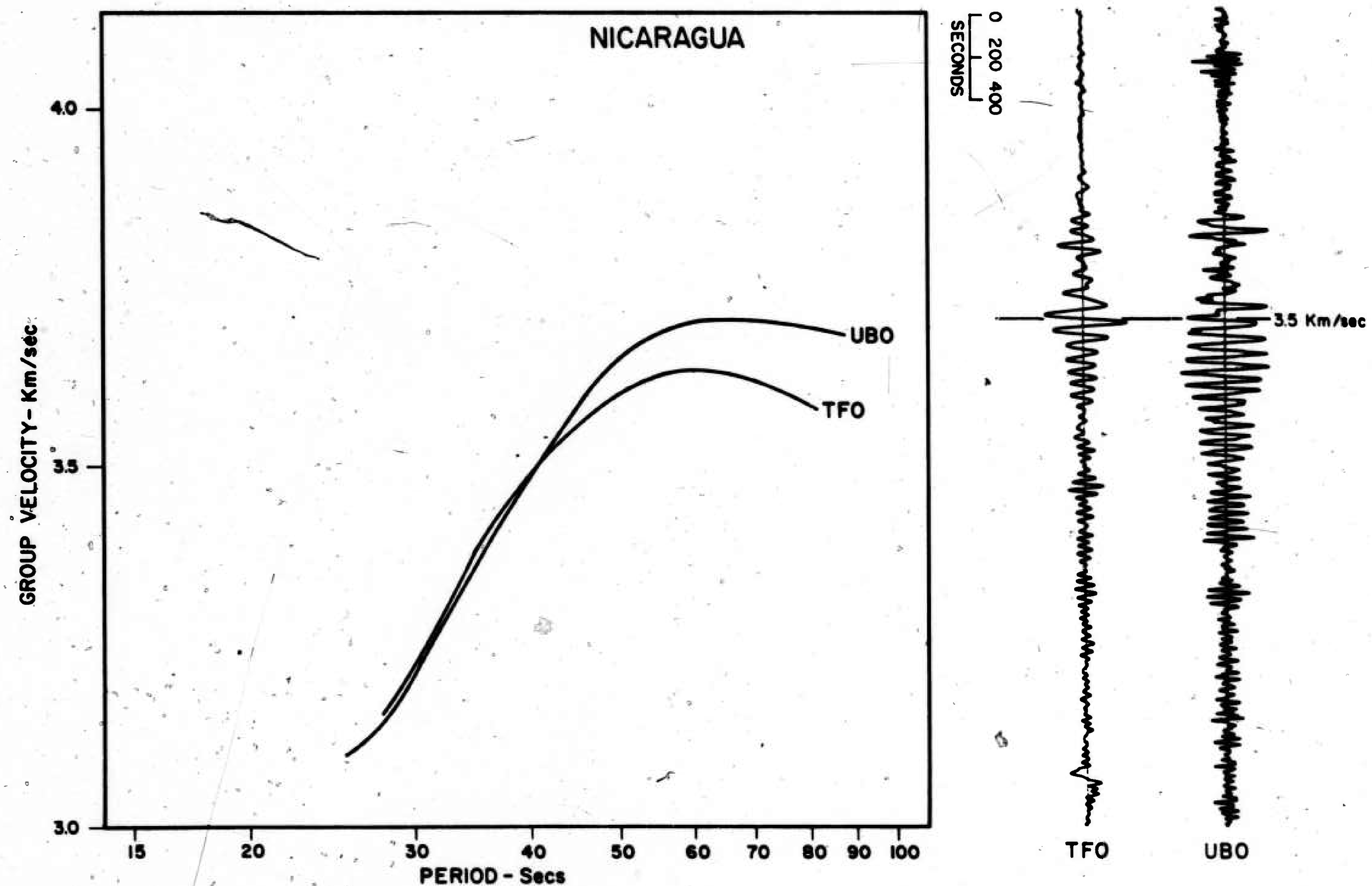

Figure 15. Dispersion of fundamental mode Rayleigh waves from an event in Nicaragua.

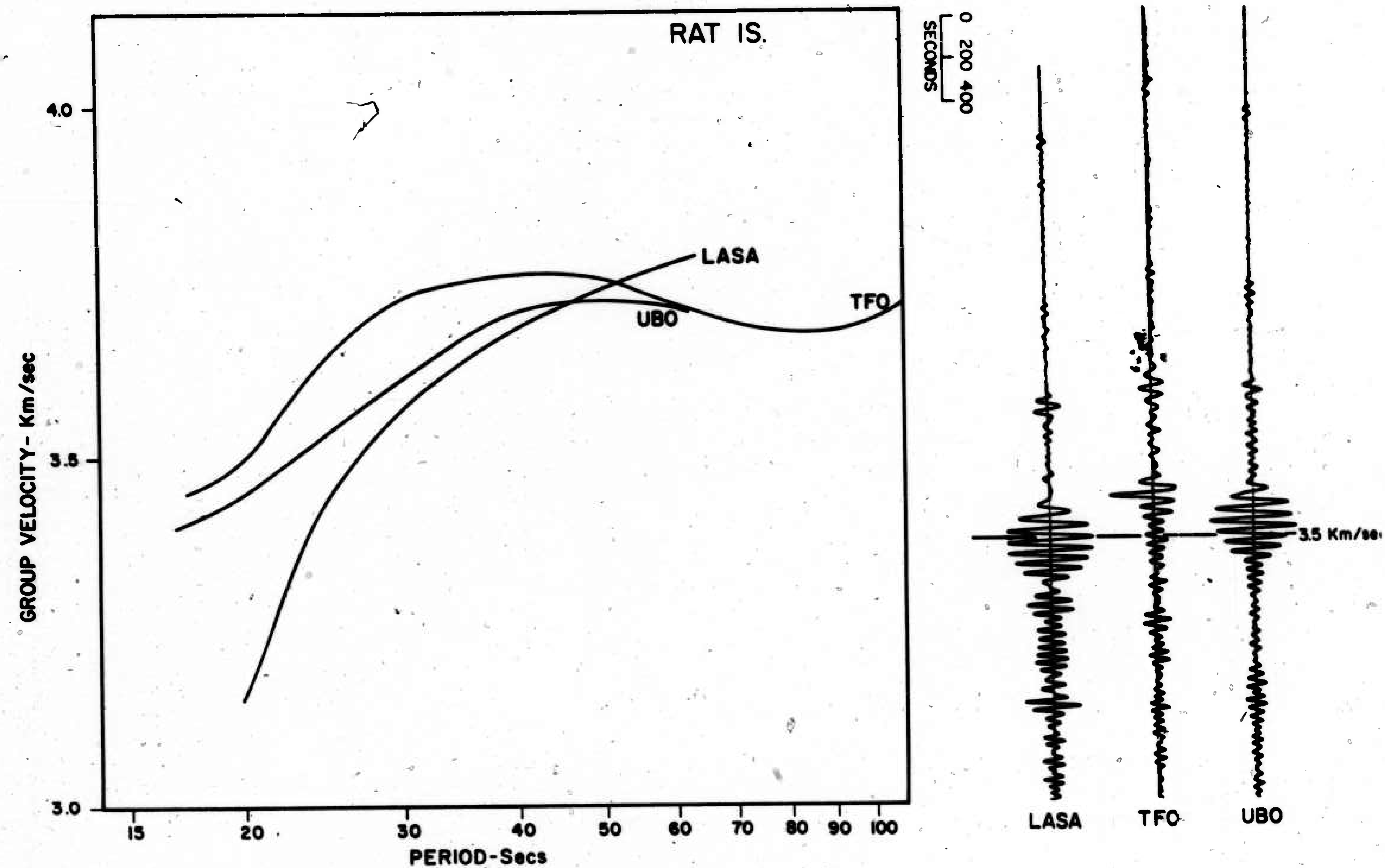

Figure 16. Dispersion of fundamental mode Rayleigh waves from an event in the Rat Islands.

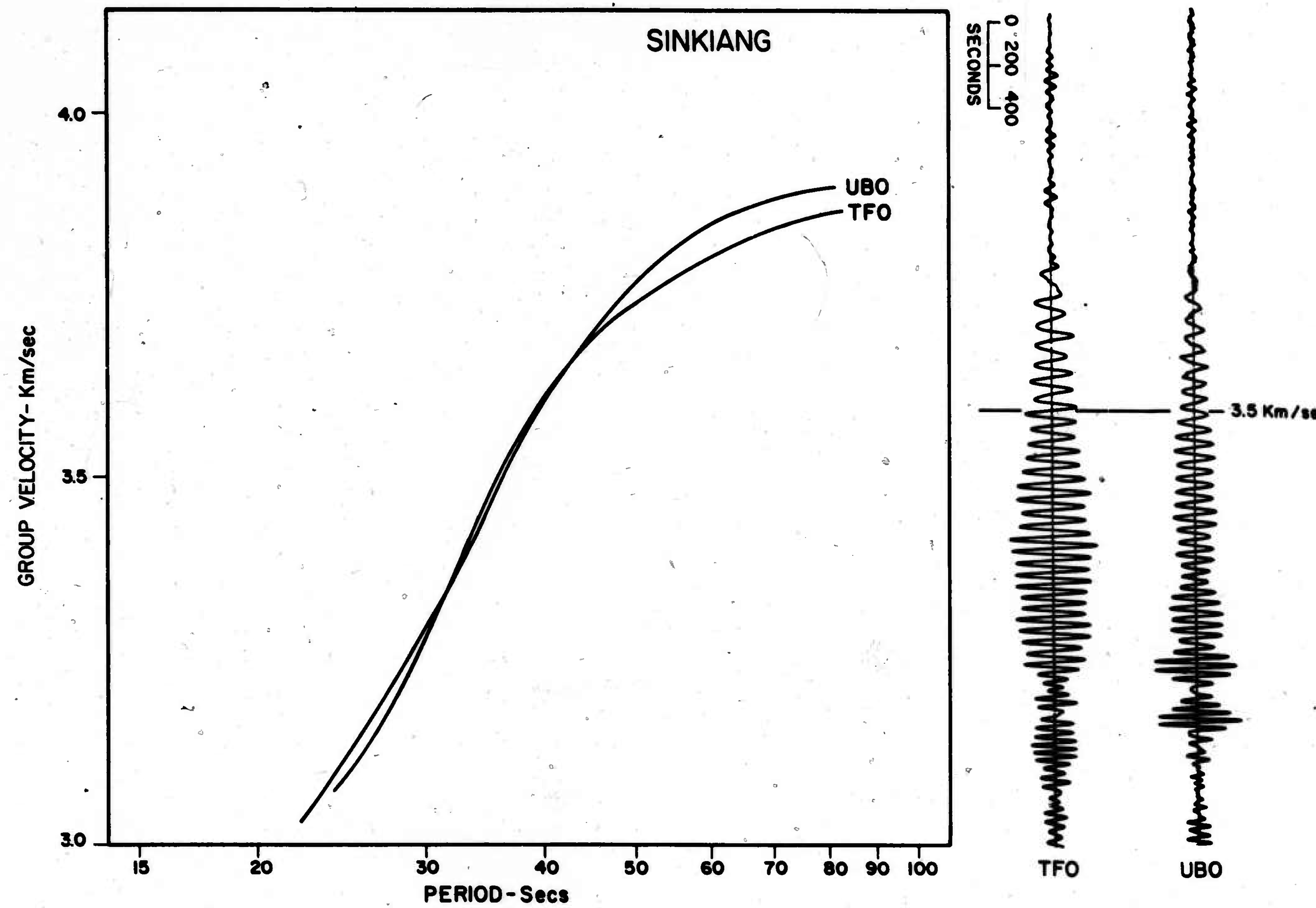

Figure 17. Dispersion of fundamental mode Rayleigh waves from an event in Sinkiang.

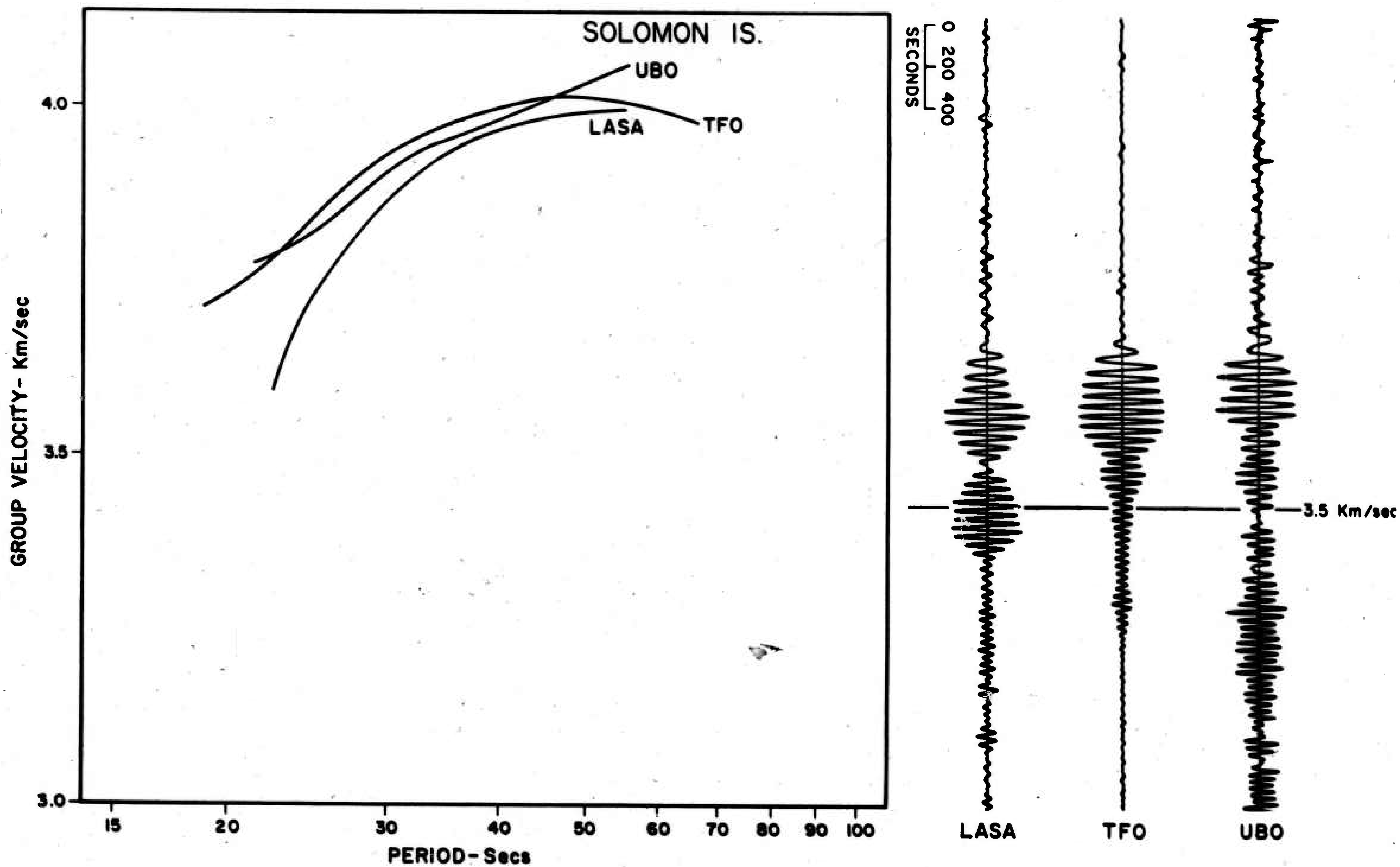

Figure 18. Dispersion of fundamental mode Rayleigh waves from an event in the Solomon Islands.

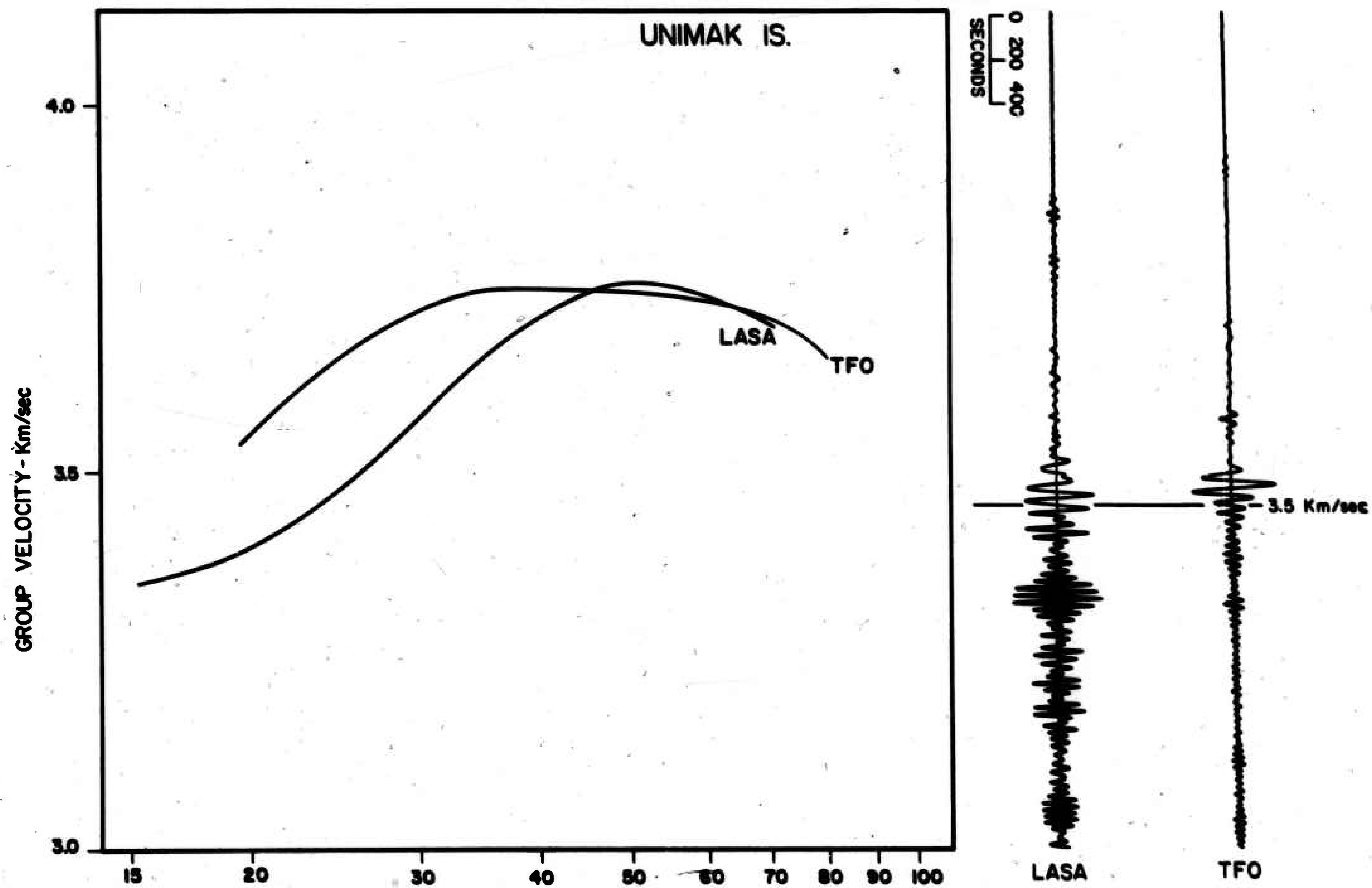

Figure 19. Dispersion of fundamental mode Rayleigh waves from an event in the Unimak Islands.

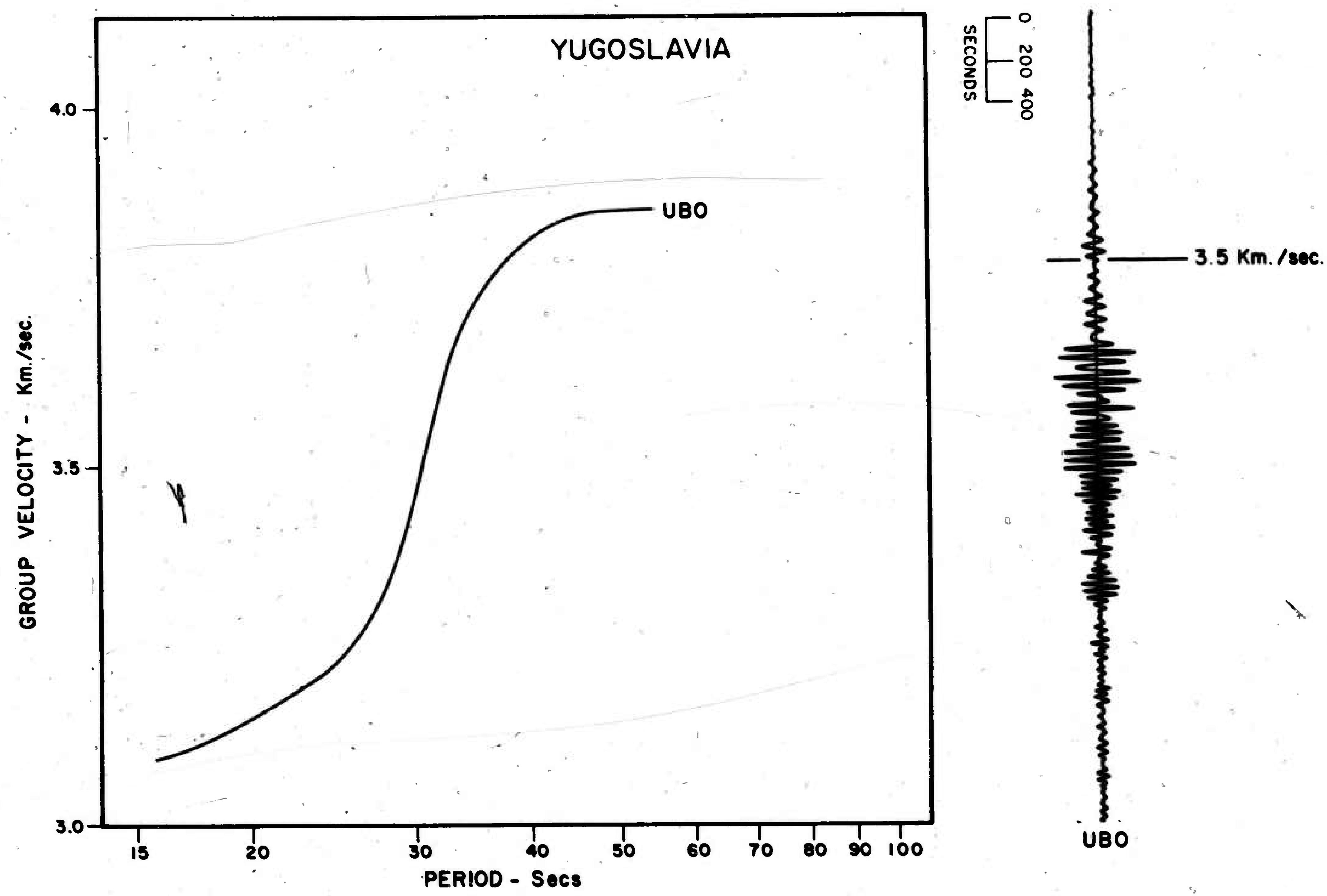

Figure 20. Dispersion of fundamental mode Rayleigh waves from an event in Yugoslavia.

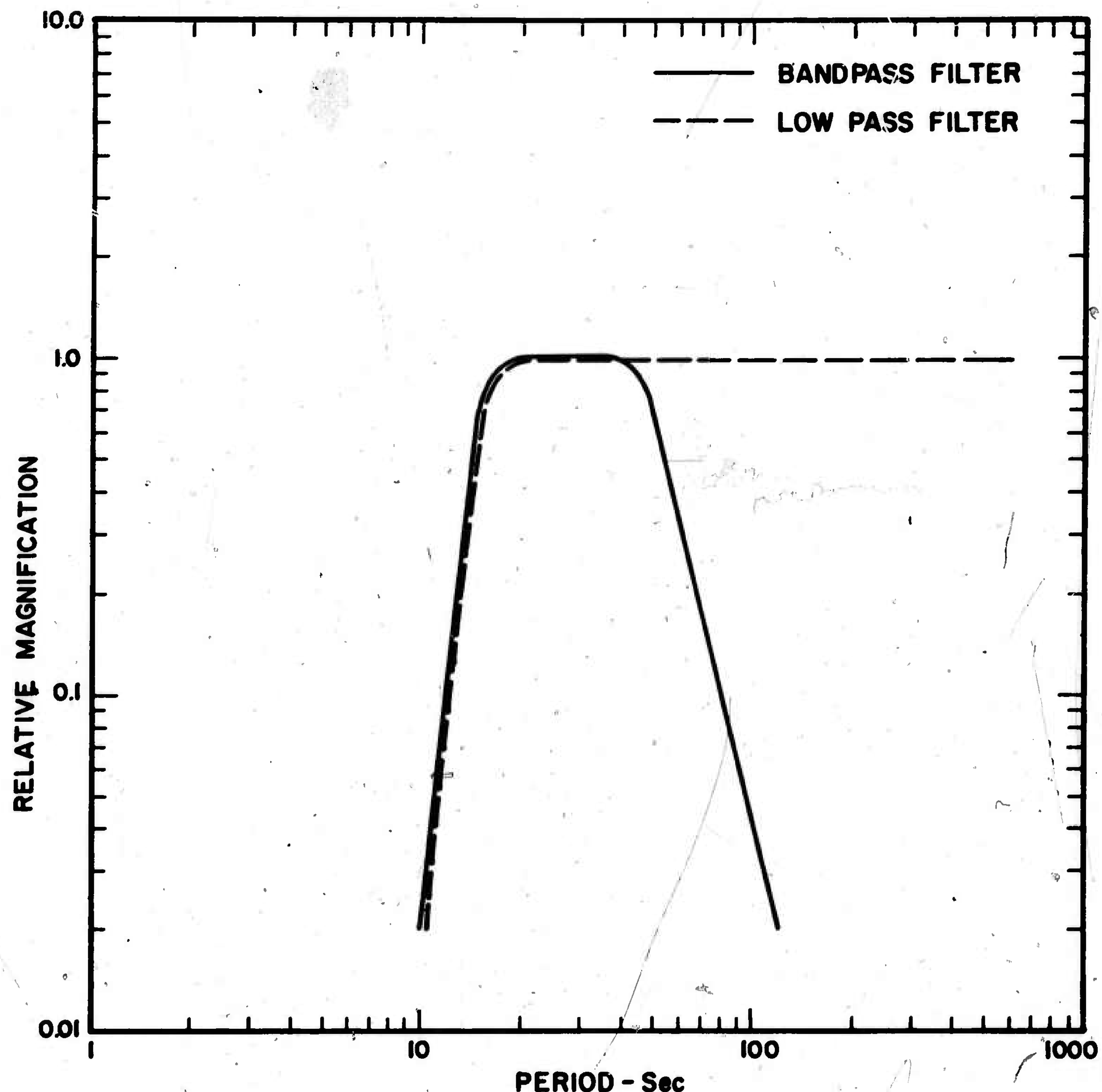

Figure 21. Low pass and band pass filters used in long period data processing.

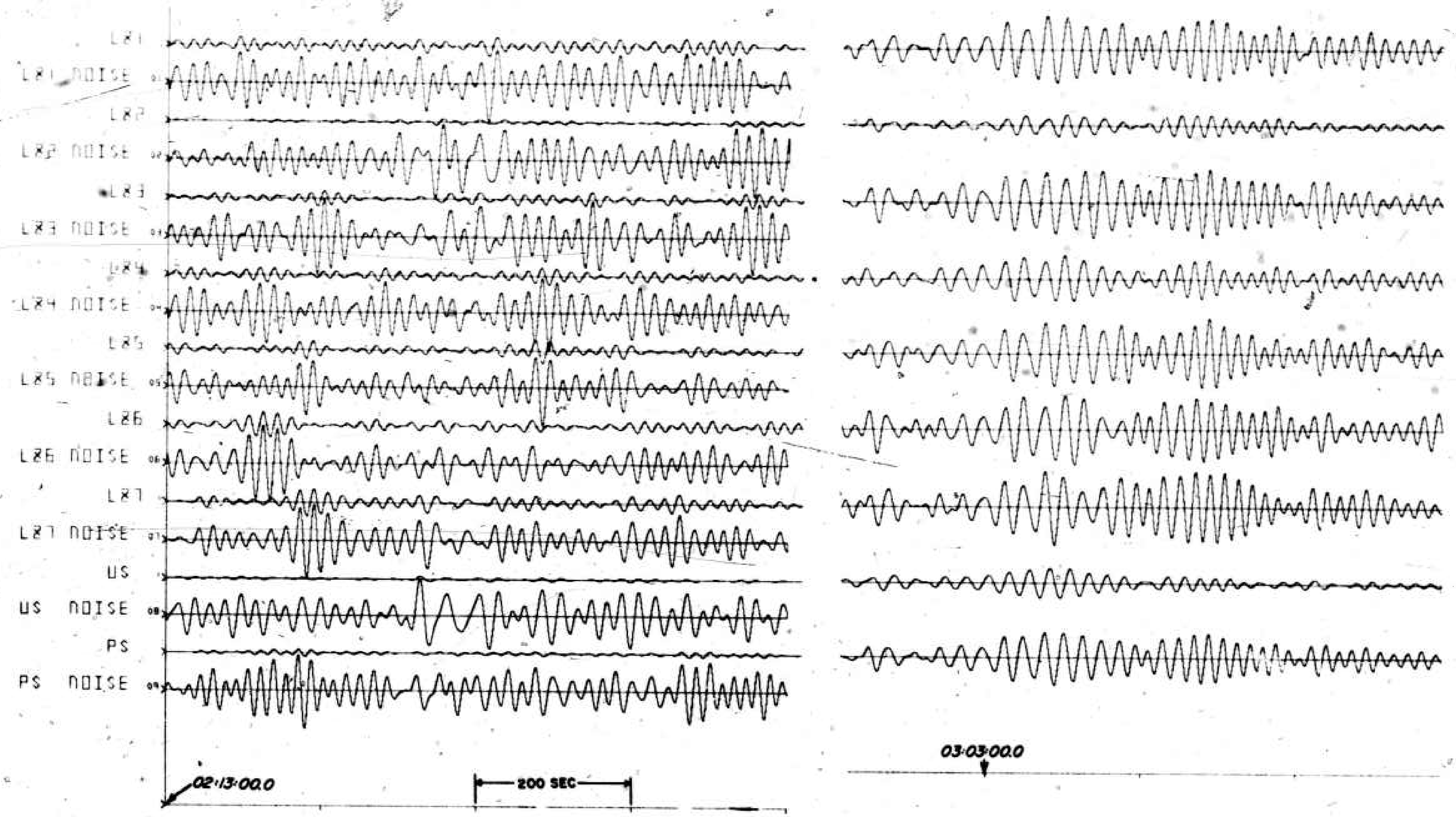

Figure 22. Band pass filtered noise and signal traces with unphased and phased sums for an event in Albania recorded at UBO.

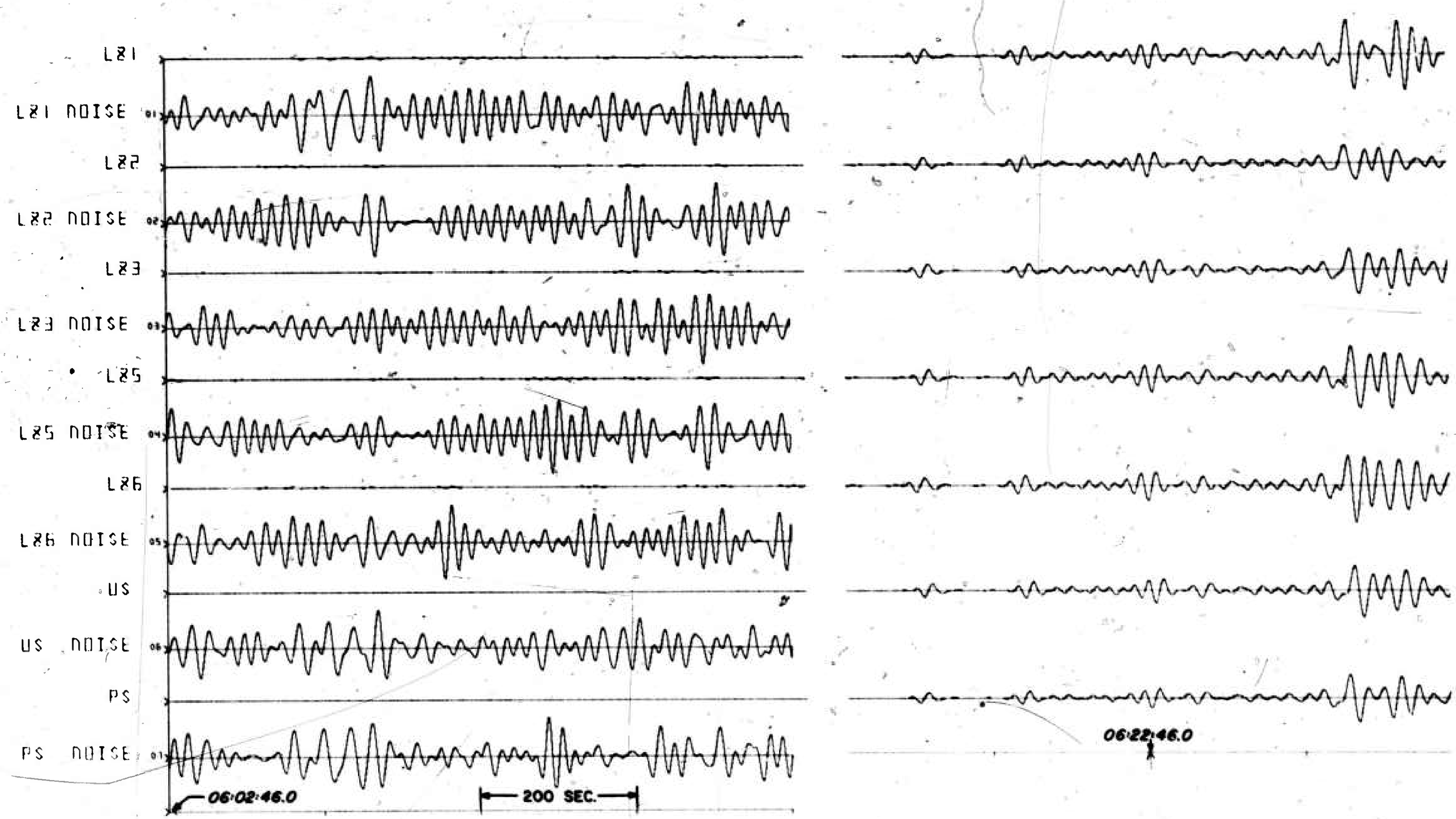

Figure 23. Band pass filtered noise and signal traces with unphased and phased sums for an event in Argentina recorded at UBO.

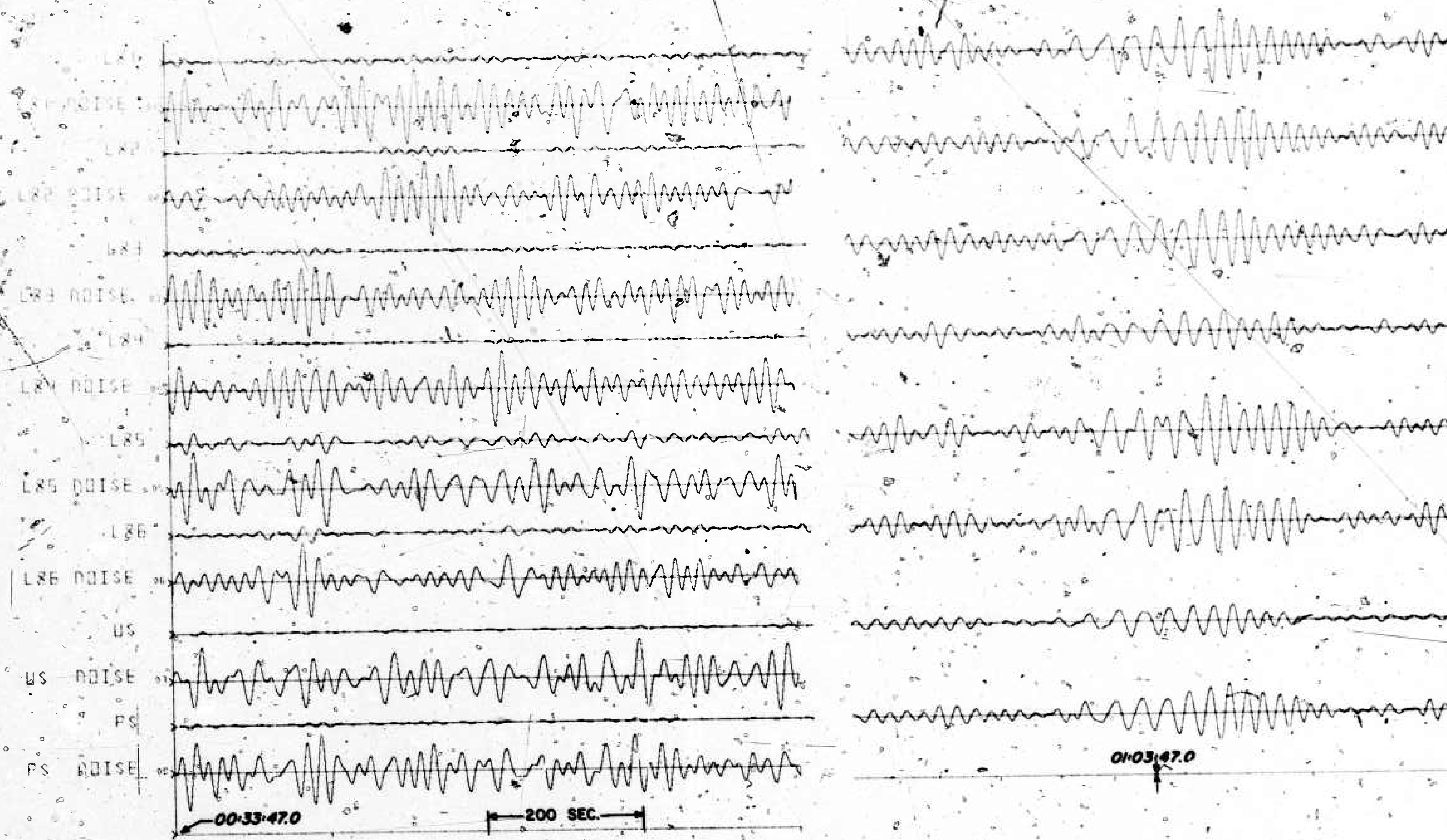

Figure 24. Band pass filtered noise and signal traces with unphased and phased sums for an event in the North Atlantic recorded at UBO.

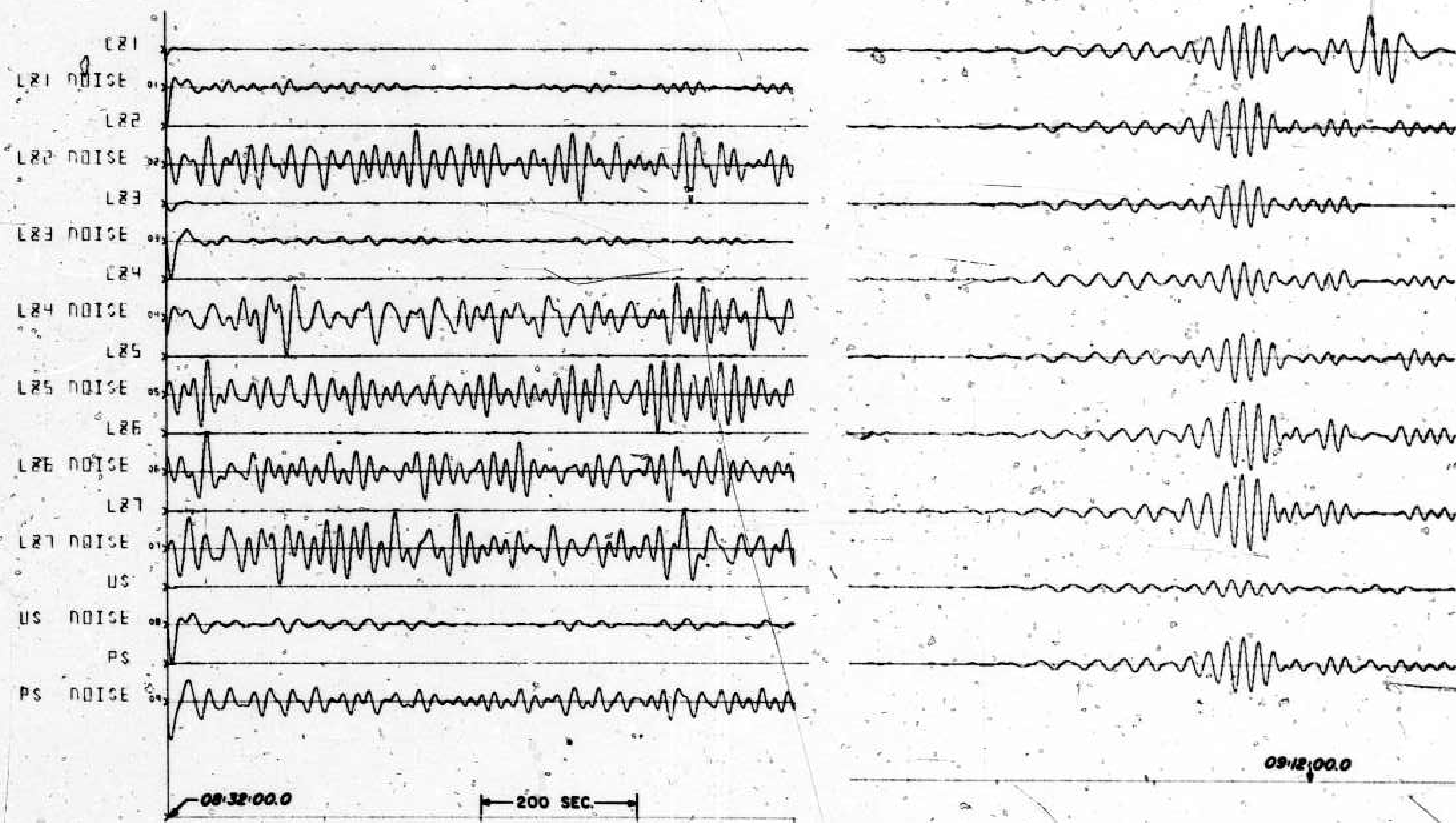

Figure 25. Band pass filtered noise and signal traces with unphased and phased sums for an event in the North Atlantic Ridge recorded at UBO.

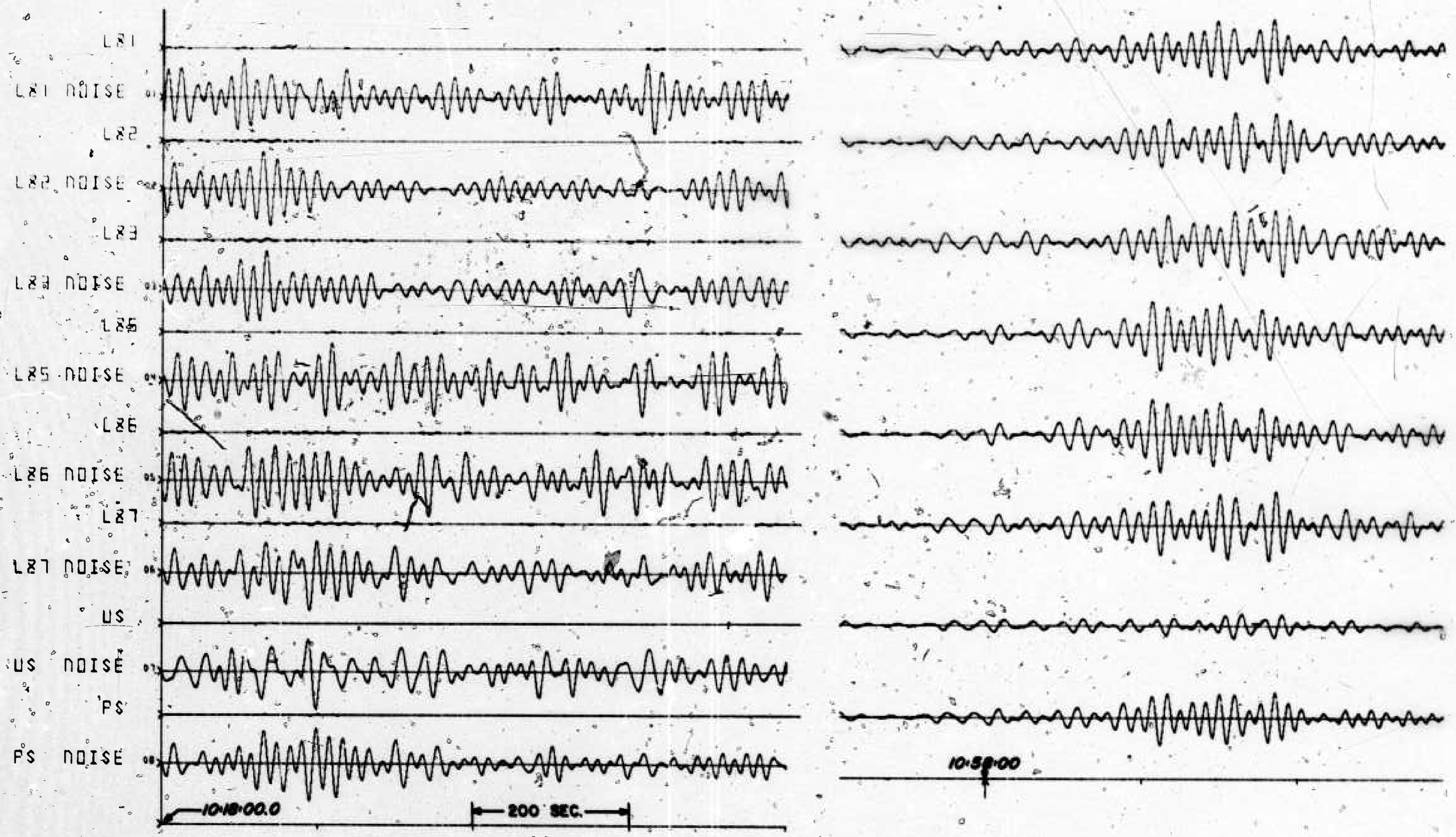

Figure 26. Band pass filtered noise and signal traces with unphased and phased sums for an event at the Coast of Chile recorded at UBO.

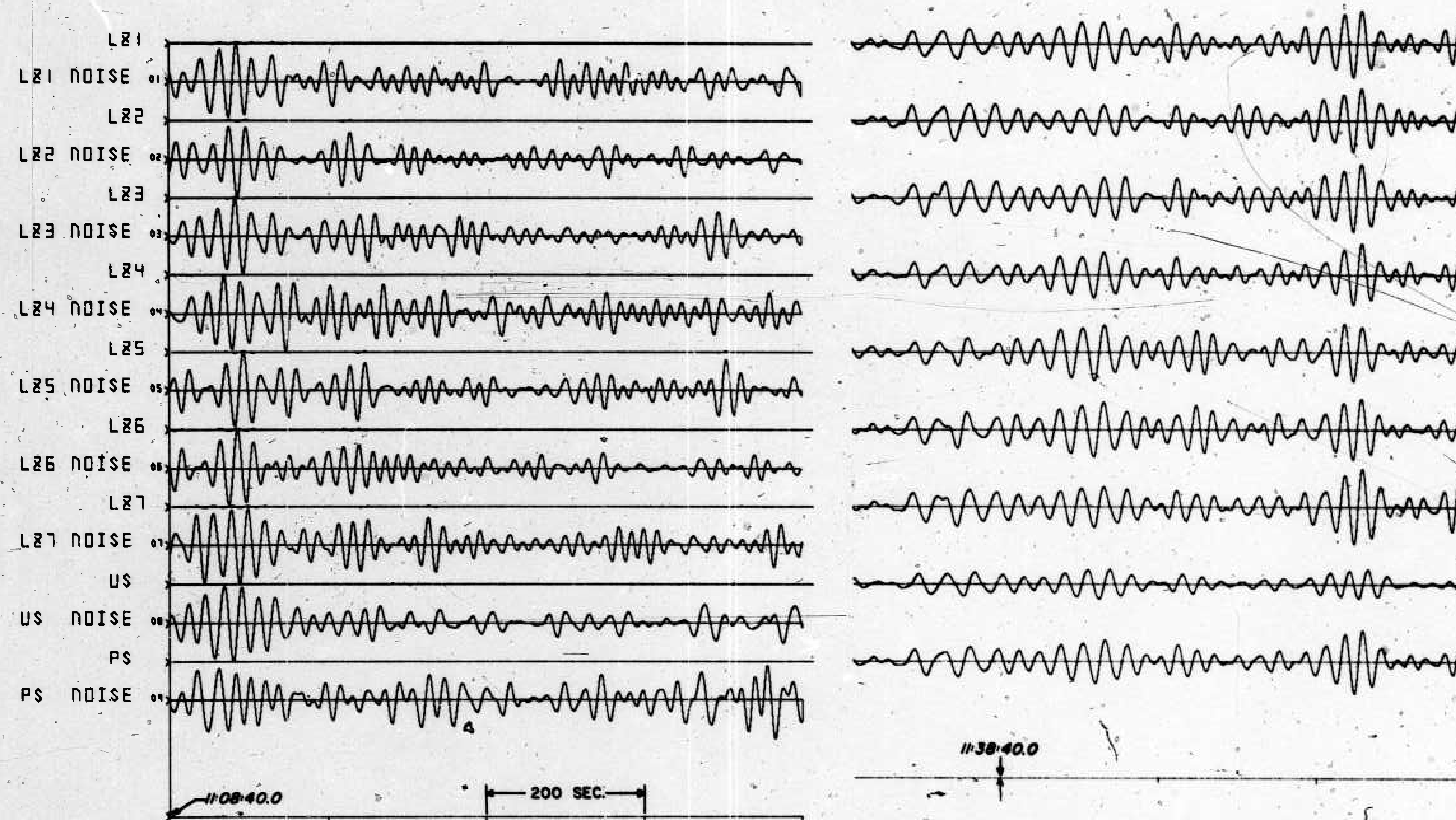

Figure 27. Band pass filtered noise and signal traces with unphased and phased sums for an event in Costa Rica recorded at UBO.

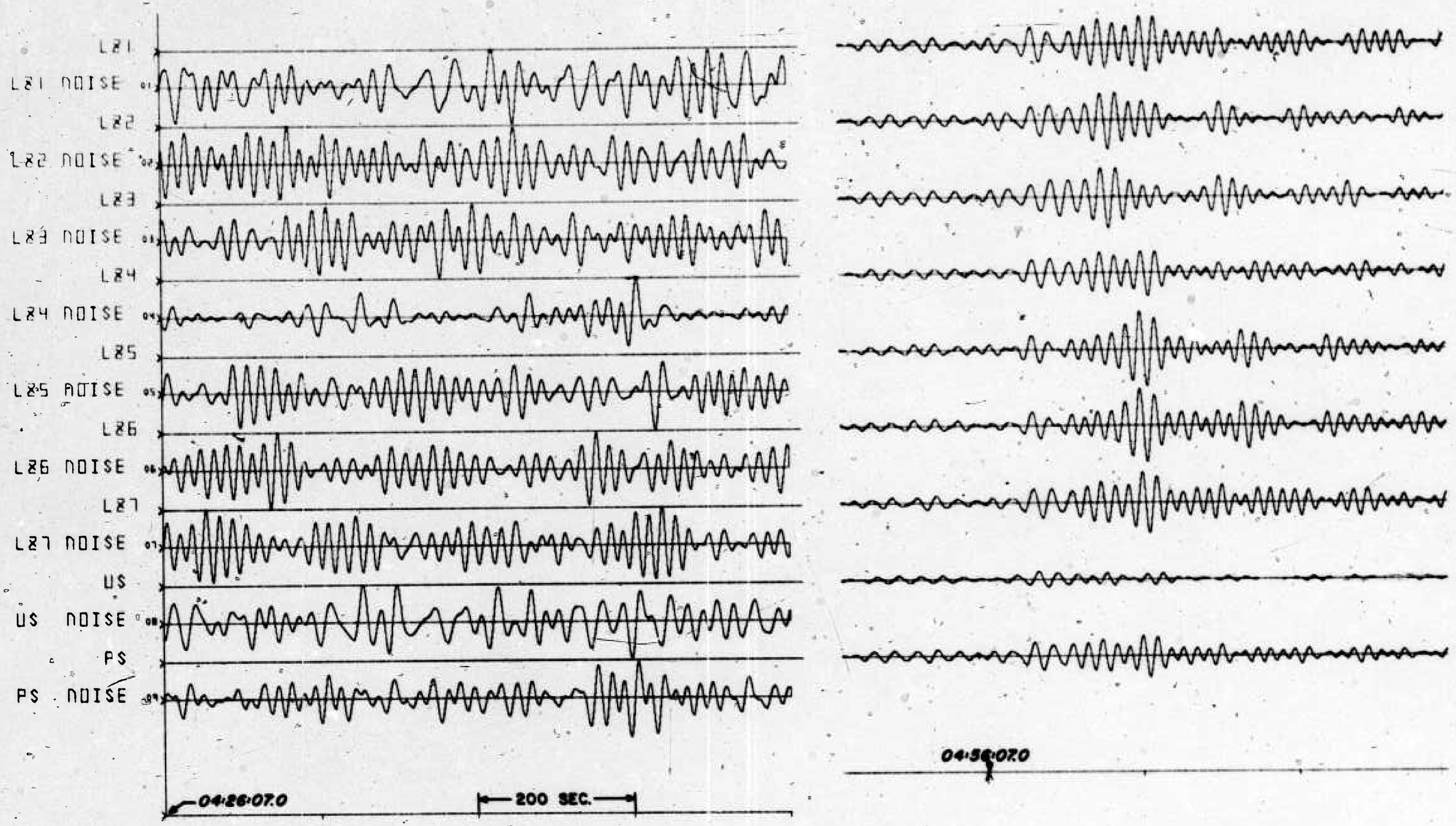

Figure 28. Band pass filtered noise and signal traces with unphased and phased sums for an event in El Salvador recorded at UBO.

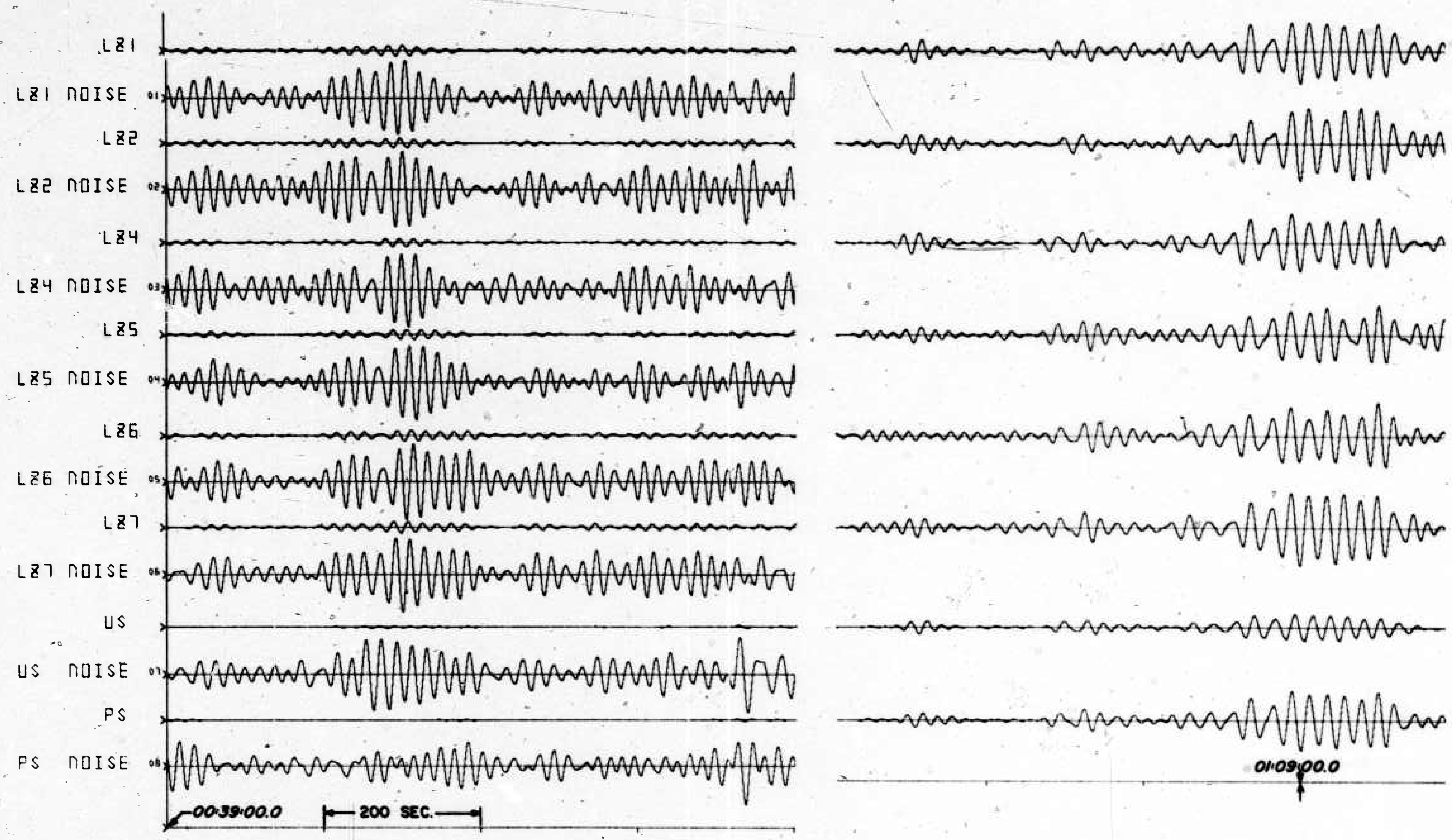

Figure 29. Band pass filtered noise and signal traces with unphased and phased sum for an event in the Fox Islands recorded at UBO.

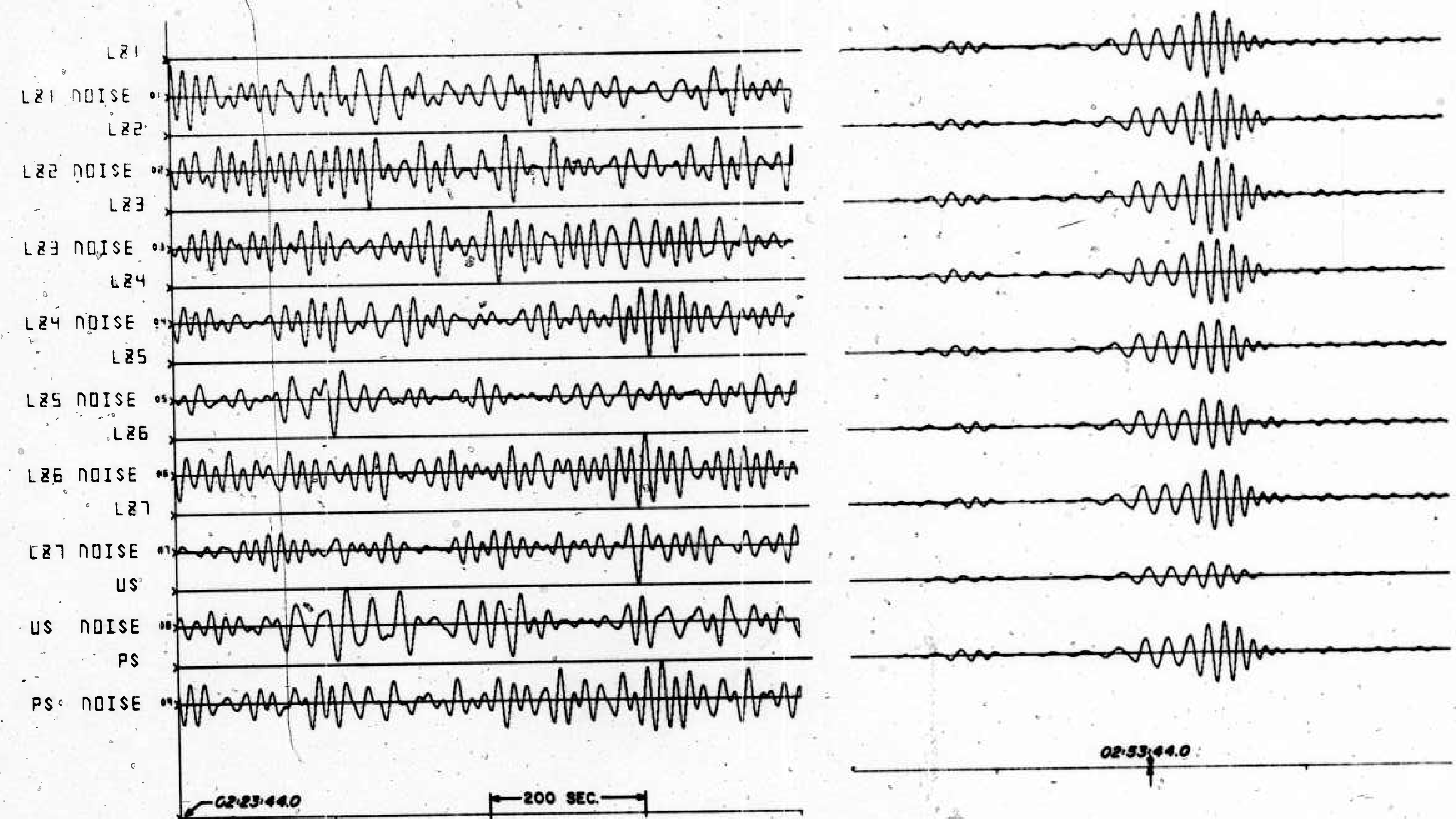

Figure 30. Band pass filtered noise and signal traces with unphased and phased sums for an event in the Galapagos recorded at UBO.

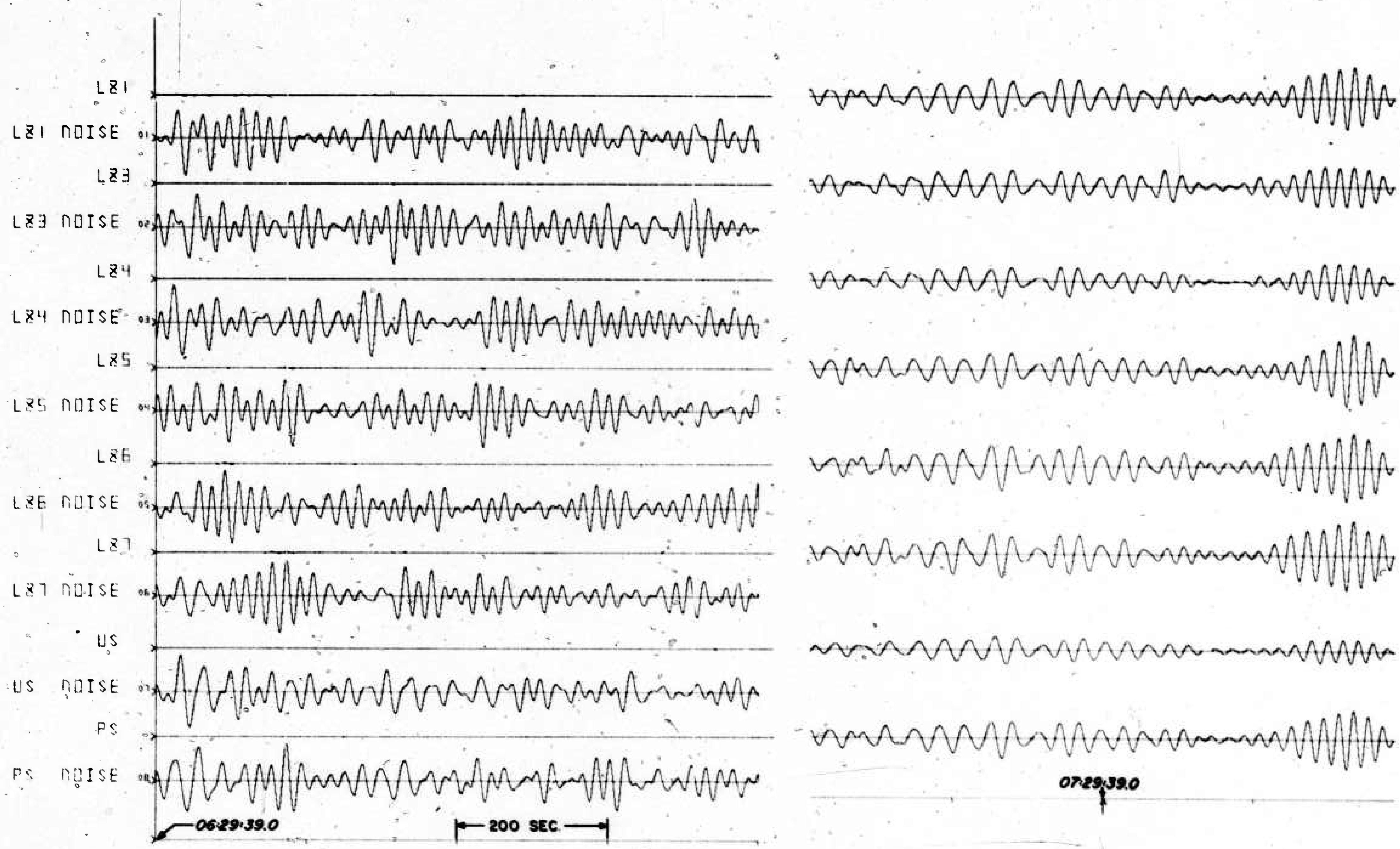

Figure 31. Band pass filtered noise and signal traces with unphased and phased sums for an event in the Hindu Kush recorded at UBO.

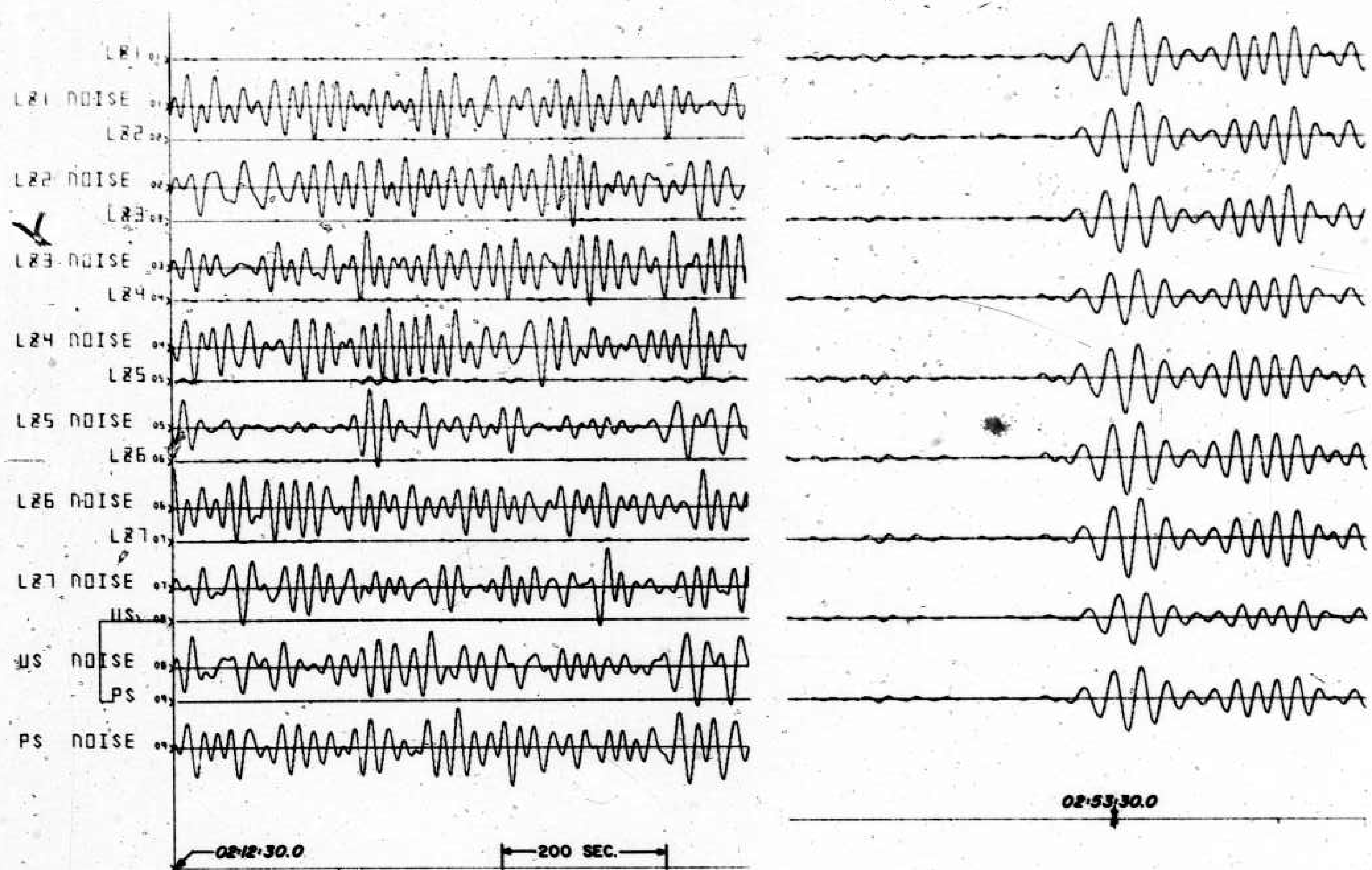

Figure 32. Band pass filtered noise and signal traces with unphased and phased sums for an event in Hokkaido recorded at UBO.

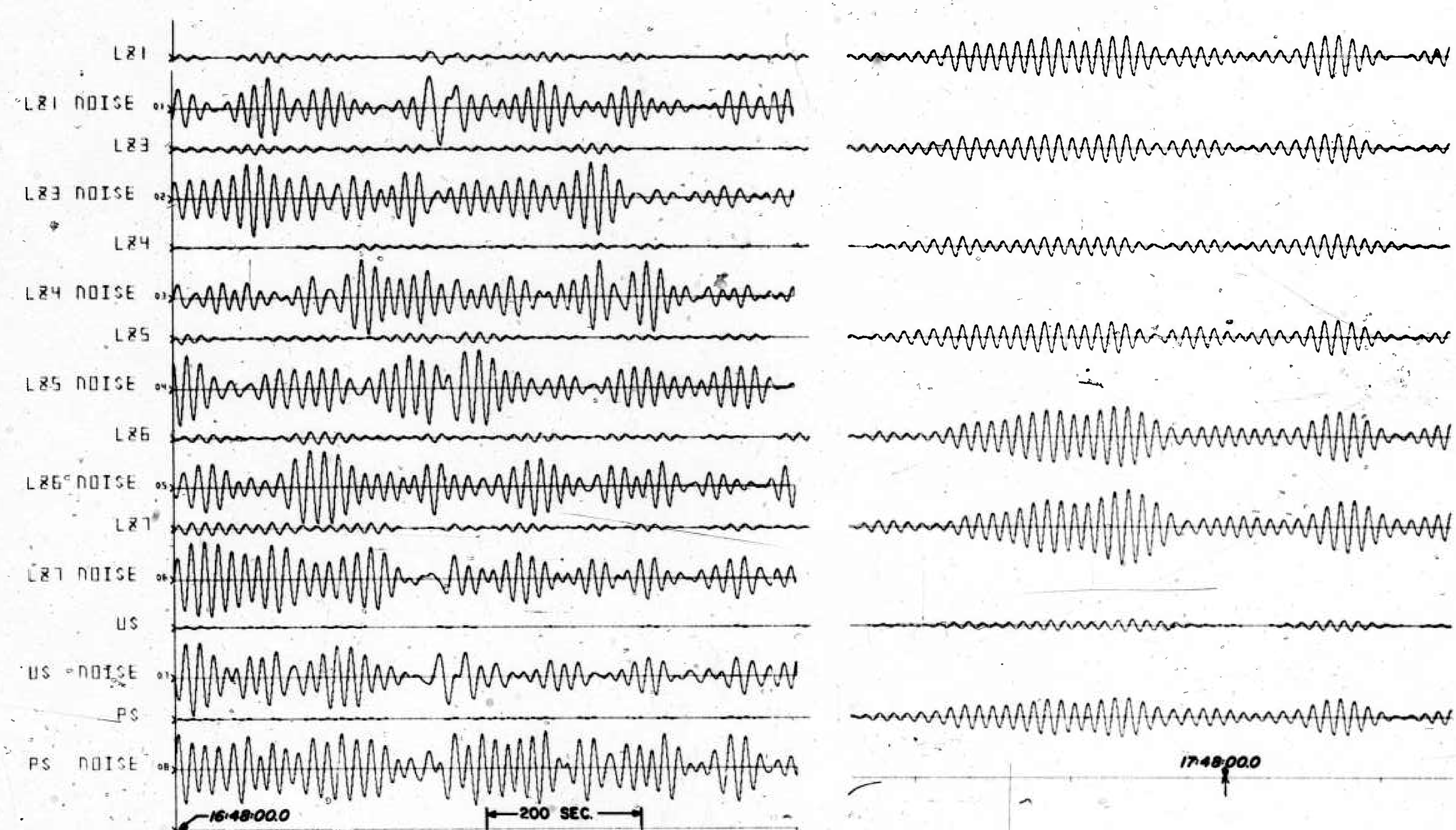

Figure 33. Band pass filtered noise and signal traces with unphased and phased sums for an event in the Kermadec Islands recorded at UBO.

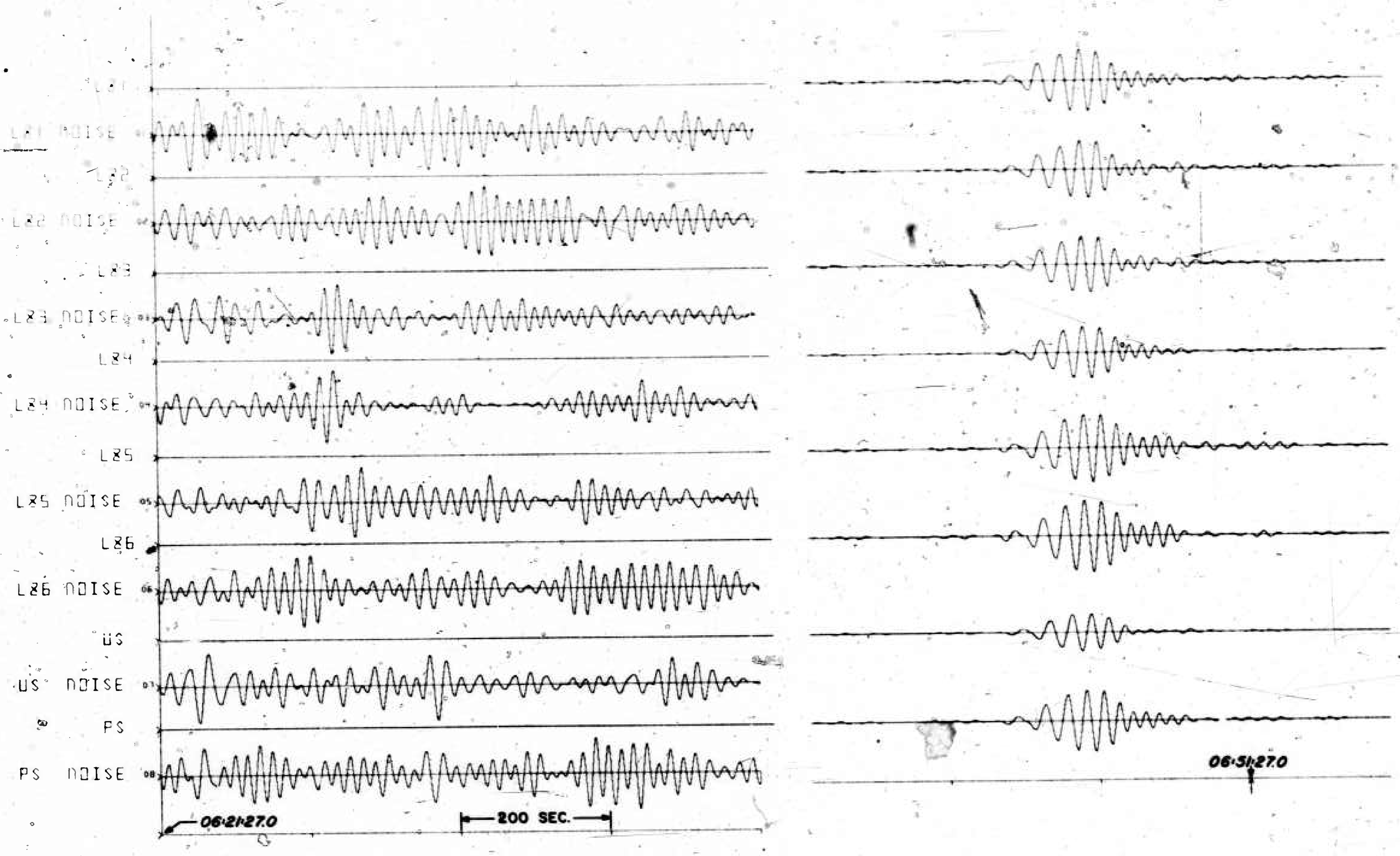

Figure 34. Band pass filtered noise and signal traces with unphased and phased sums for an event in the Kodiac Islands recorded at UBO.

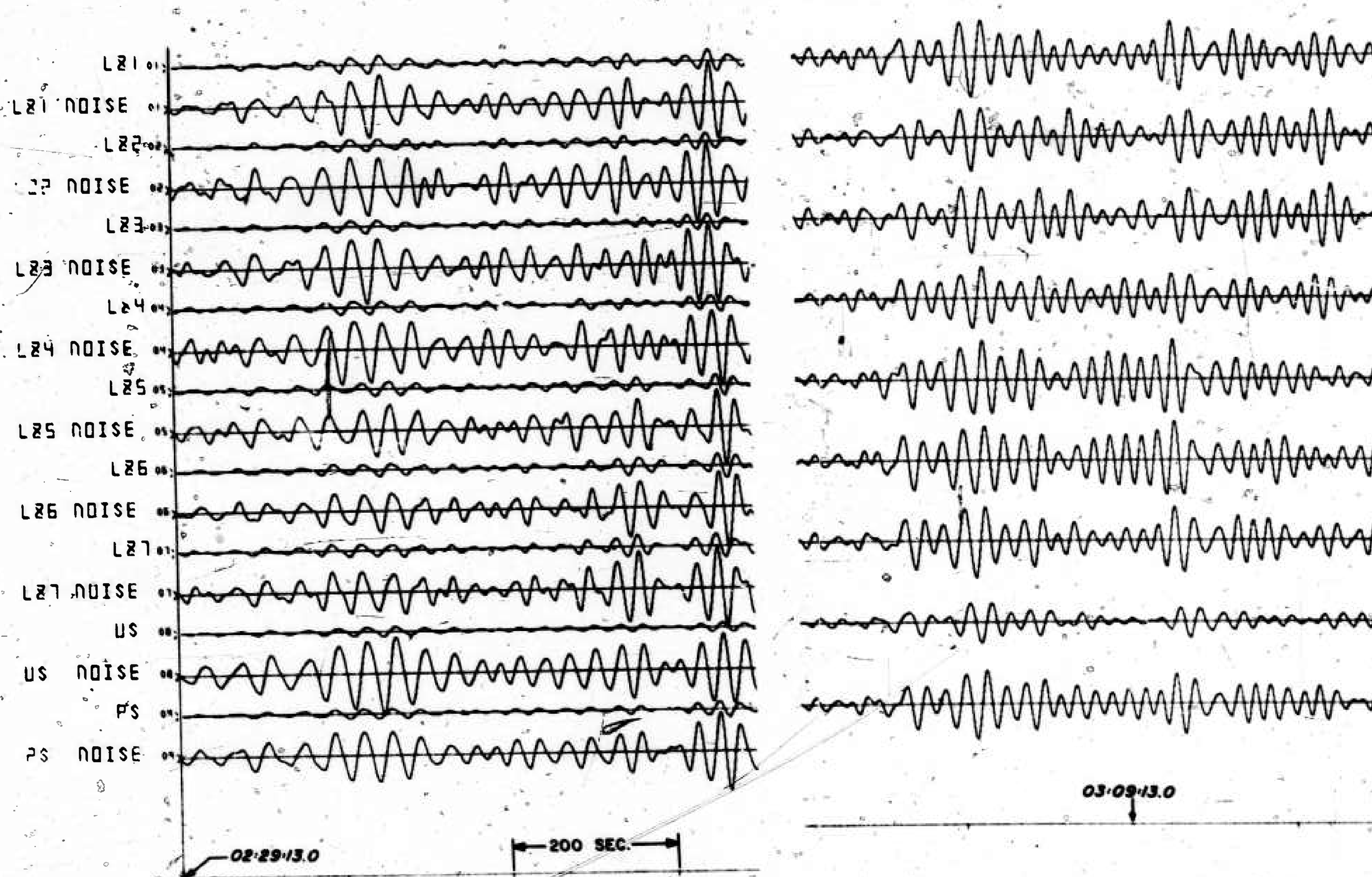

Figure 35. Band pass filtered noise and signal traces with unphased and phased sums for an event in the Kuril Islands recorded at UBO.

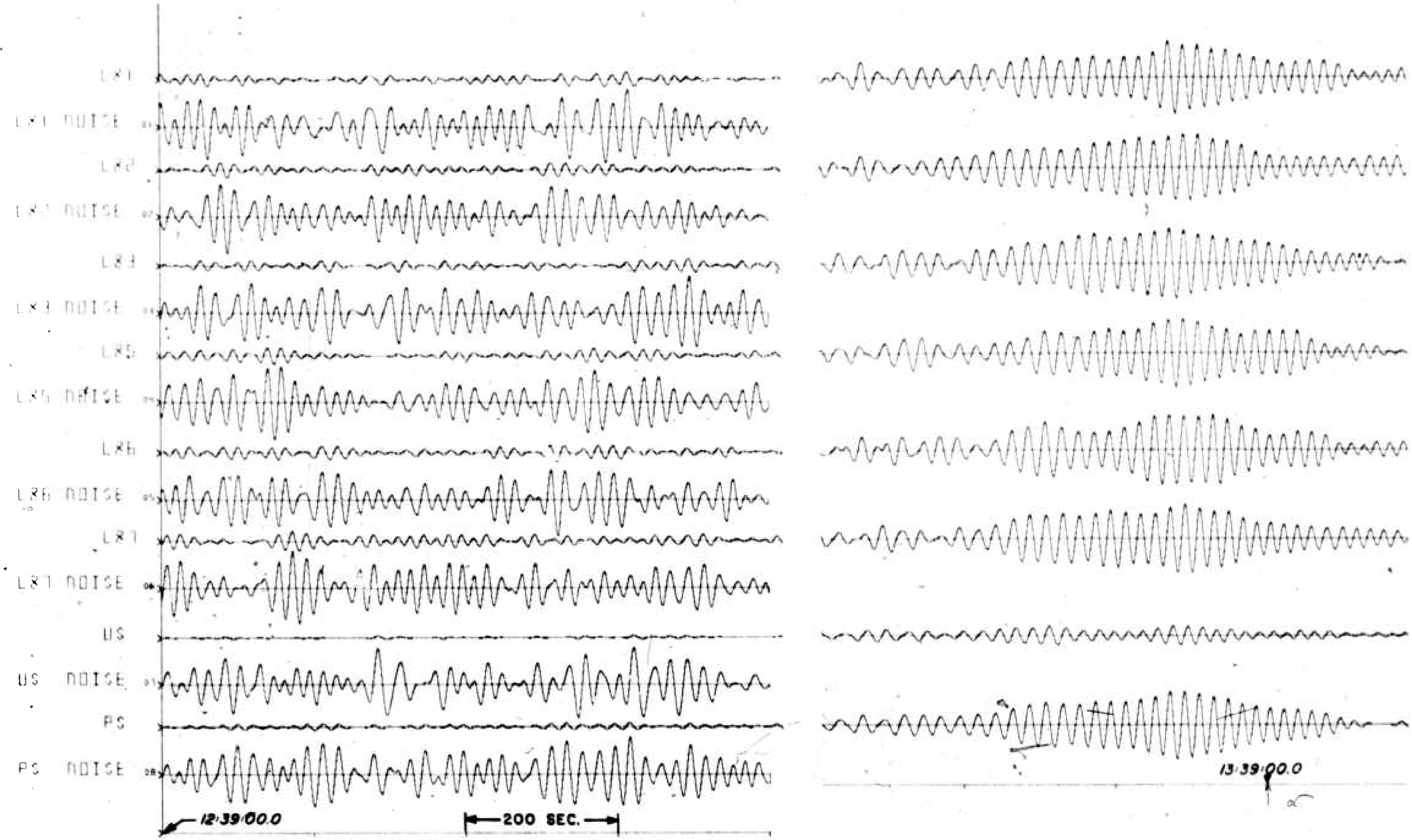

Figure 36. Band pass filtered noise and signal traces with unphased and phased sums for an event in East New Guinea recorded at UBO.

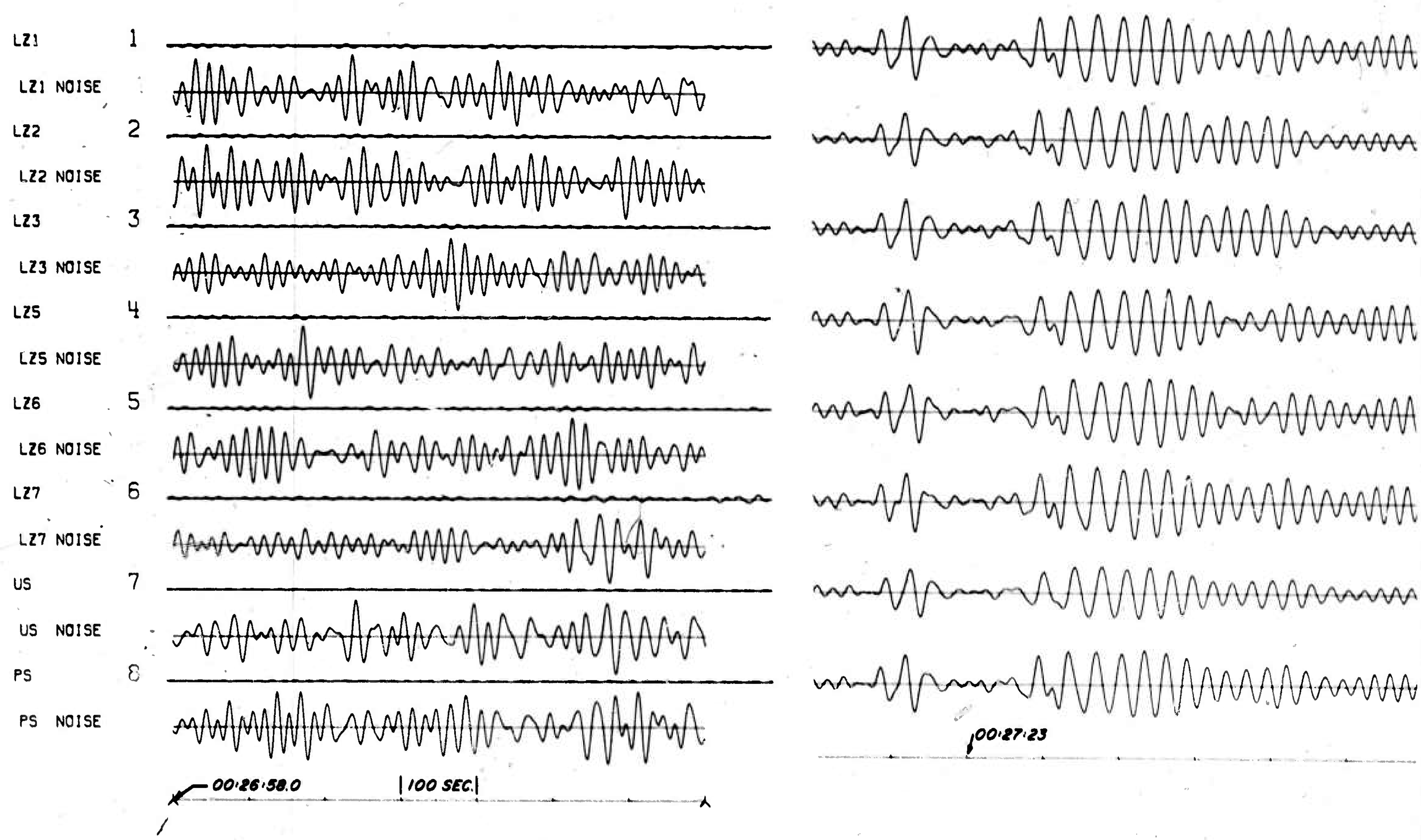

Figure 37. Band pass filtered noise and signal traces with unphased and phased sums for an event in Nicaragua recorded at UBO.

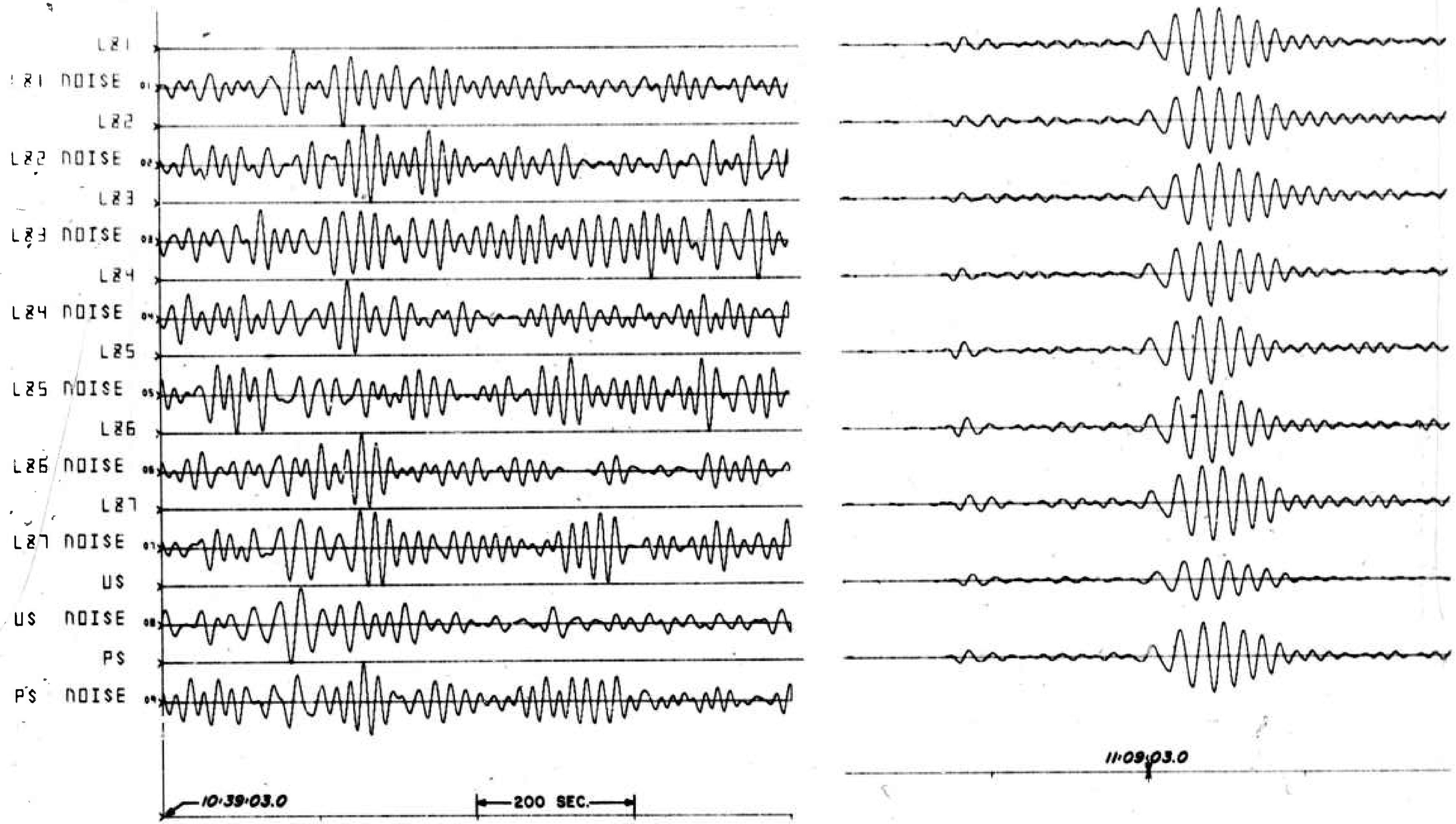

Figure 38. Band pass filtered noise and signal traces with unphased and phased sums for an event in the Rat Islands recorded at UBO.

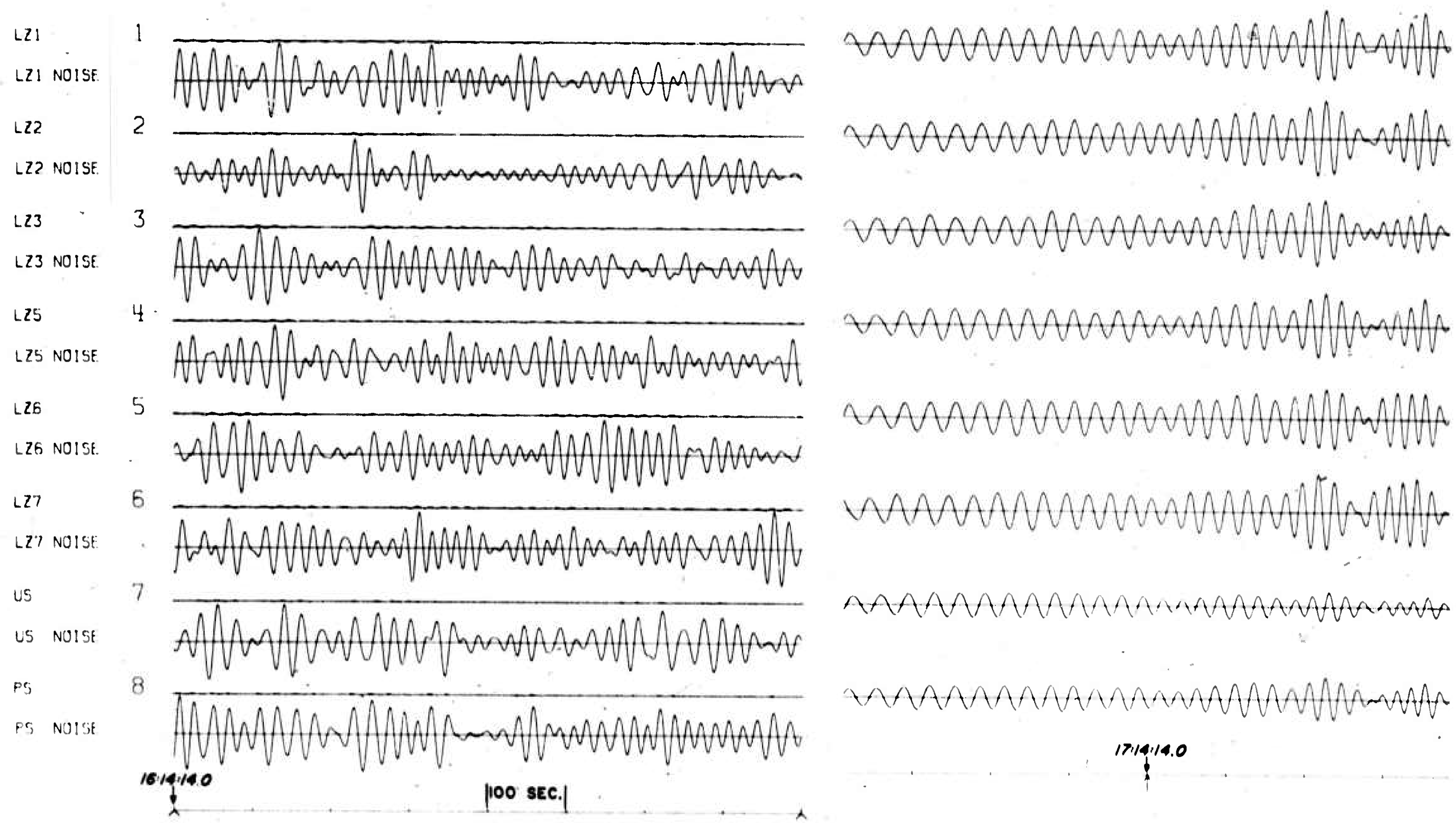

Figure 39. Band pass filtered noise and signal traces with unphased and phased sums for an event in Sinkiang recorded at UBO.

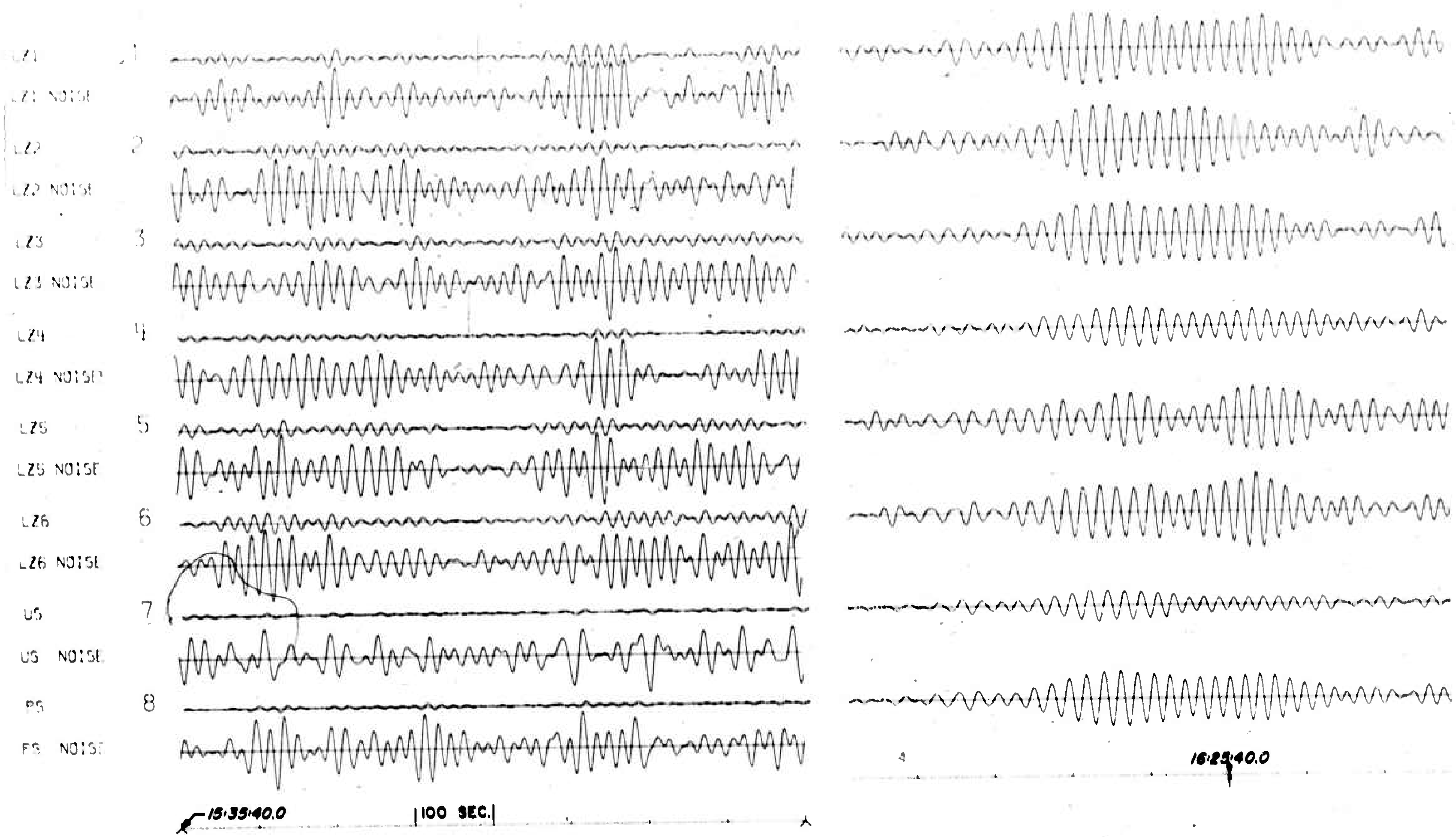

Figure 40. Band pass filtered noise and signal traces with unphased and phased sums for an event in the Volcano Islands recorded at UBO.

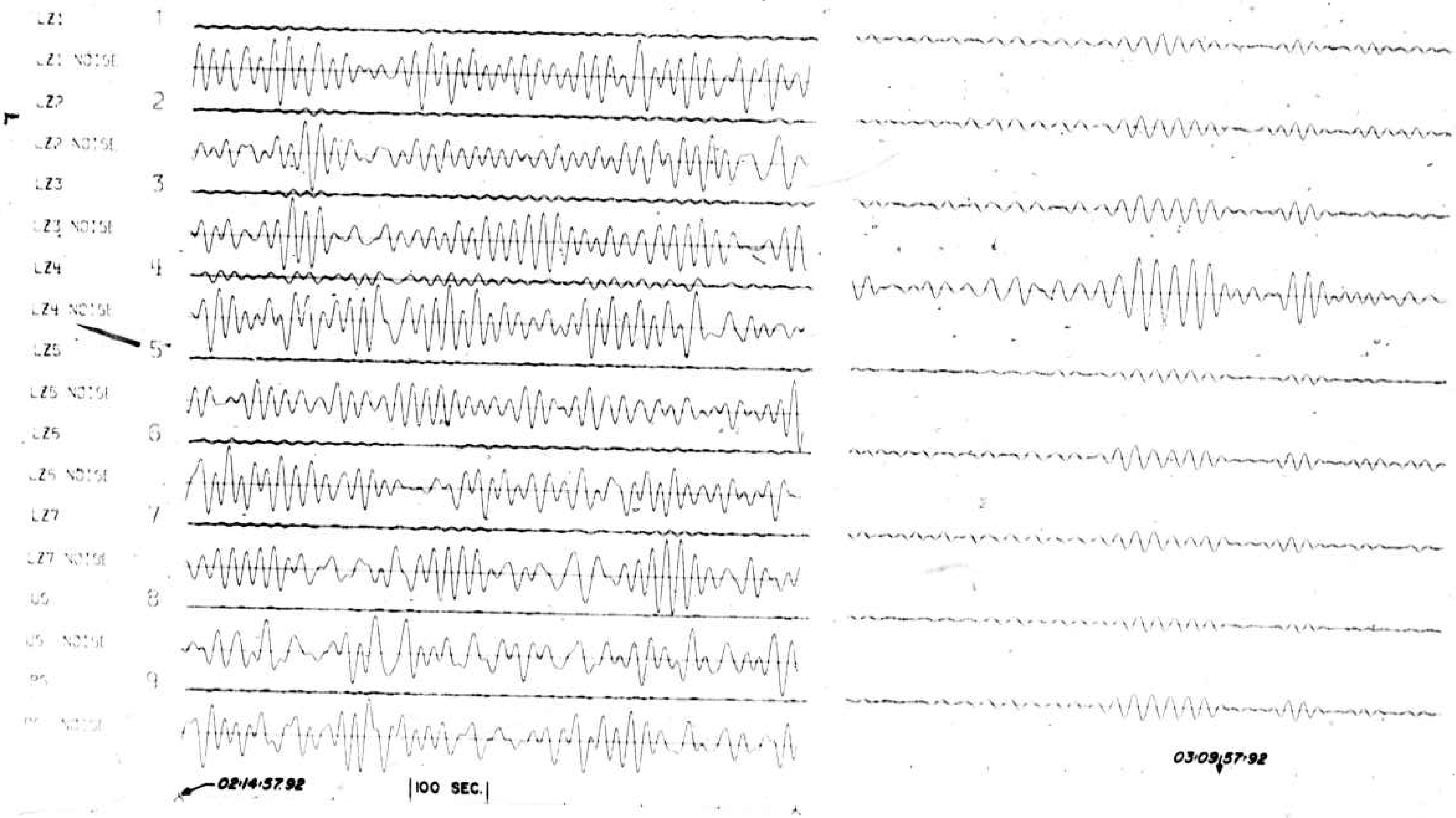

Figure 41. Band pass filtered noise and signal traces with unphased and phased sums for an event in Albania recorded at TFO.

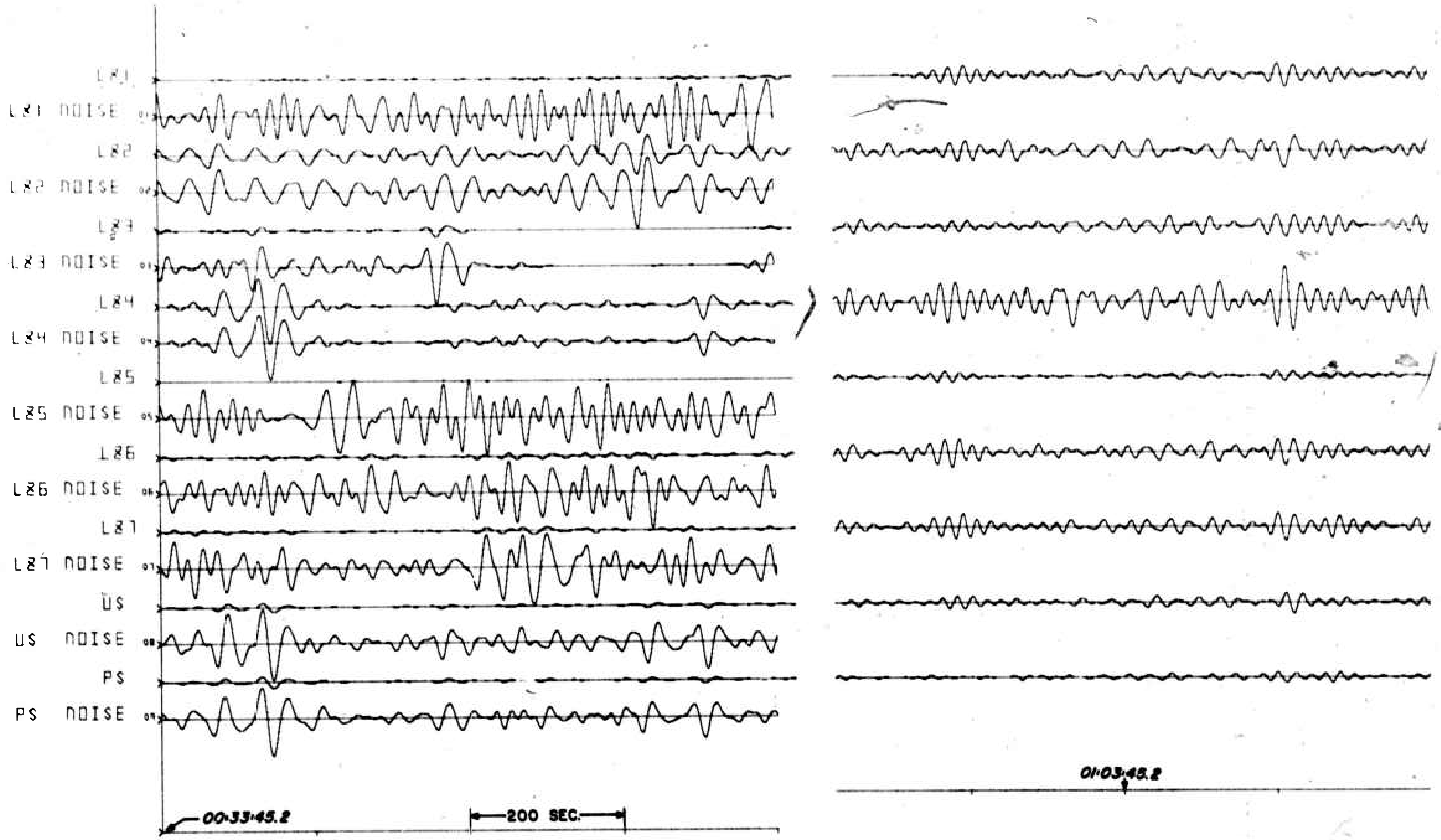

Figure 42. Band pass filtered noise and signal traces with unphased and phased sums for an event in the North Atlantic recorded at TFO.

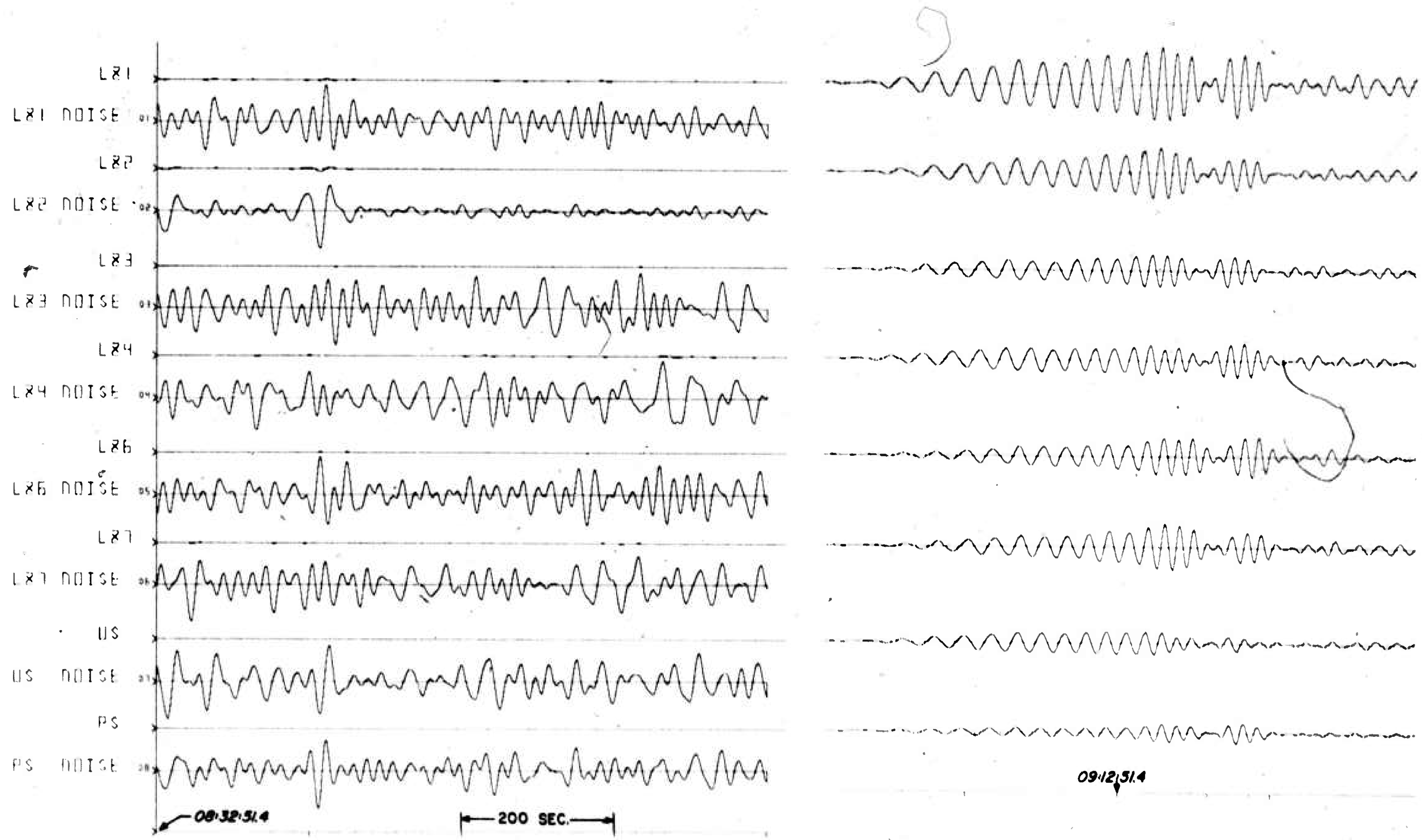

Figure 43. Band pass filtered noise and signal traces with unphased and phased sums for an event in the North Atlantic Ridge recorded at TFO.

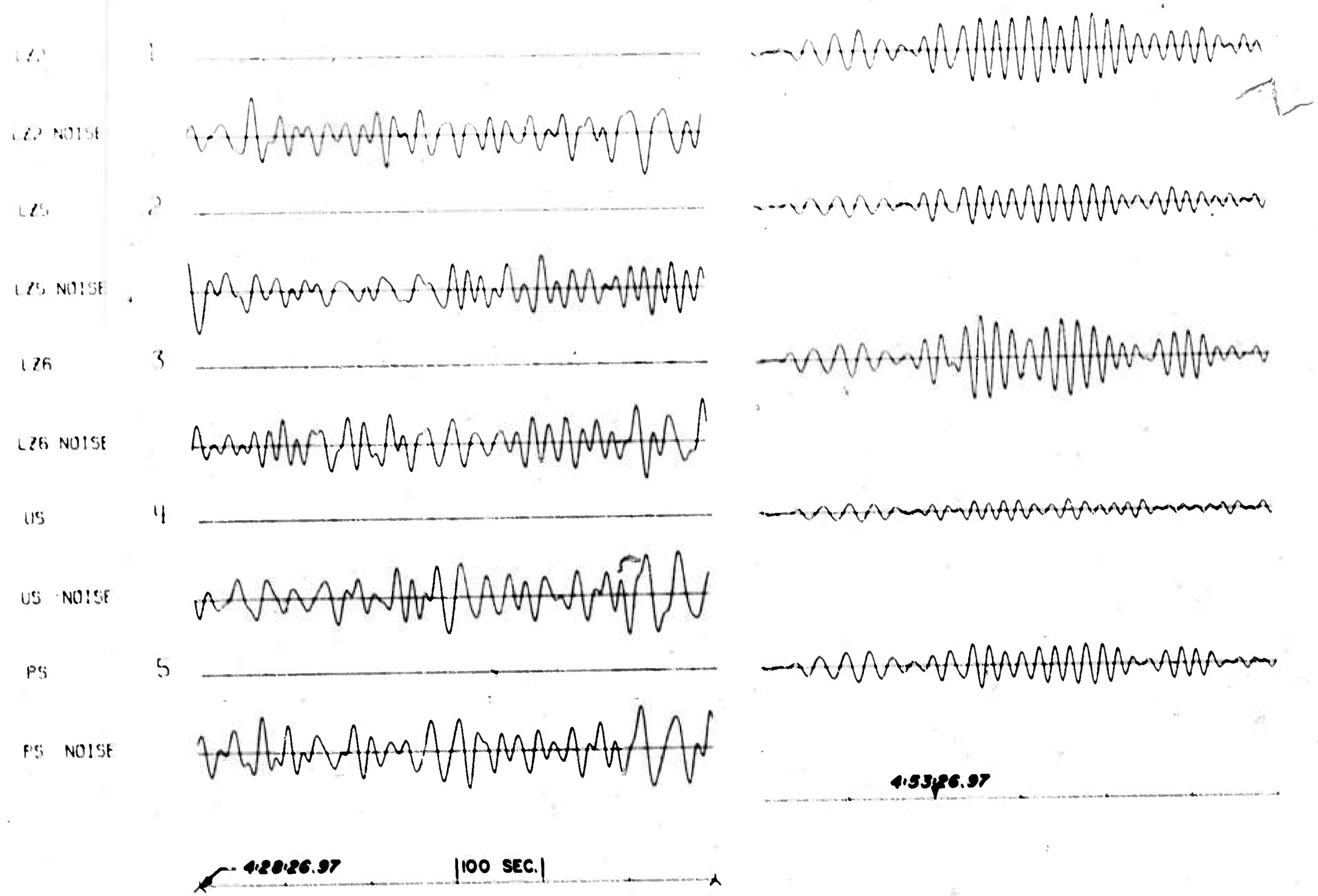

Figure 44. Band pass filtered noise and signal traces with unphased and phased sums for an event in El Salvador recorded at TFO.

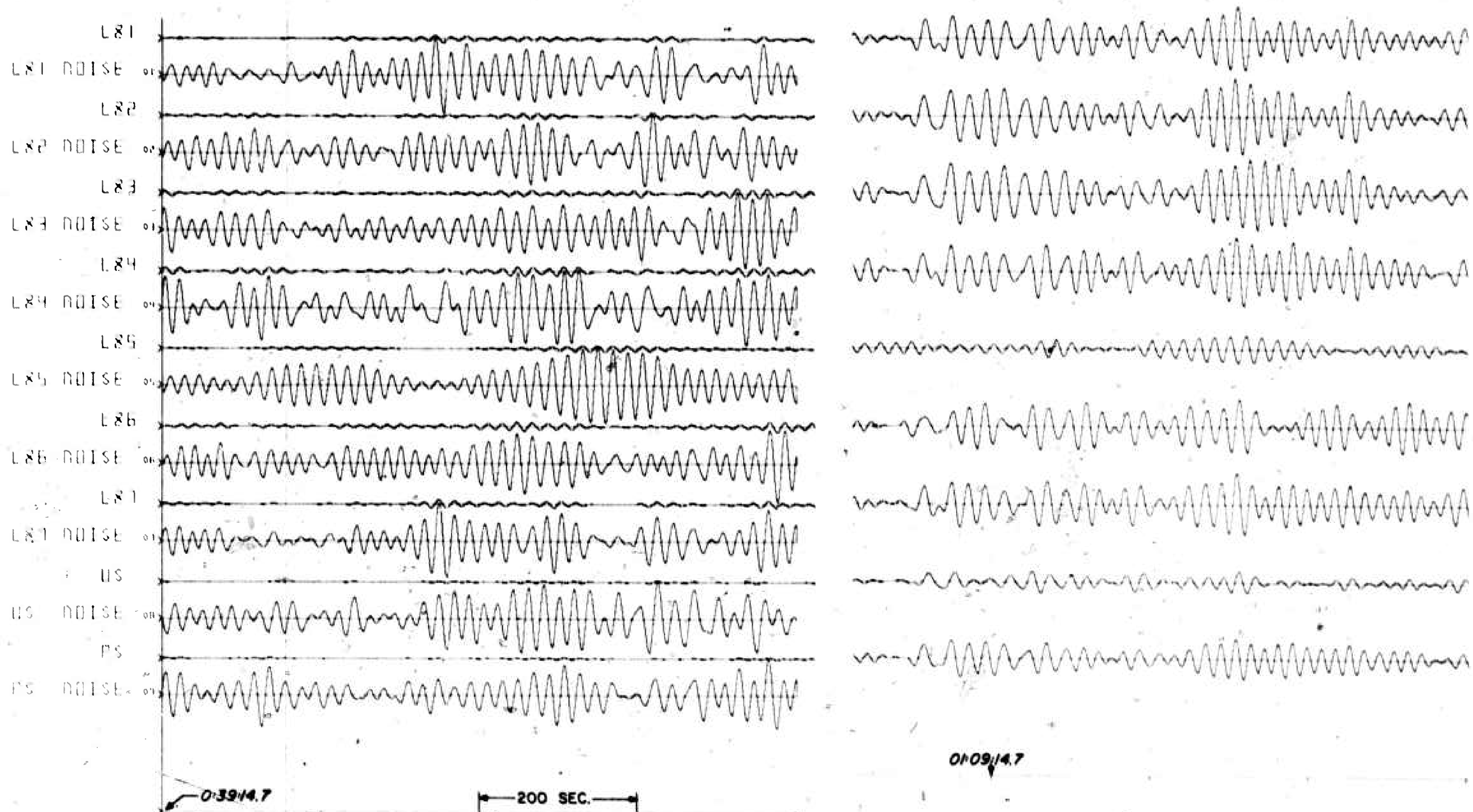

Figure 45. Band pass filtered noise and signal traces with unphased and phased sums for an event in the Fox Islands recorded at TFO.

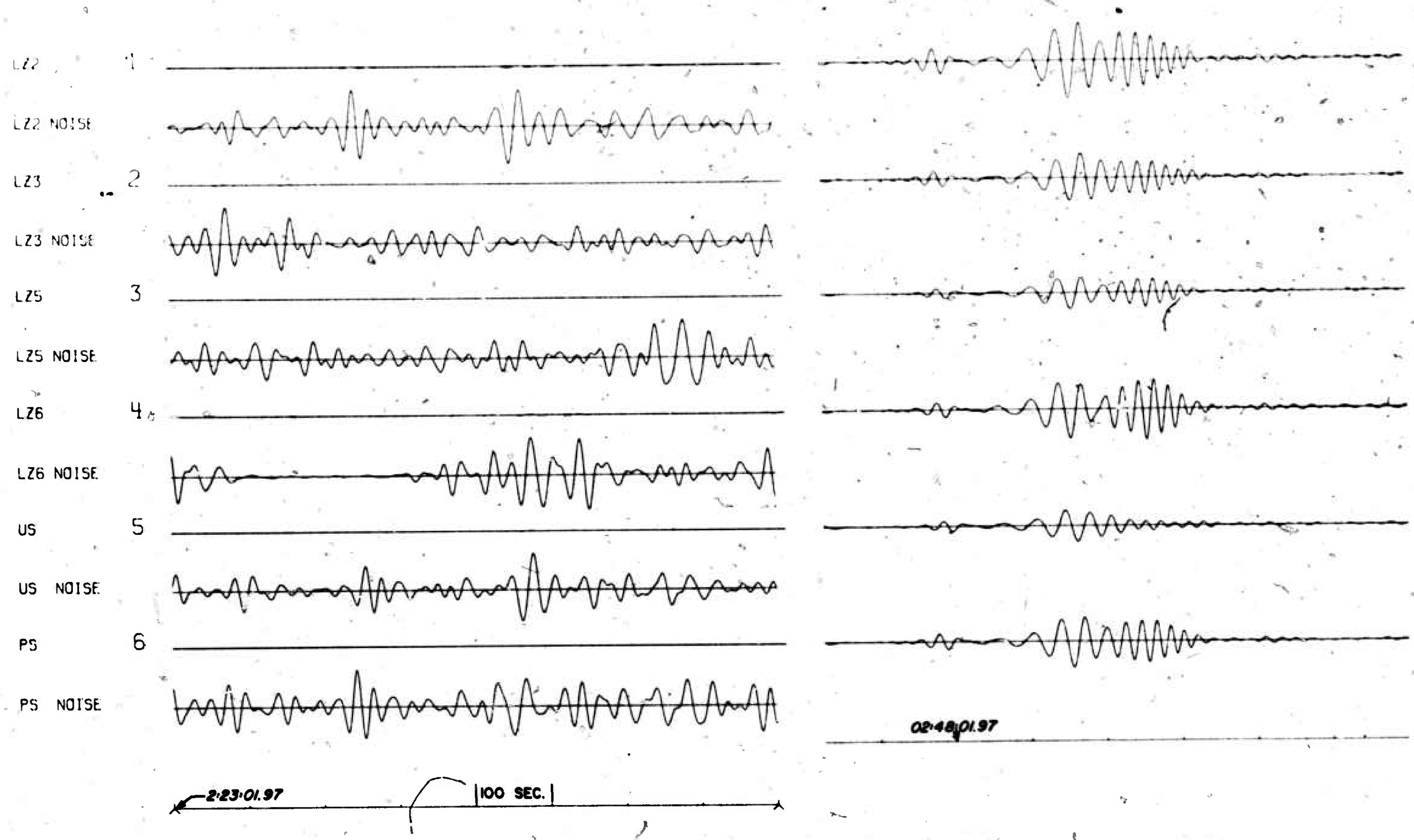

Figure 46. Band pass filtered noise and signal traces with unphased and phased sums for an event in Galapagos recorded at TFO.

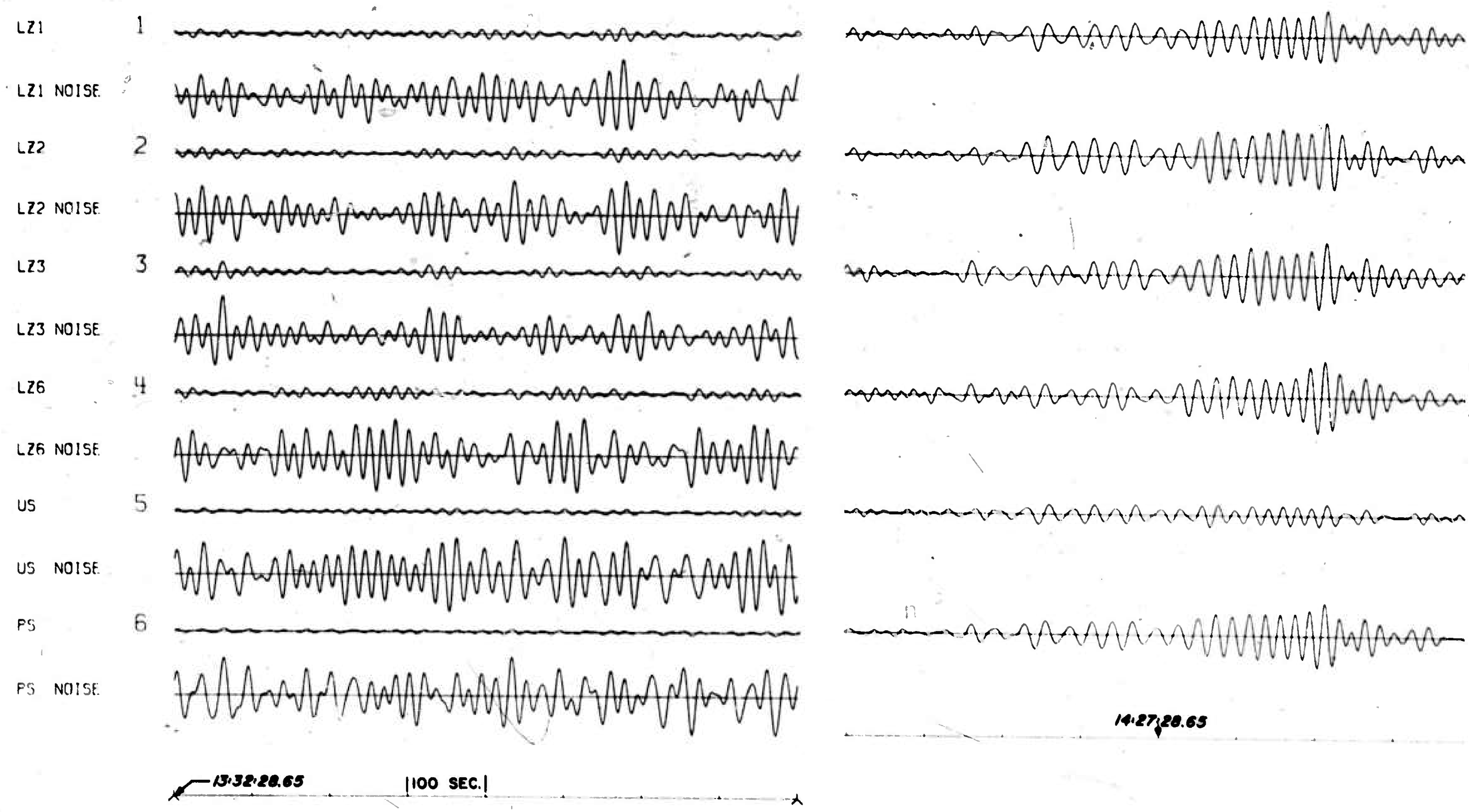

Figure 47. Band pass filtered noise and signal traces with unphased and phased sums for an event in the Border Region of Greece - Albania recorded at TFO.

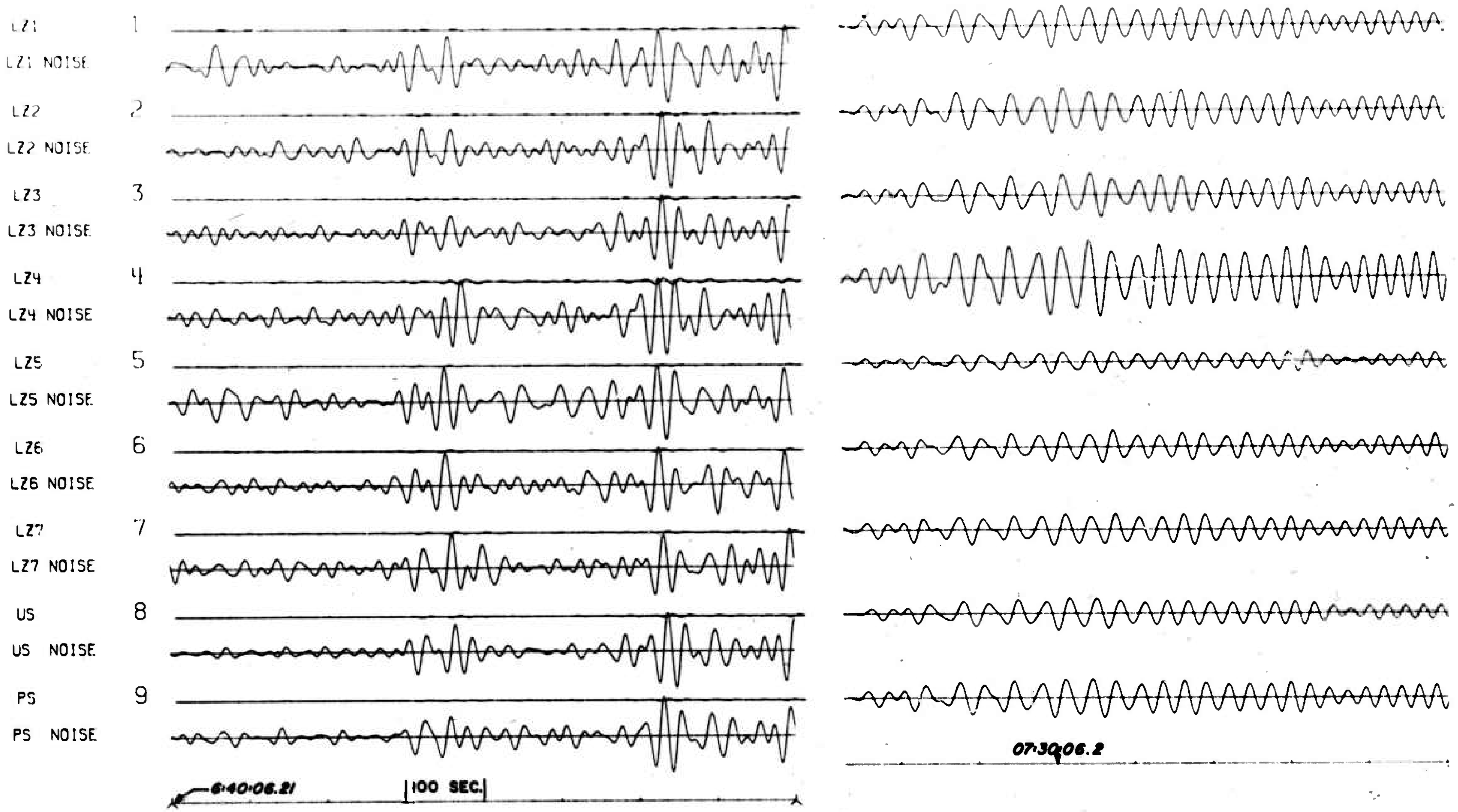

Figure 48. Band pass filtered noise and signal traces with unphased and phased sums for an event in the Hindu Kush recorded at TFO.

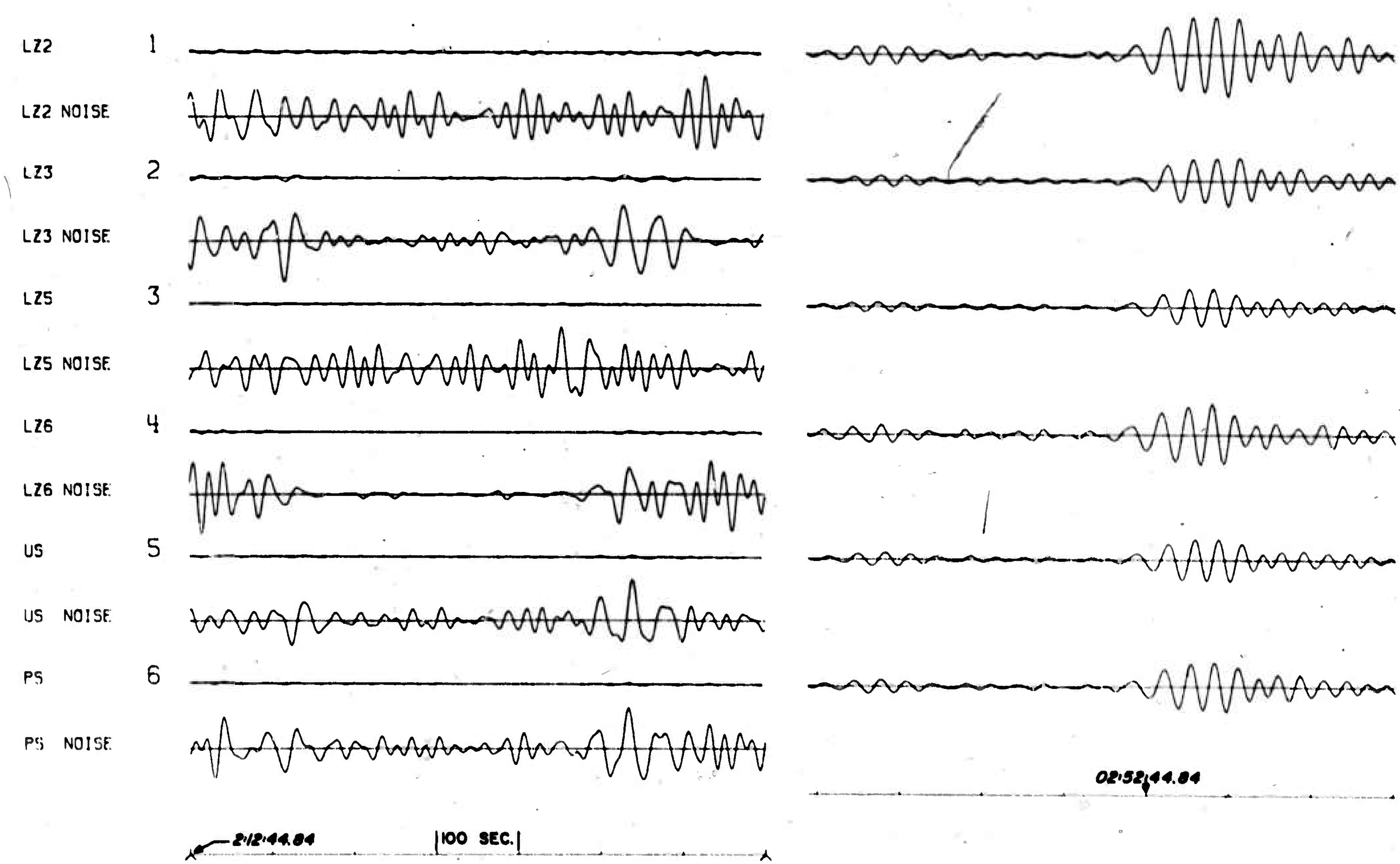

Figure 49. Band pass filtered noise and signal traces with unphased and phased sums for an event in Hokkaido recorded at TFO.

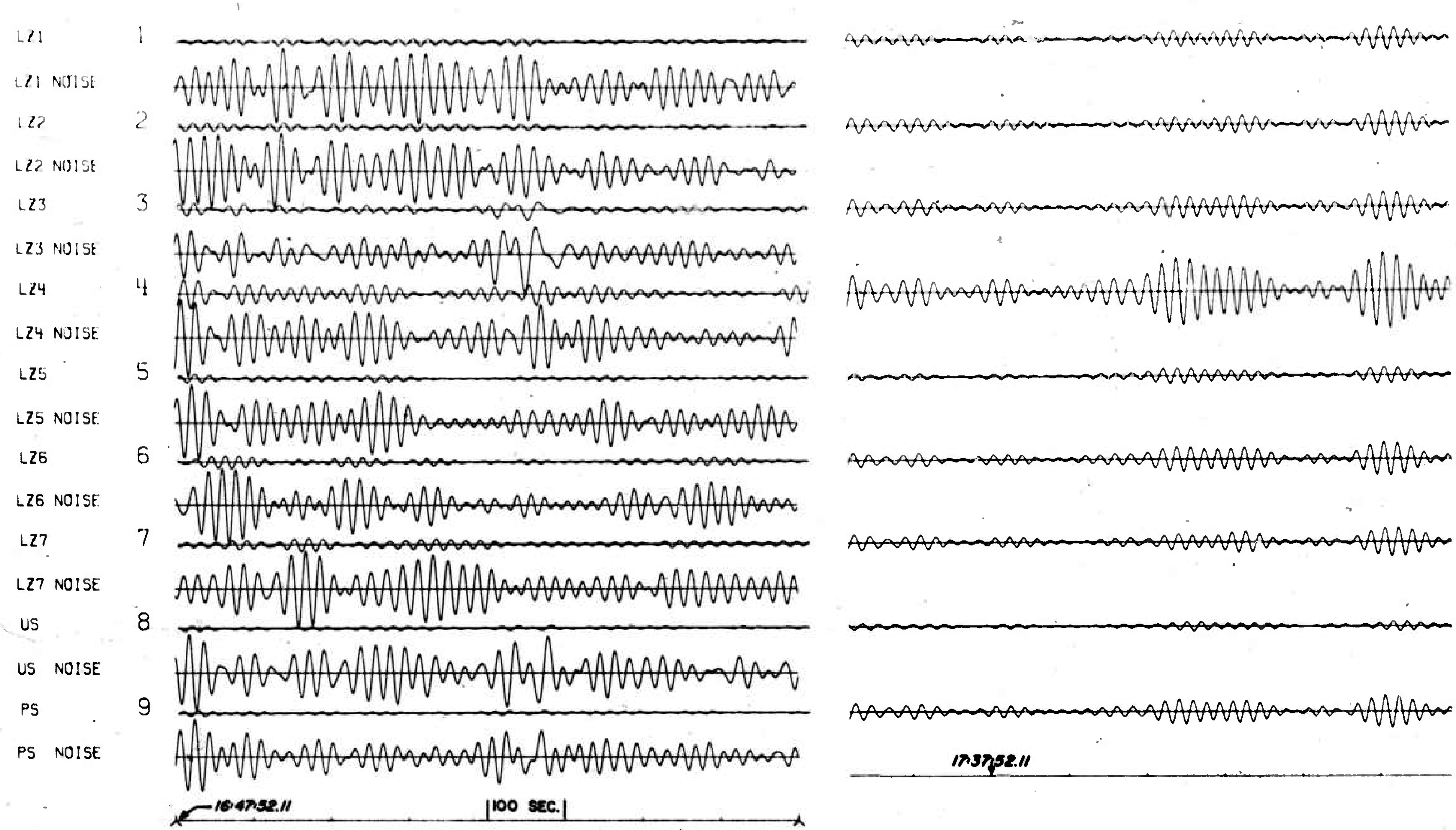

Figure 50. Band pass filtered noise and signal traces with unphased and phased sums for an event in the Kermadec Islands recorded at TFO.

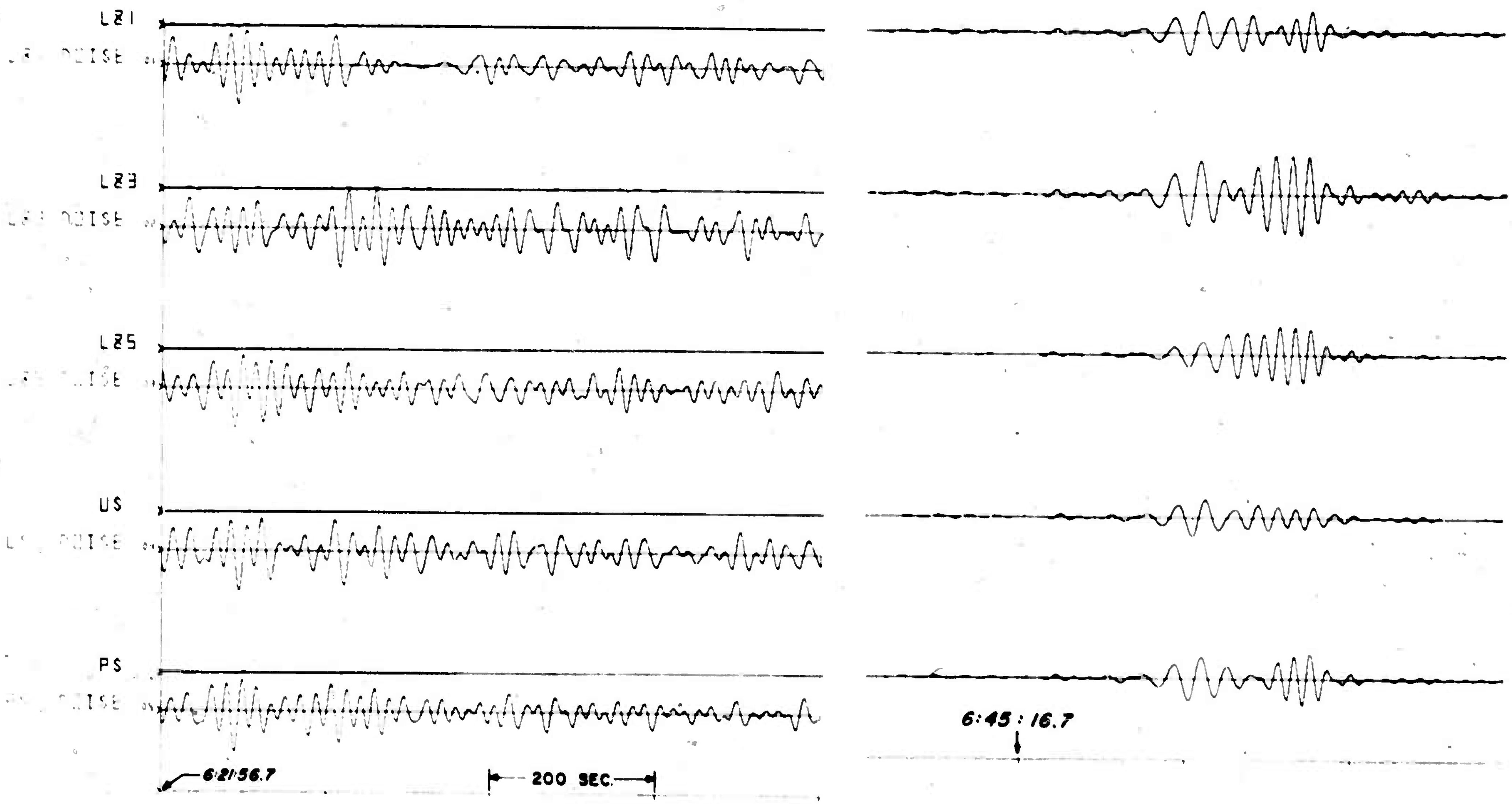

Figure 51. Band pass filtered noise and signal traces with unphased and phased sums for an event in the Kodiac Islands recorded at TFO.

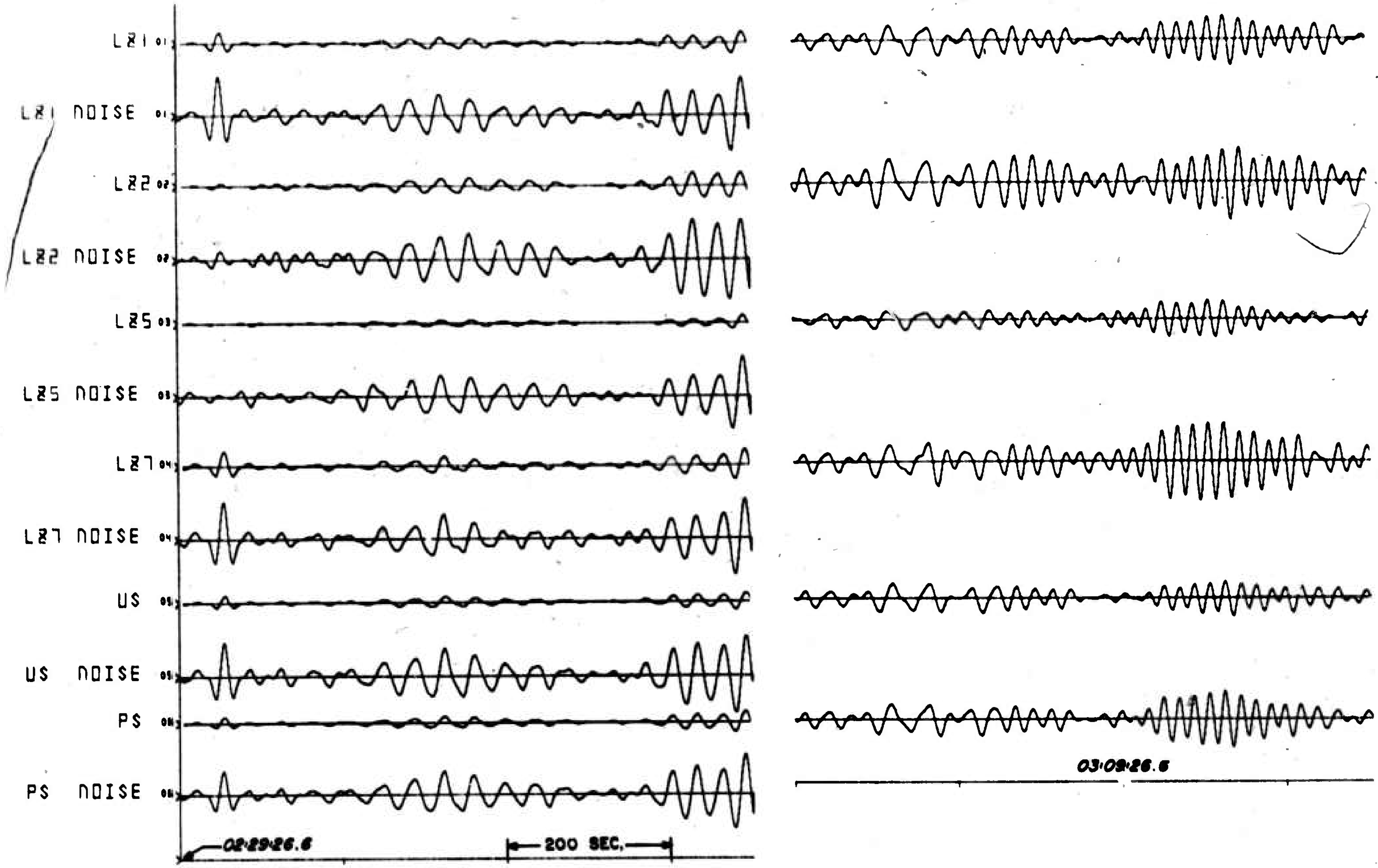

Figure 52. Band pass filtered noise and signal traces with unphased and phased sums for an event in the Kurile Islands recorded at TFO.

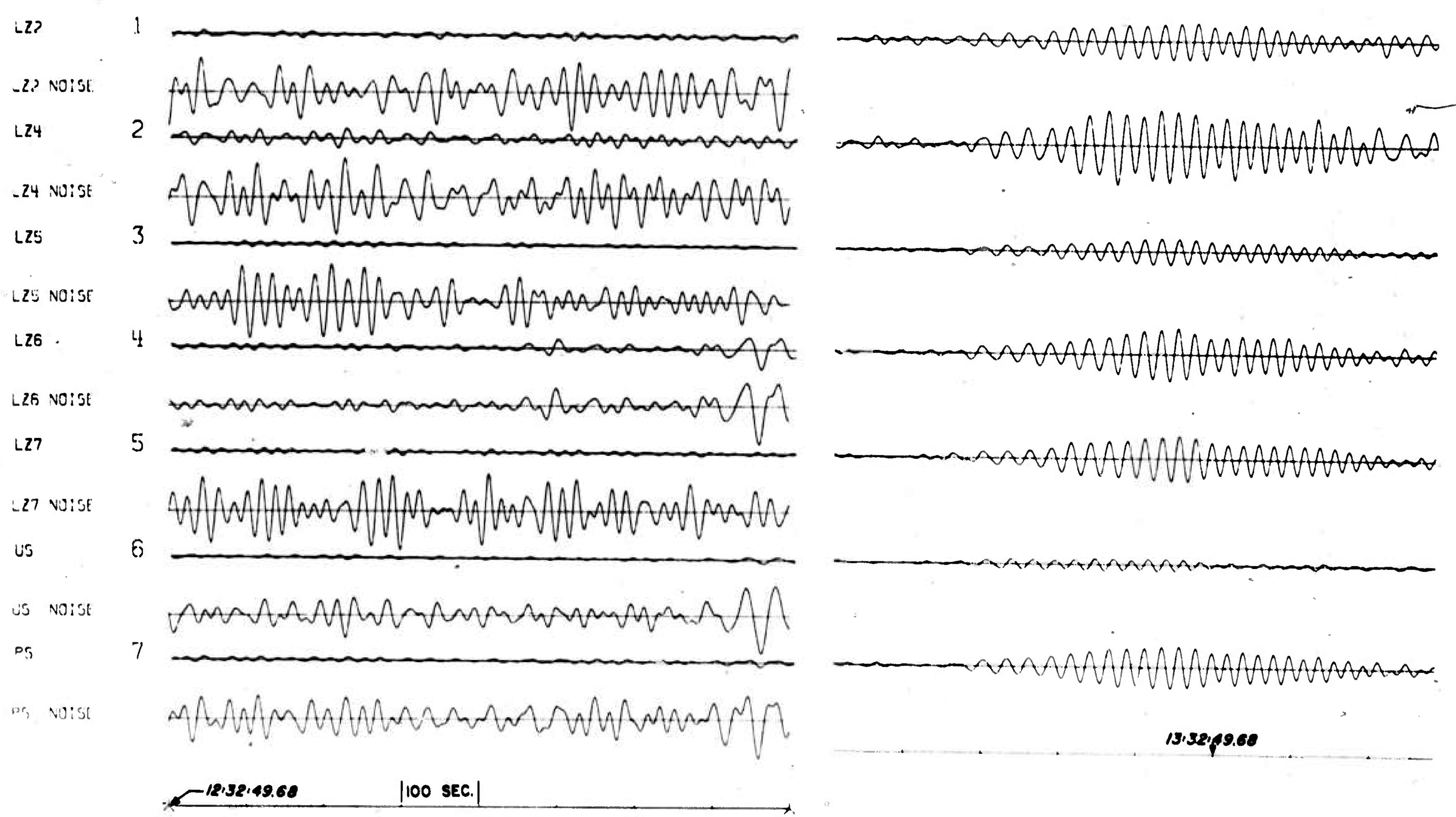

Figure 53. Band pass filtered noise and signal traces with unphased and phased sums for an event in East New Guinea recorded at TFO.

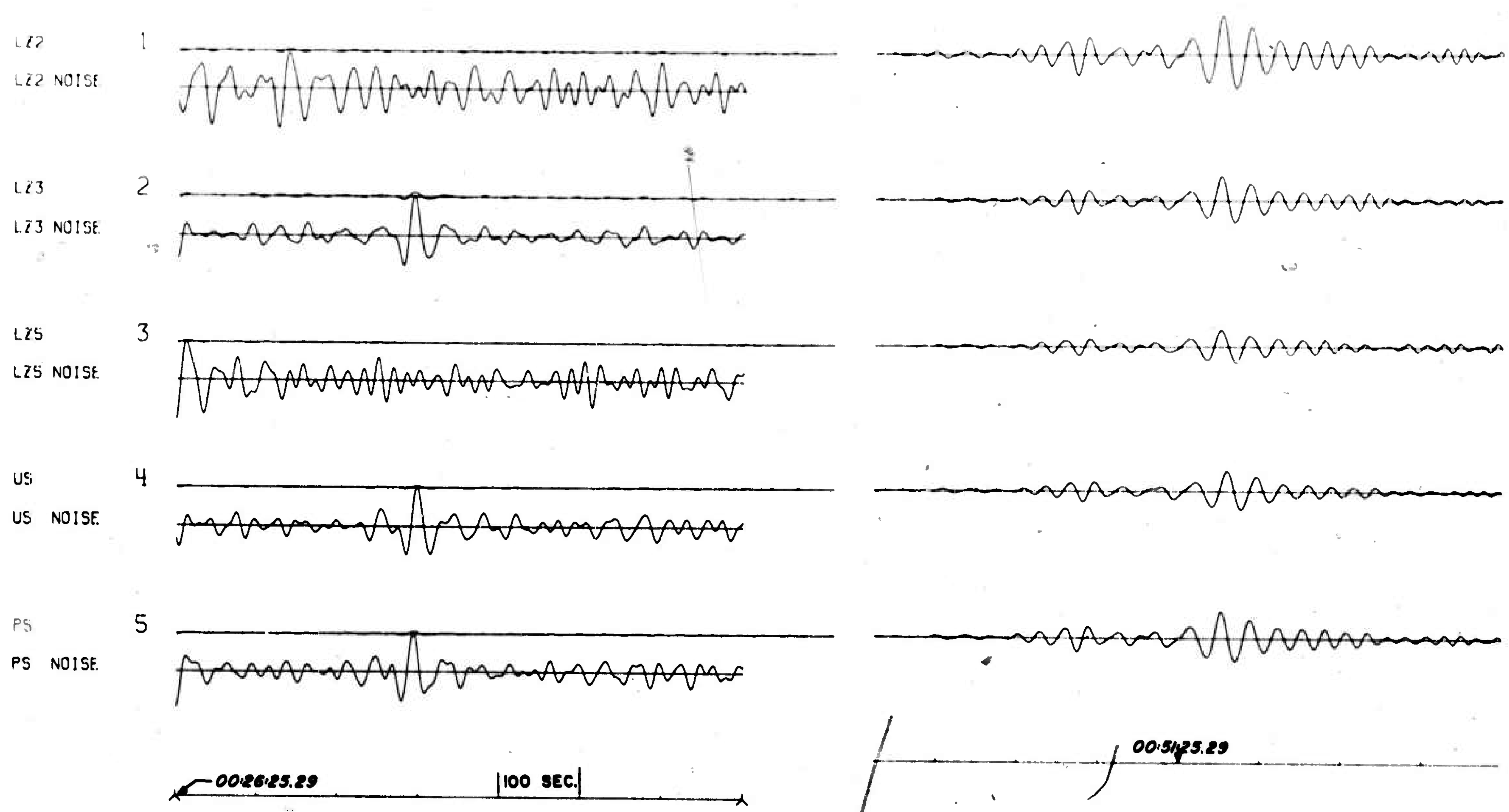

Figure 54. Band pass filtered noise and signal traces with unphased and phased sums for an event in Nicaragua recorded at TFO.

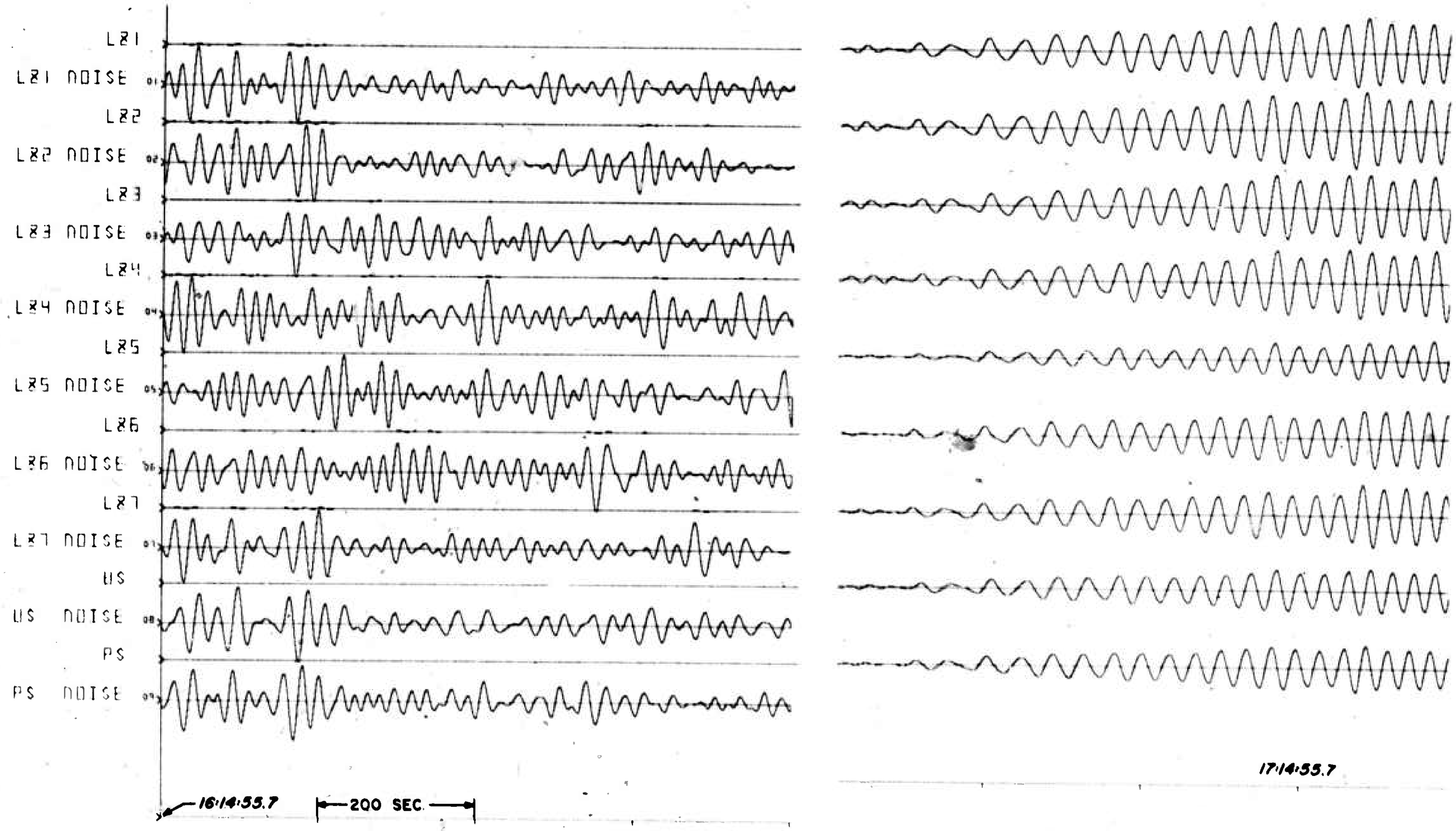

Figure 55. Band pass filtered noise and signal traces with unphased and phased sums for an event in Sinkiang recorded at TFO.

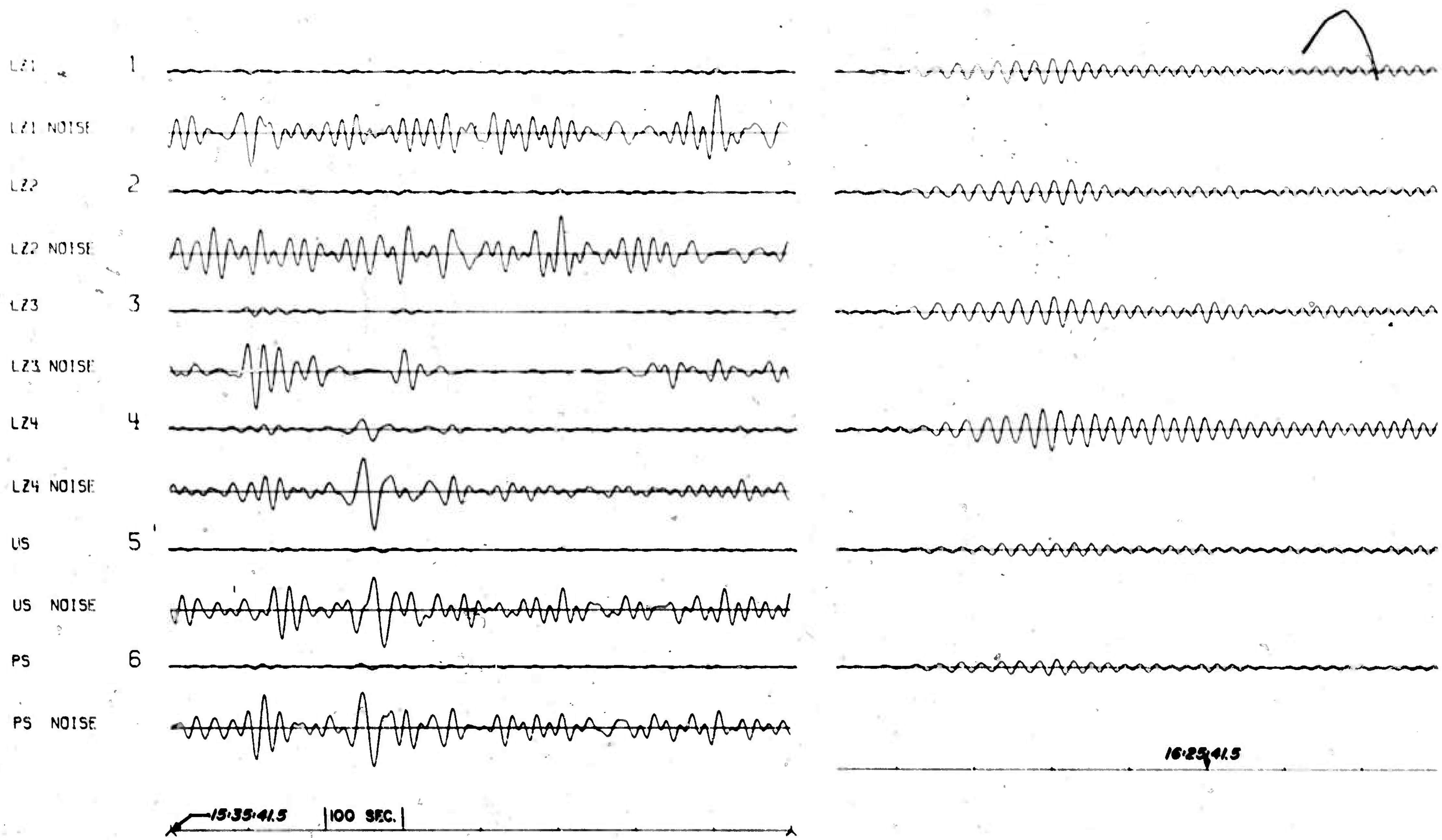

Figure 56. Band pass filtered noise and signal traces with unphased and phased sums for an event in the Volcano Islands recorded at TFO.

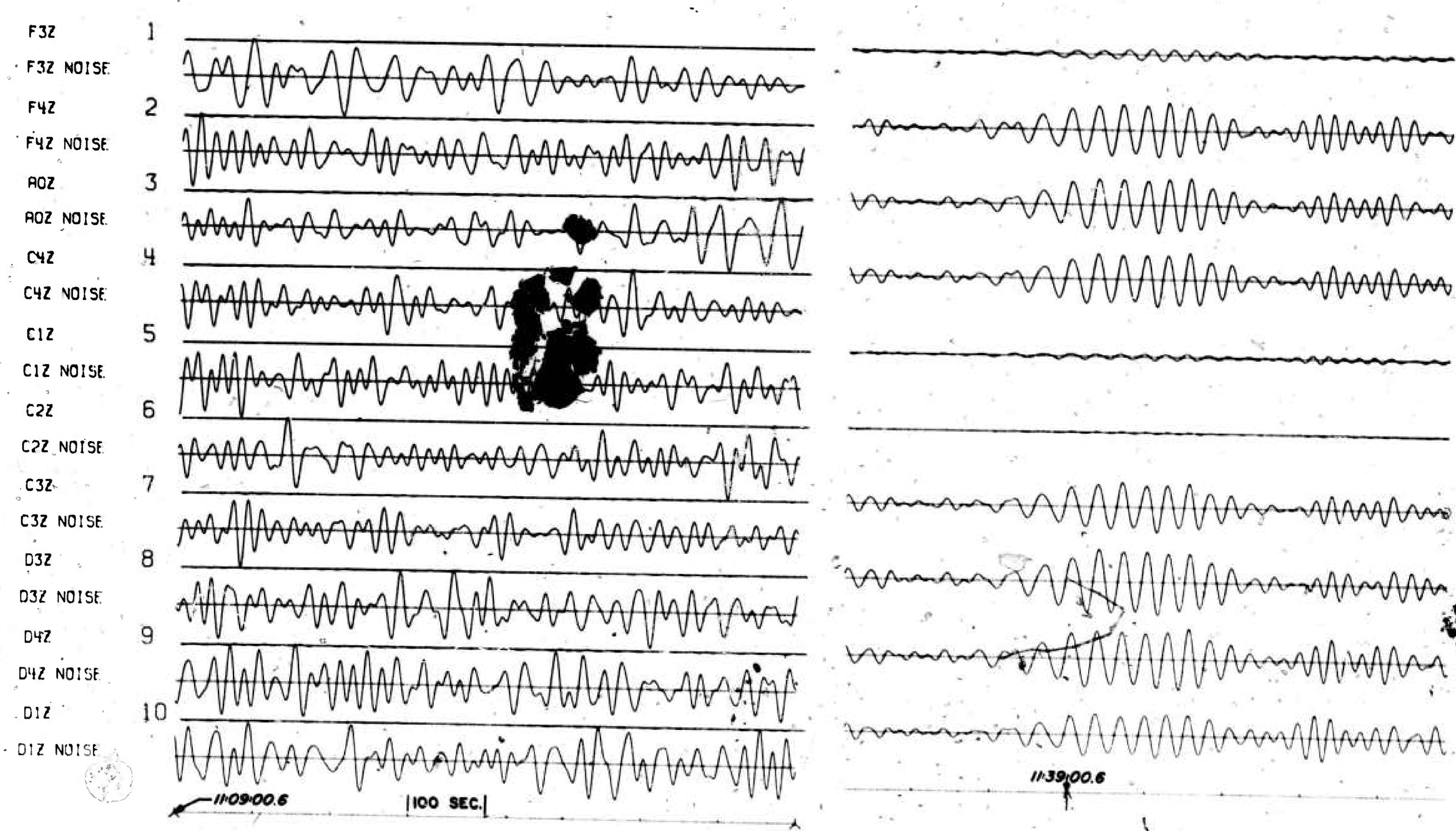

Figure 57a. Band pass filtered noise and signal traces with unphased and phased sums for an event in Costa Rica recorded at LASA.

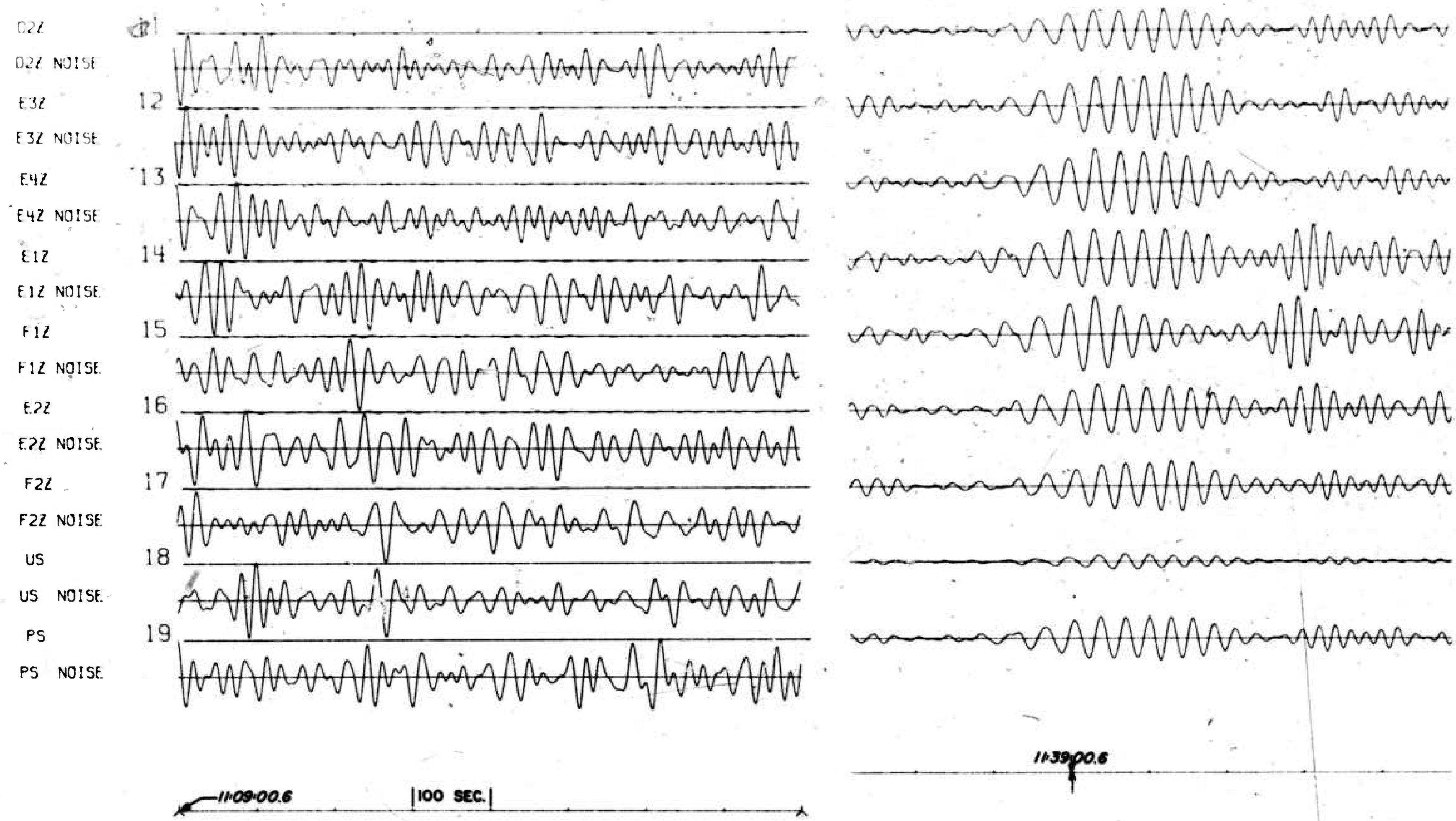

Figure 57b. Band pass filtered noise and signal traces with unphased and phased sums for an event in Costa Rica recorded at LASA.

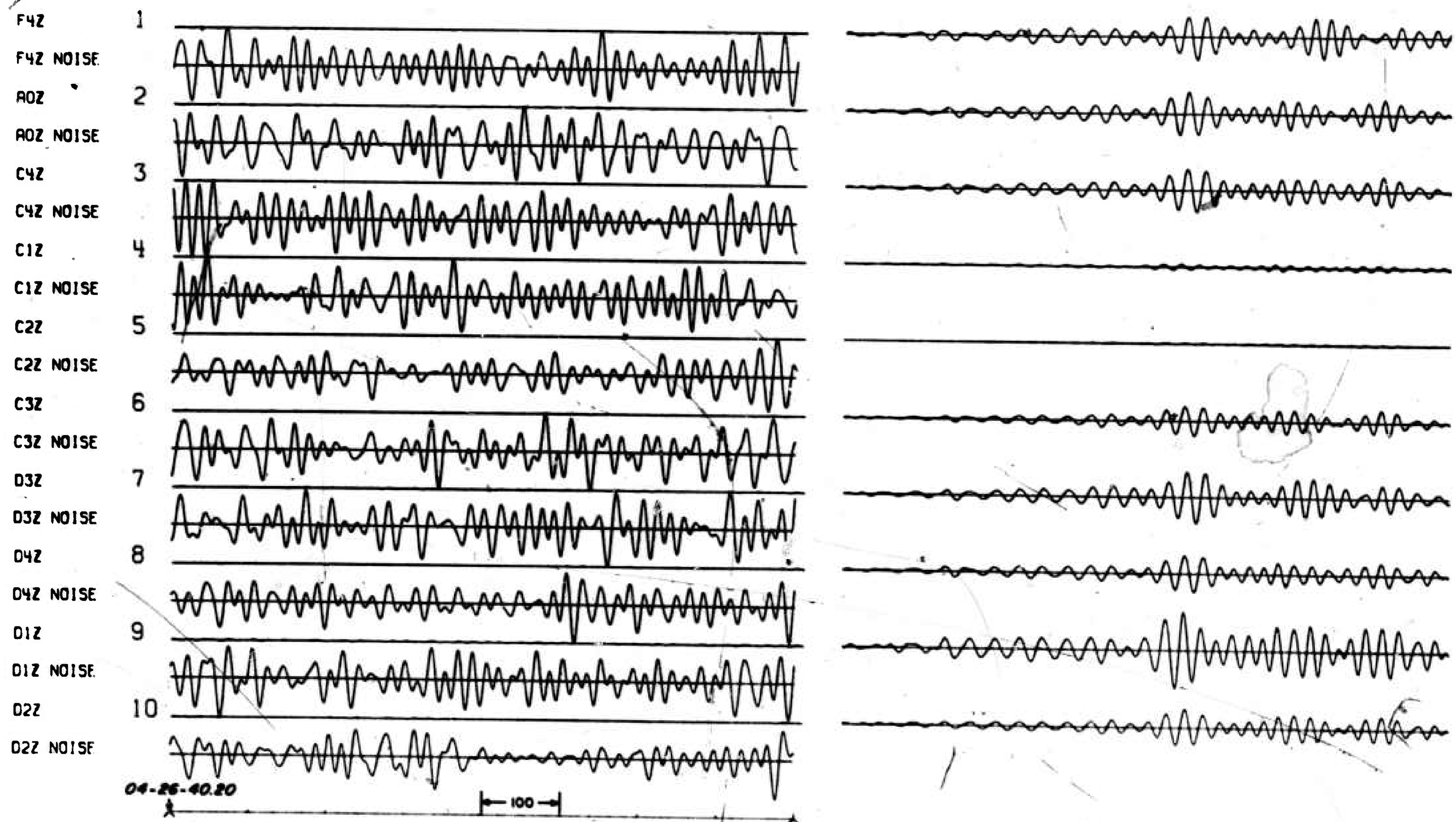

Figure 58a. Band pass filtered noise and signal traces with unphased and phased sums for an event in El Salvador recorded at LASA.

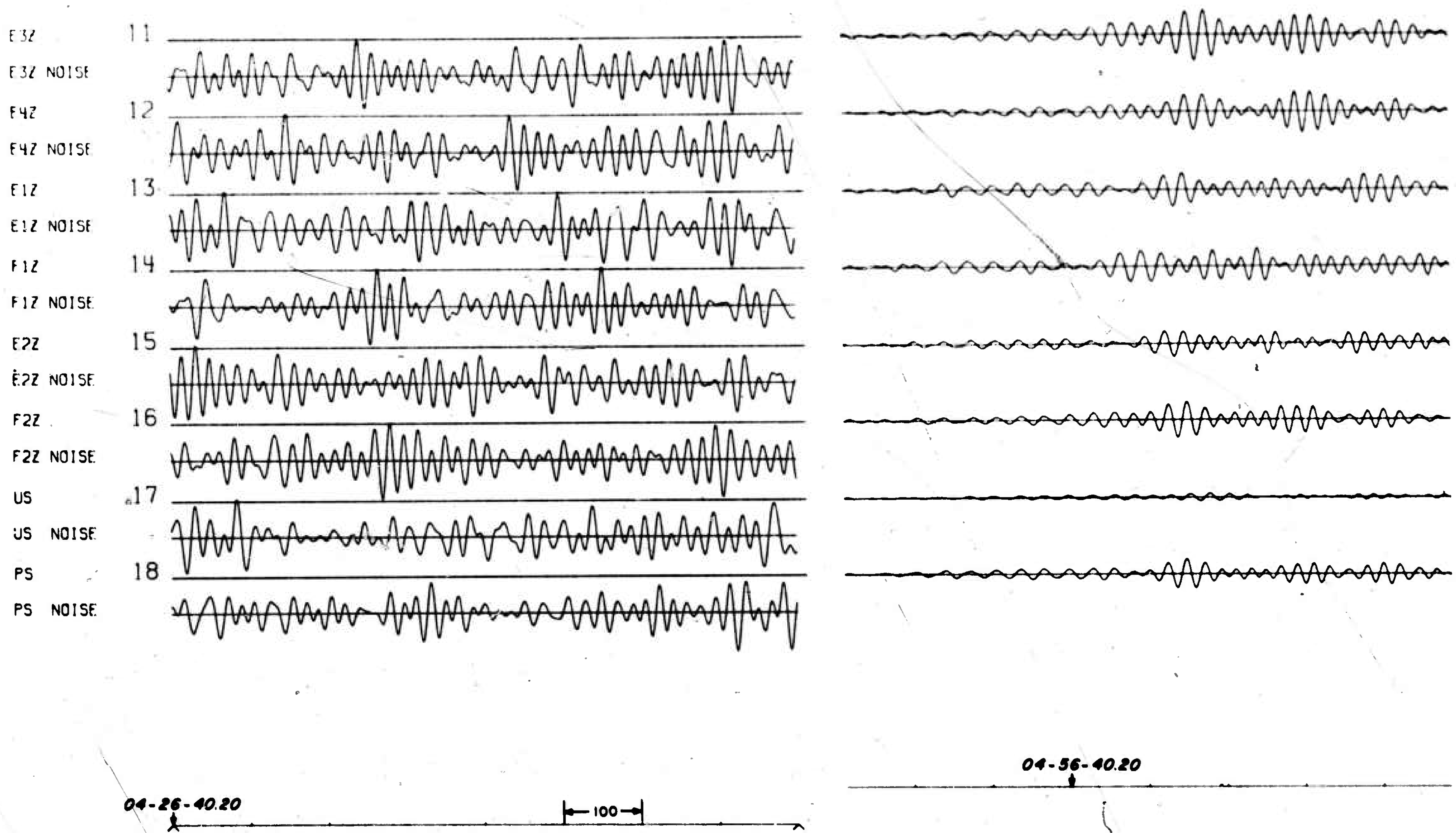

Figure 58b. Band pass filtered noise and signal traces with unphased and phased sums for an event in El Salvador recorded at LASA.

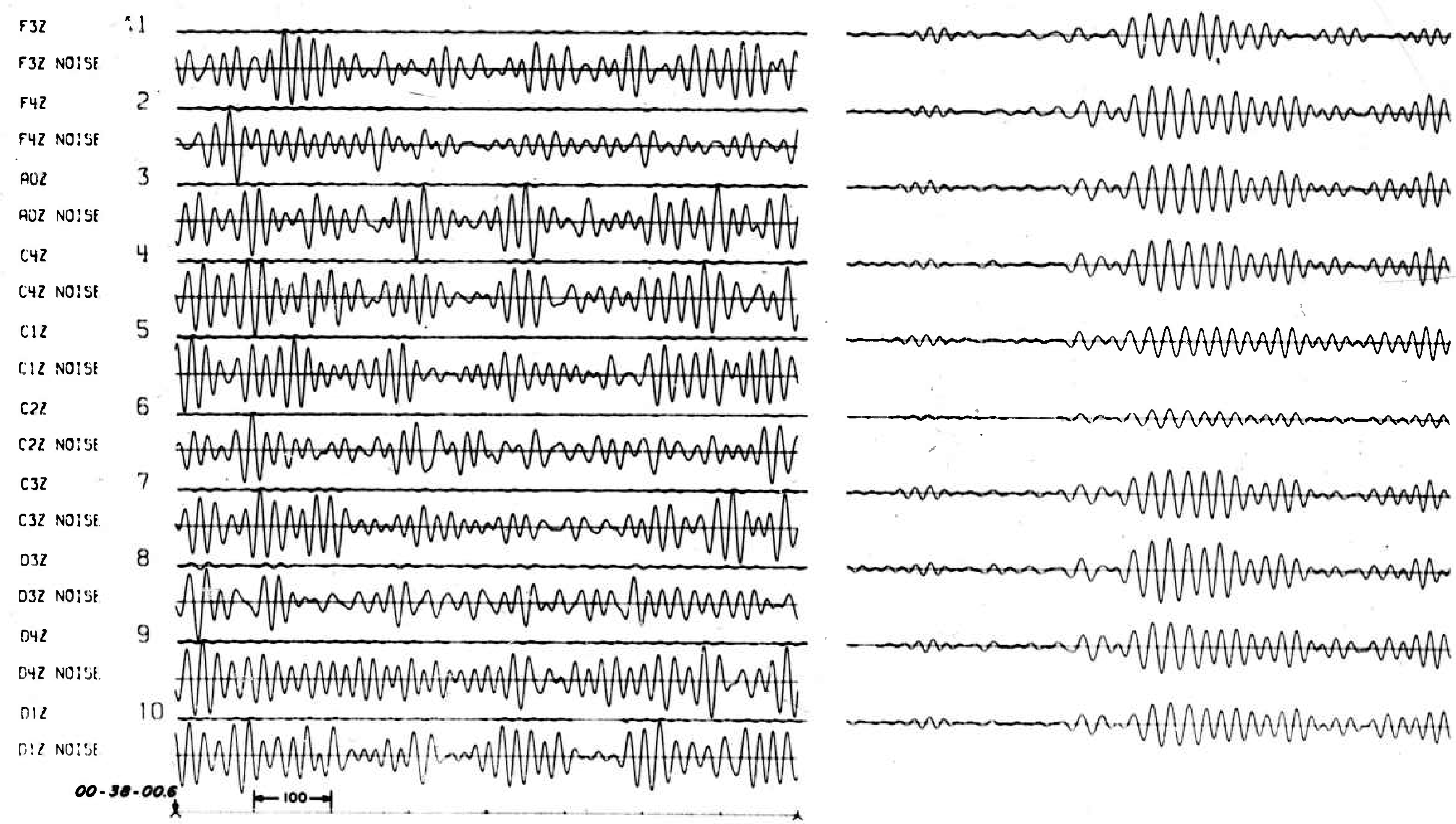

Figure 59a. Band pass filtered noise and signal traces with unphased and phased sums for an event in the Fox Islands recorded at LASA.

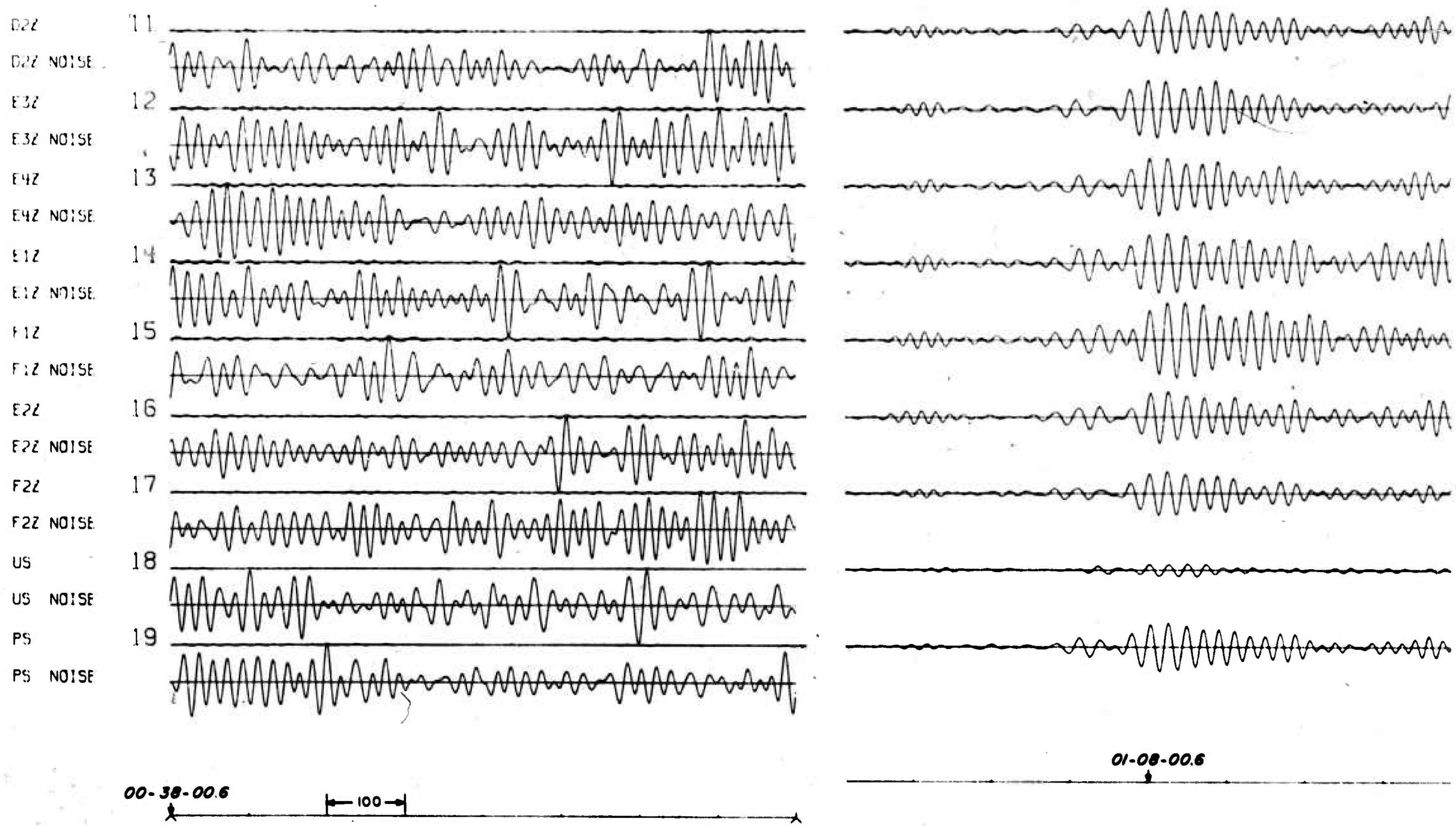

Figure 59b. Band pass filtered noise and signal traces with unphased and phased sums for an event in the Fox Islands recorded at LASA.

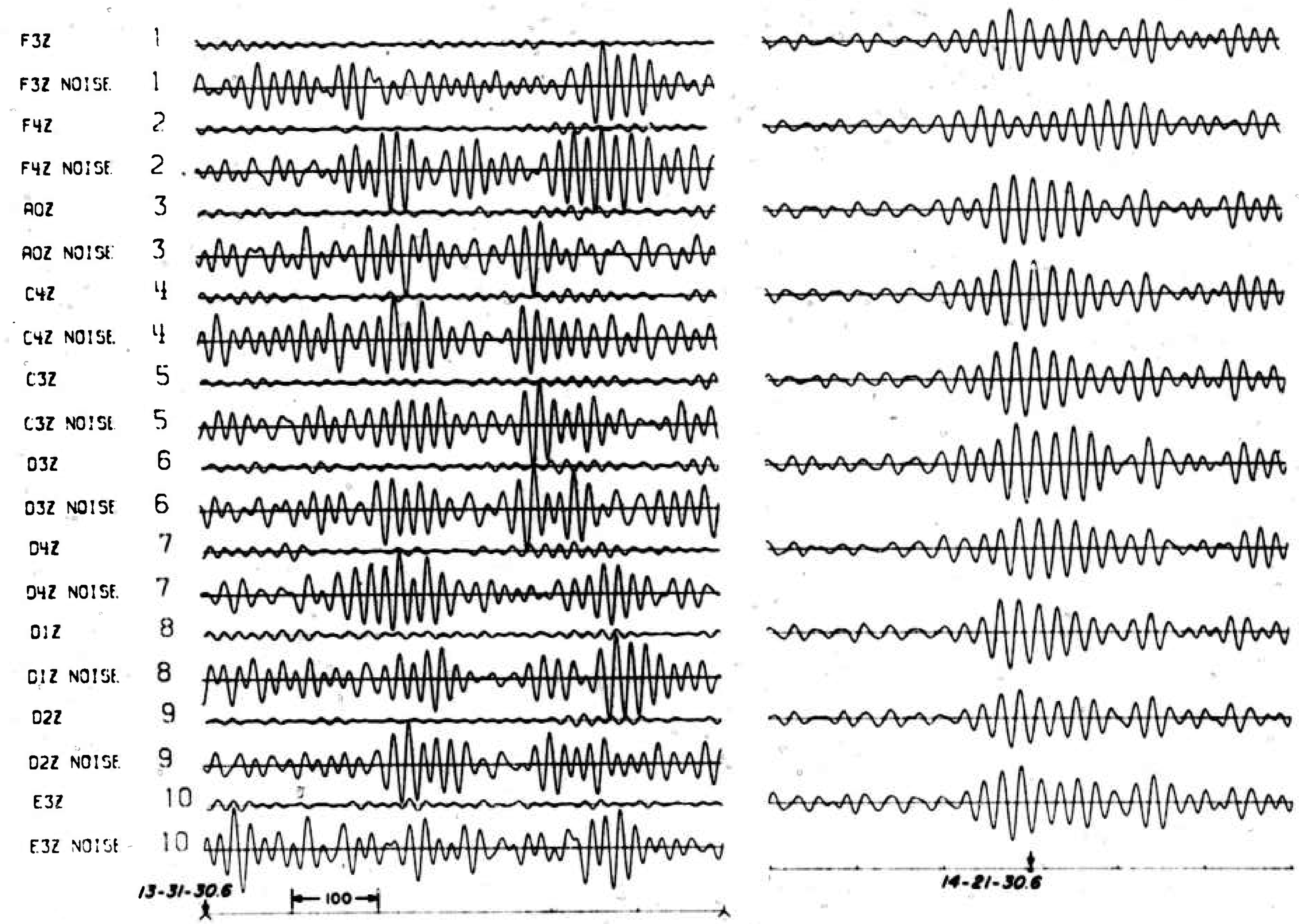

Figure 60a. Band pass filtered noise and signal traces with unphased and phased sums for an event in the Border Region of Greece - Albania recorded at LASA.

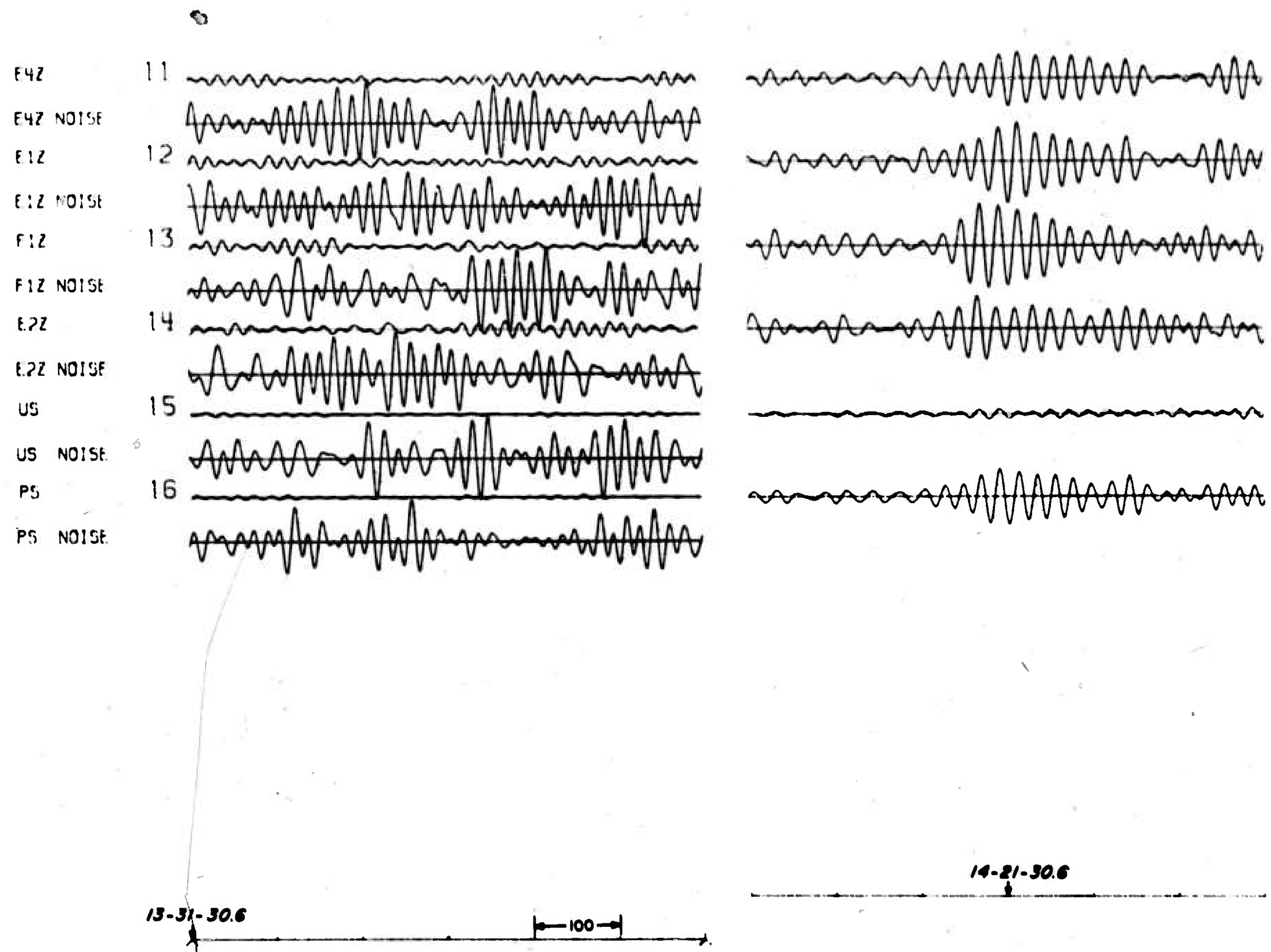

Figure 60b. Band pass filtered noise and signal traces with unphased and phased sums for an event in the Border Region of Greece - Albania recorded at LASA.

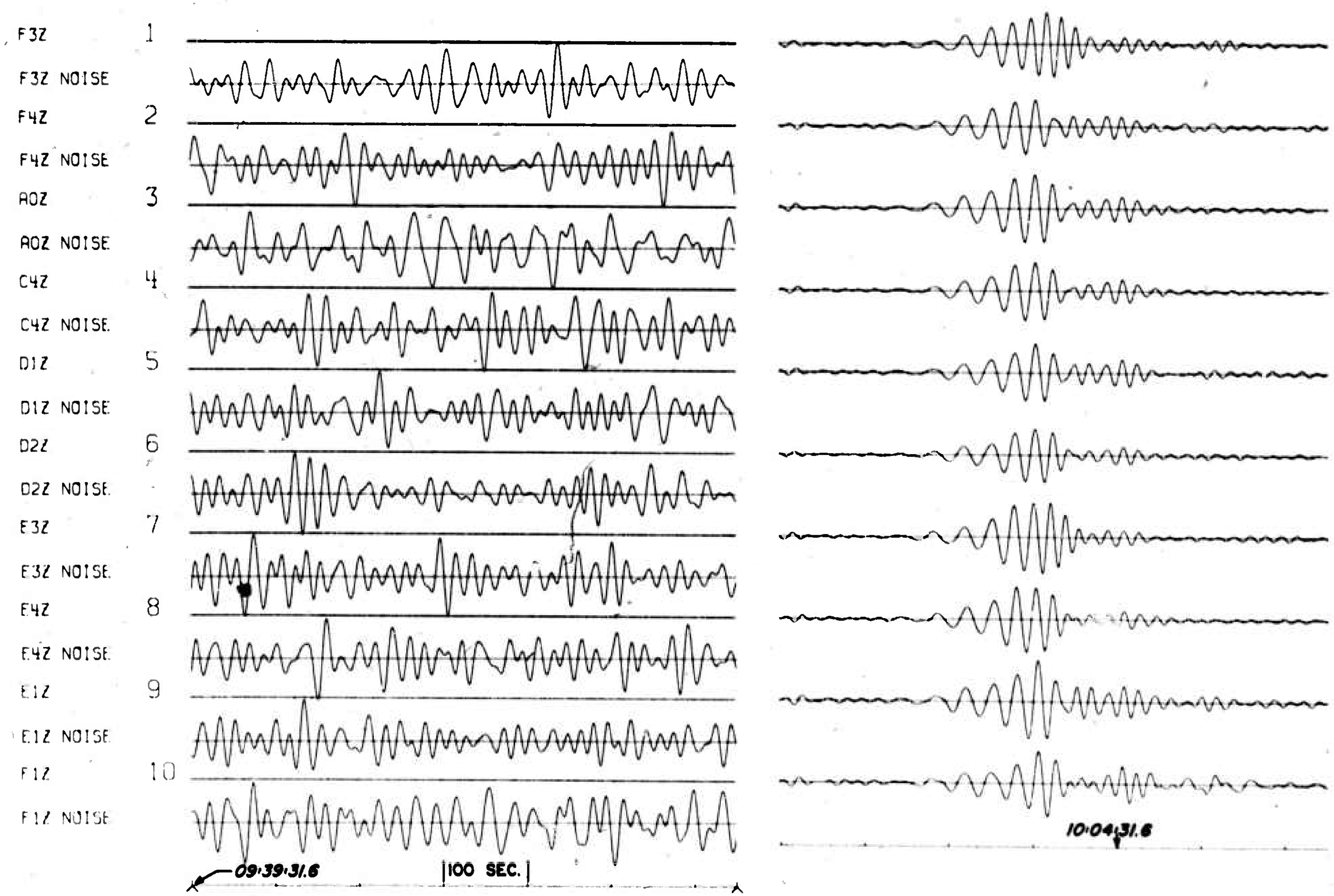

Figure 61a. Band pass filtered noise and signal traces with unphased and phased sums for an event in the Gulf of Alaska recorded at LASA.

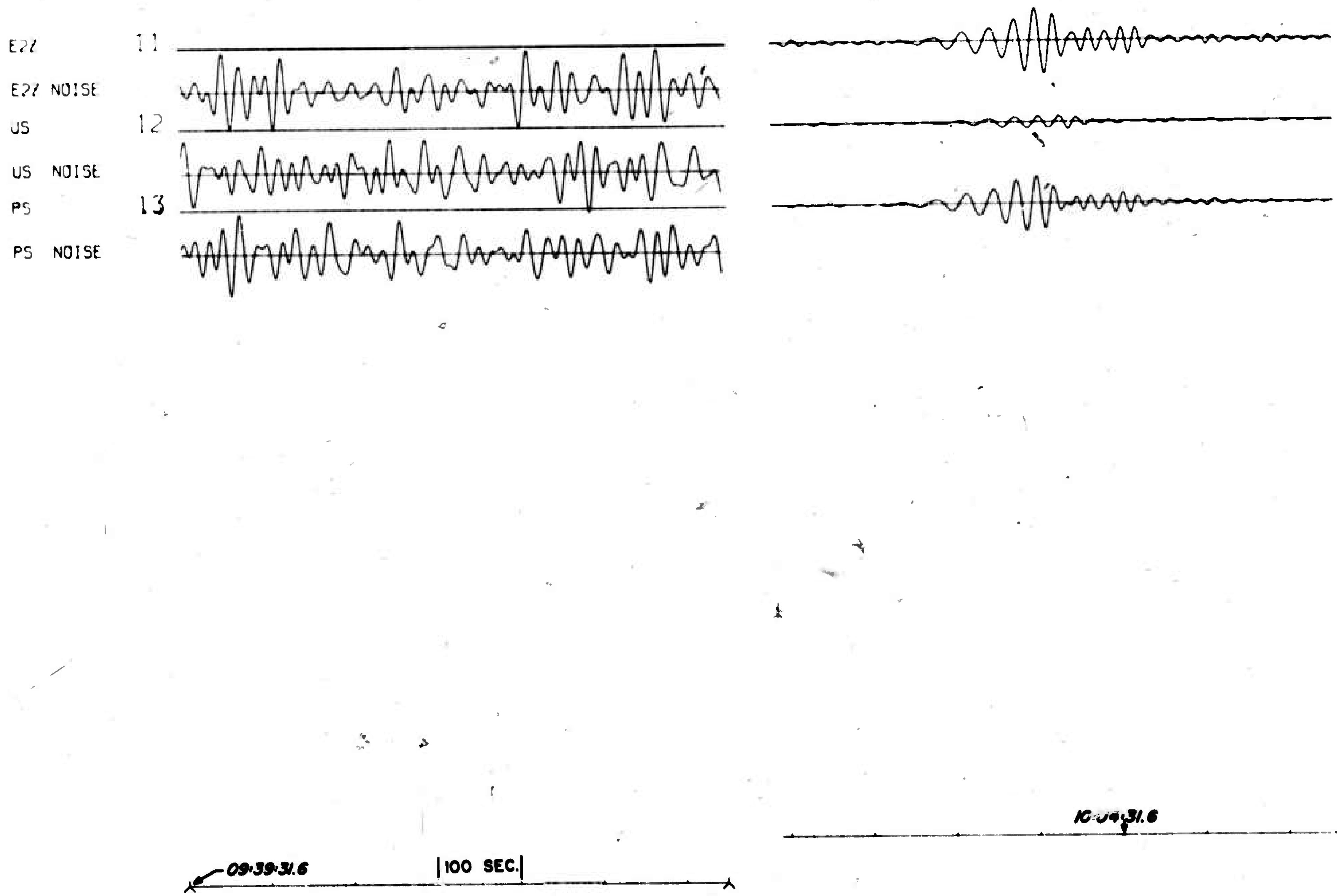

Figure 61b. Band pass filtered noise and signal traces with unphased and phased sums for an event in the Gulf of Alaska recorded at LASA.

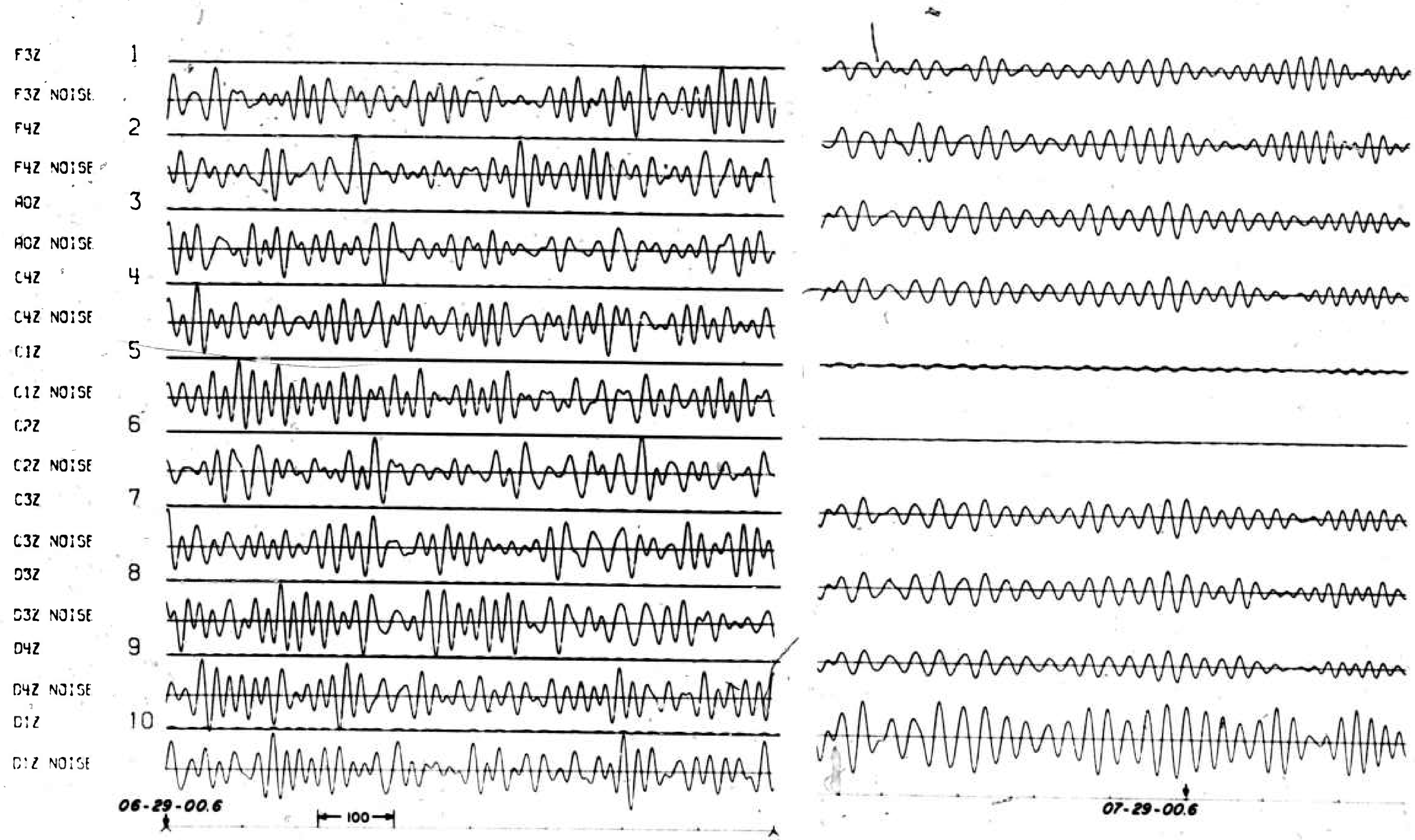

Figure 62a. Band pass filtered noise and signal traces with unphased and phased sums for an event in Hindu Kush recorded at LASA.

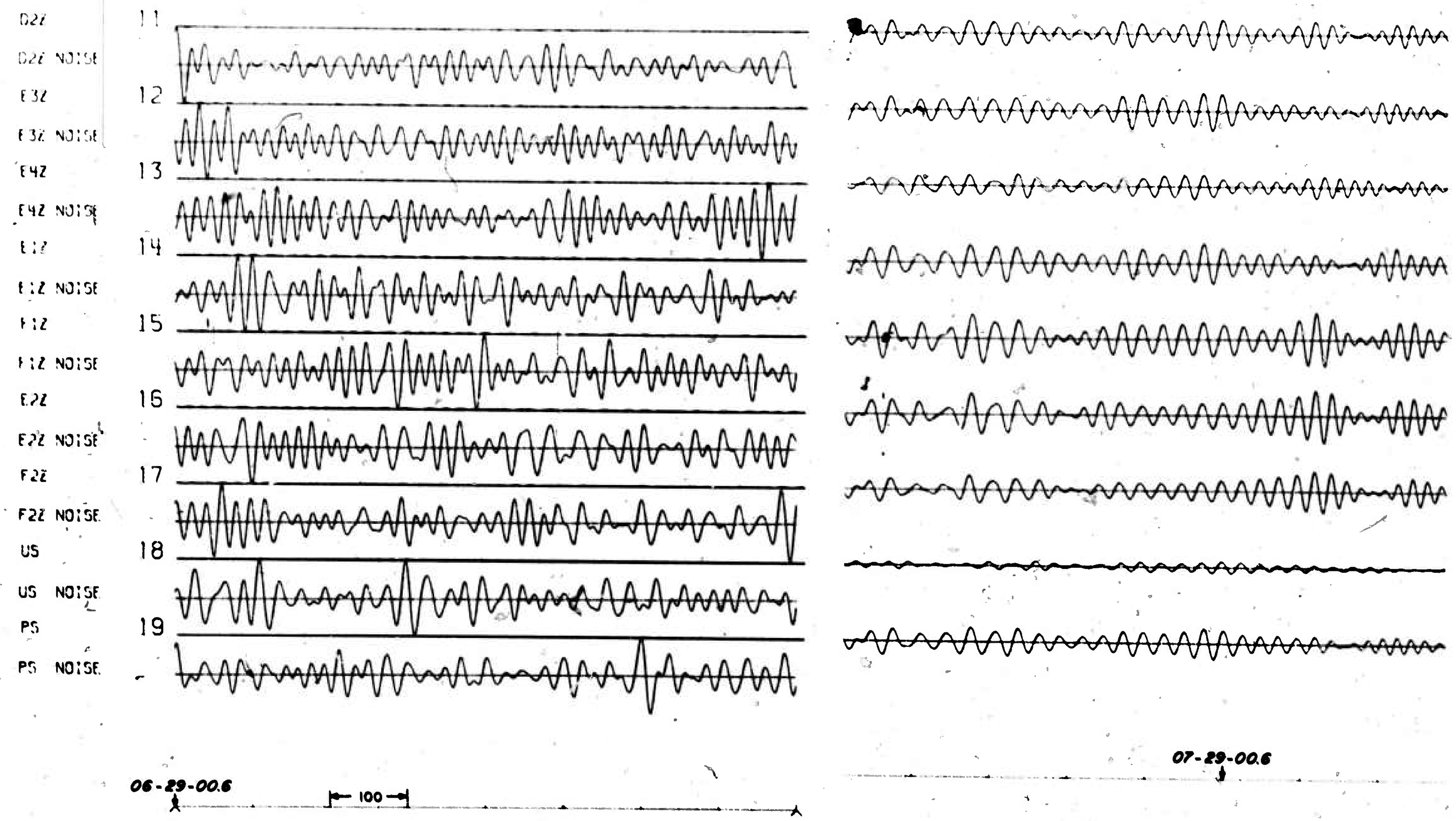

Figure 62b. Band pass filtered noise and signal traces with unphased and phased sums for an event in Hindu Kush recorded at LASA.

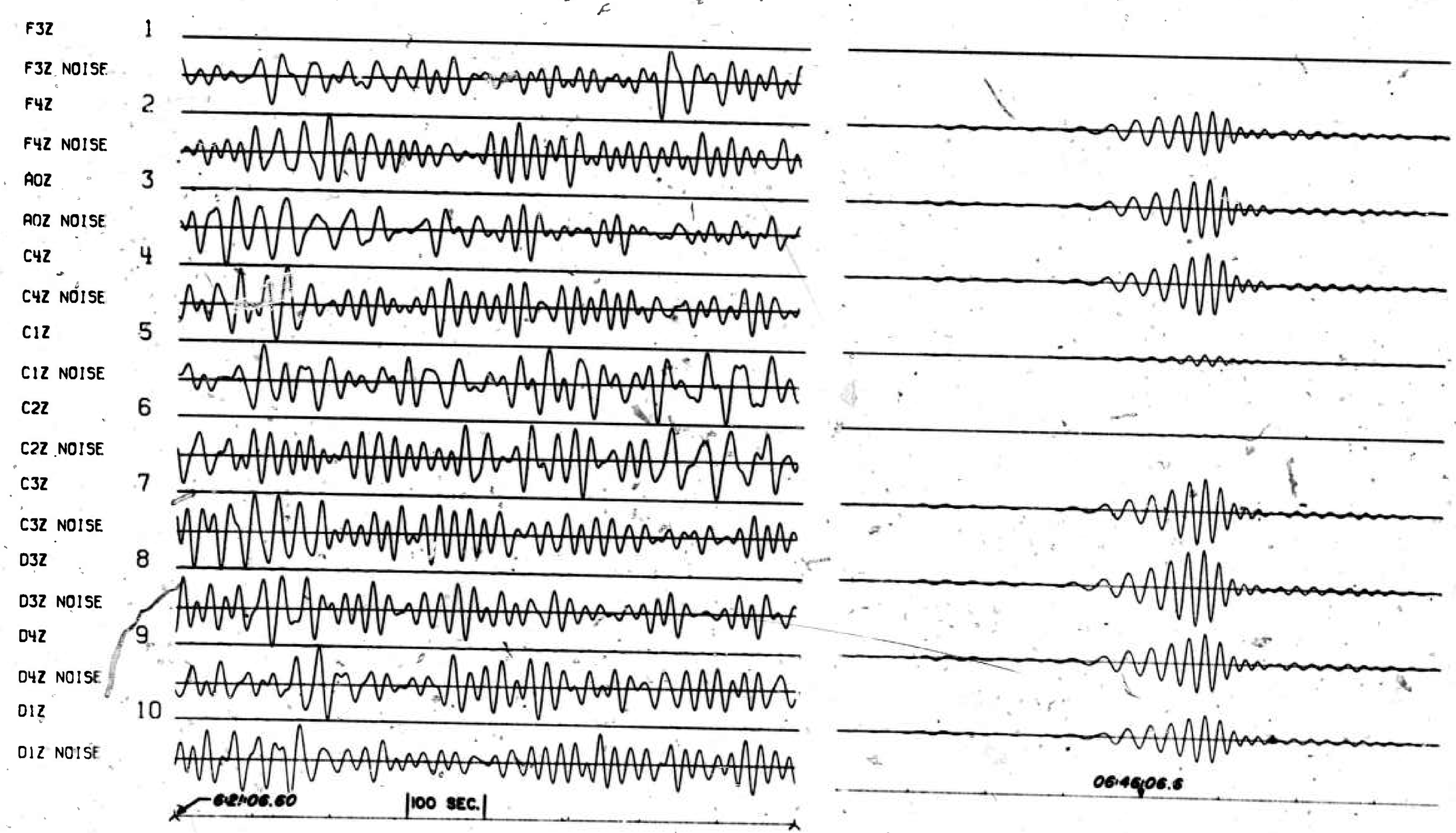

Figure 63a. Band pass filtered noise and signal traces with unphased and phased sums for an event in the Kodiac Islands recorded at LASA.

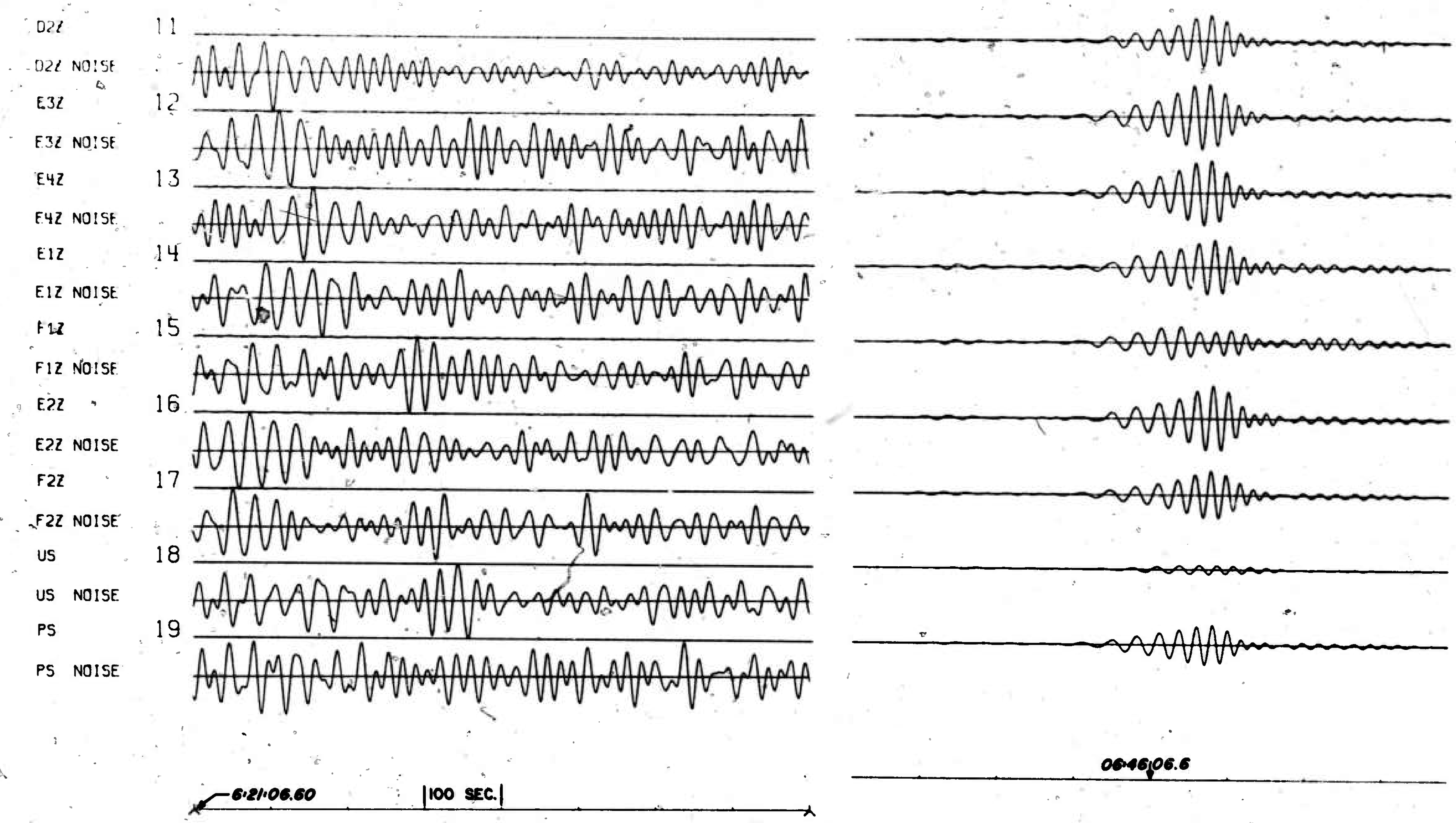

Figure 63b. Band pass filtered noise and signal traces with unphased and phased sums for an event in the Kodiac Islands recorded at LASA.

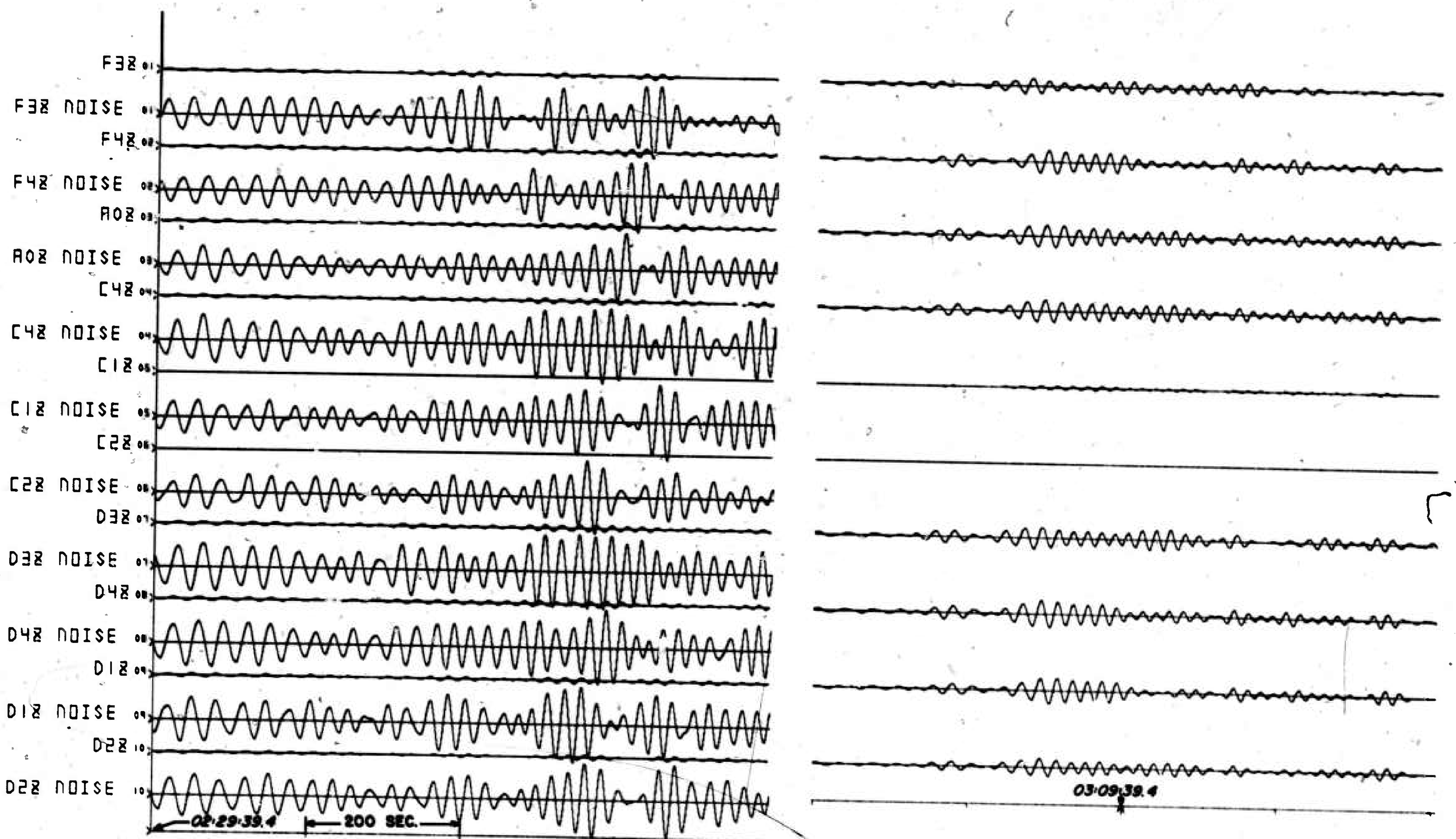

Figure 64a. Band pass filtered noise and signal traces with unphased and phased sums for an event in the Kurile Islands recorded at LASA.

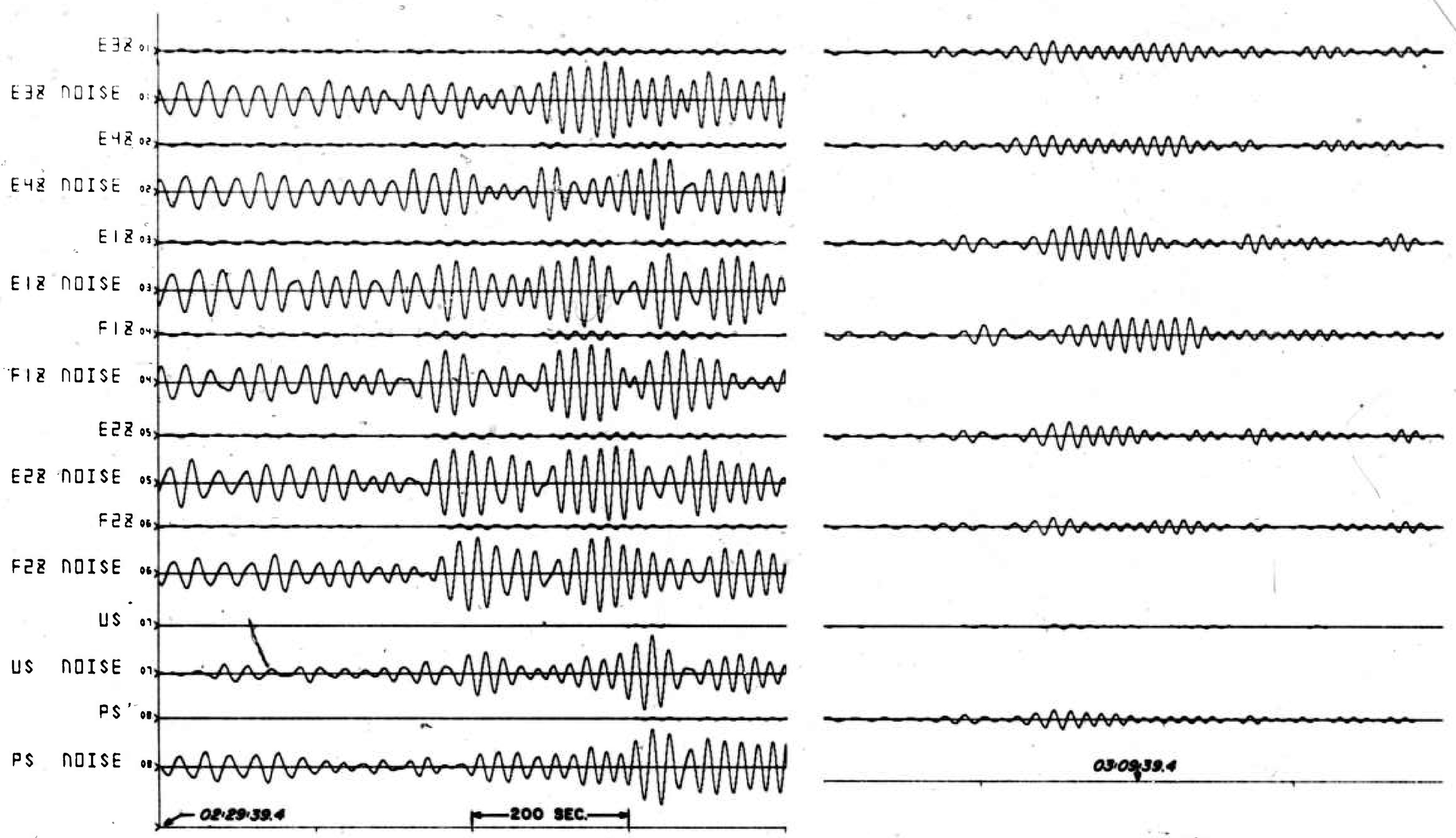

Figure 64b. Band pass filtered noise and signal traces with unphased and phased sums for an event in the Kurile Islands recorded at LASA.

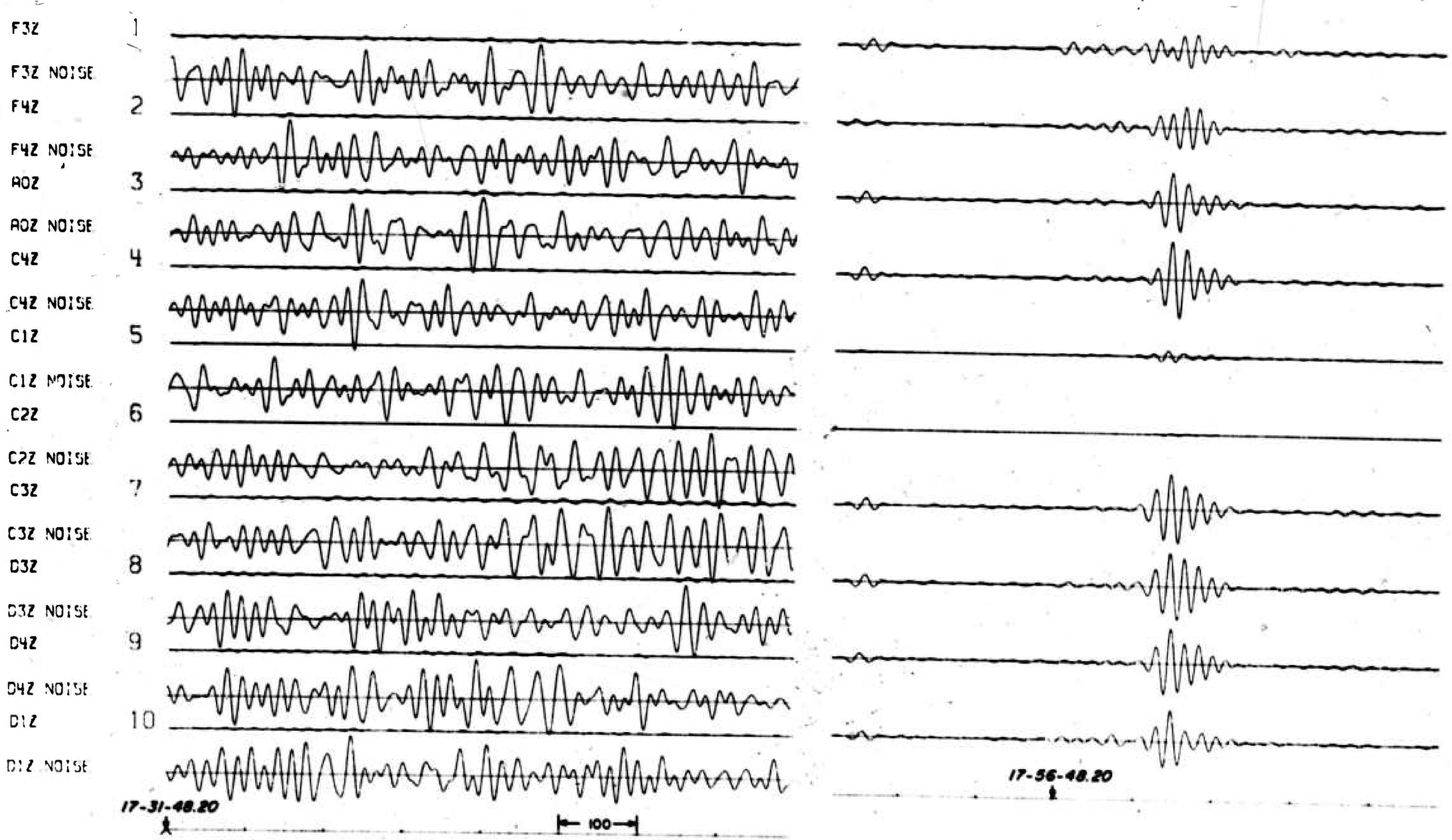

Figure 65a. Band pass filtered noise and signal traces with unphased and phased sums for an event in Mexico recorded at LASA.

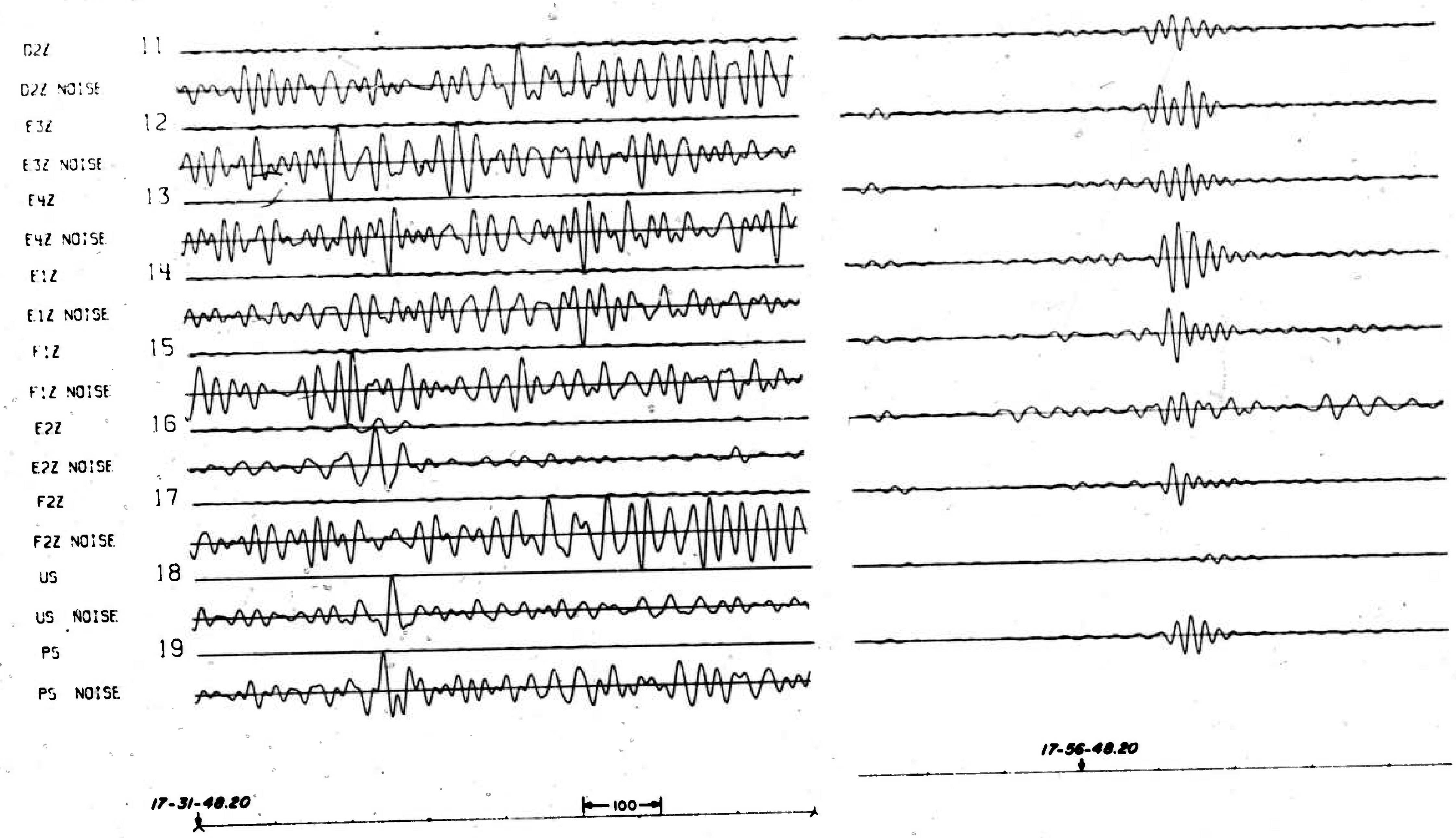

Figure 65b. Band pass filtered noise and signal traces with unphased and phased sums for an event in Mexico recorded at LASA.

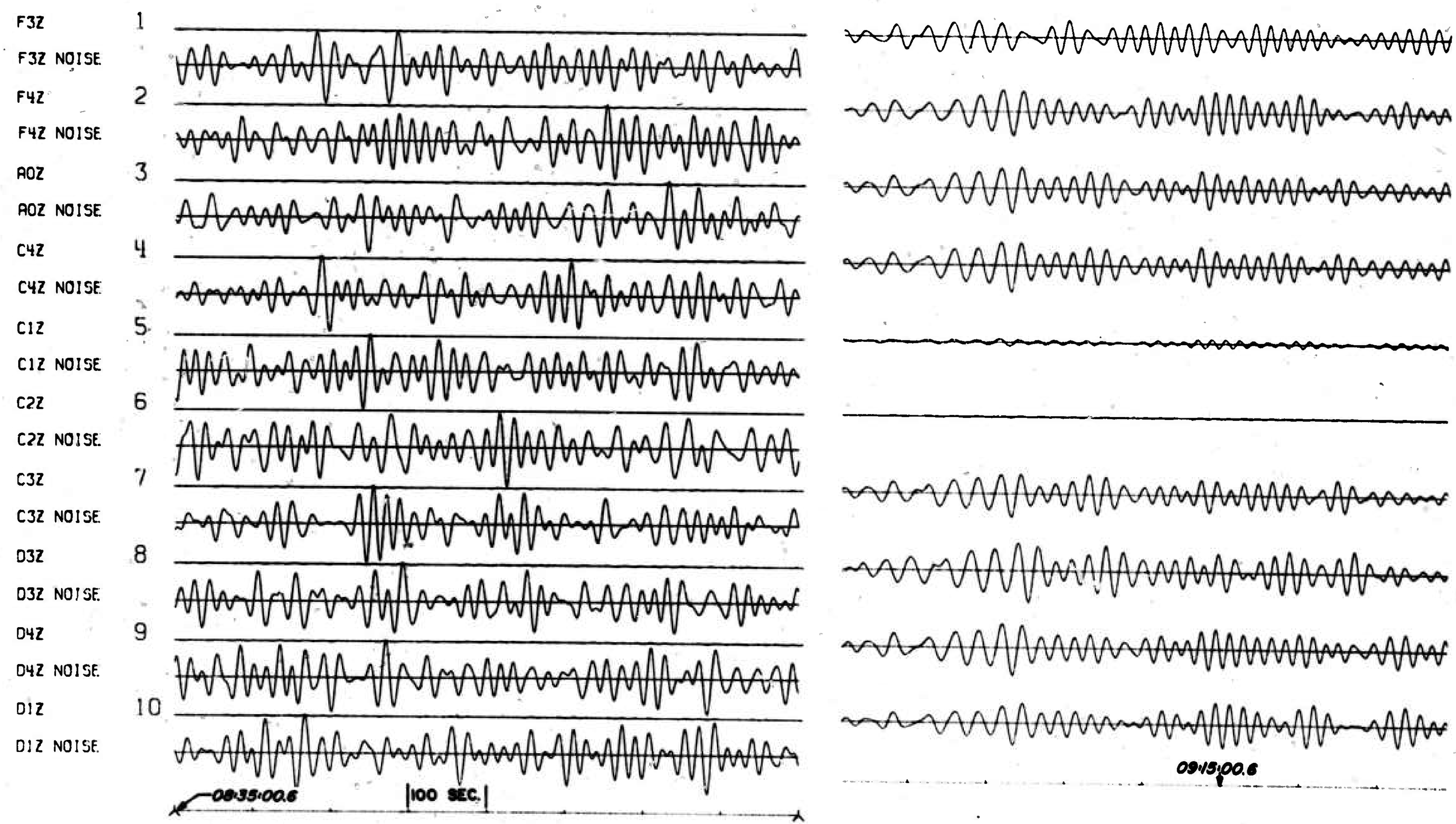

Figure 66a. Band pass filtered noise and signal traces with unphased and phased sums for an event in the Near Islands recorded at LASA.

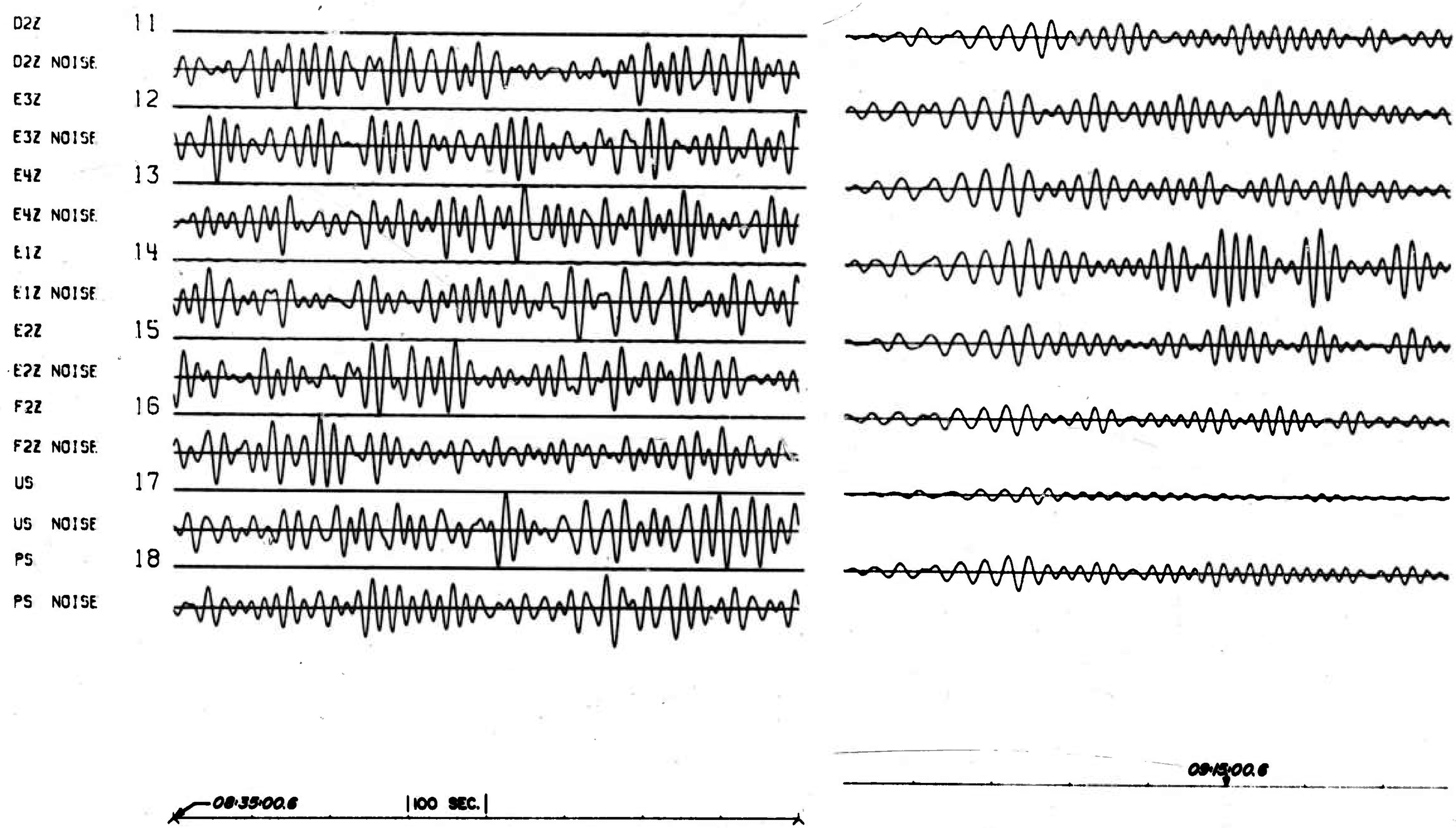

Figure 66b. Band pass filtered noise and signal traces with unphased and phased sums for an event in the Near Islands recorded at LASA.

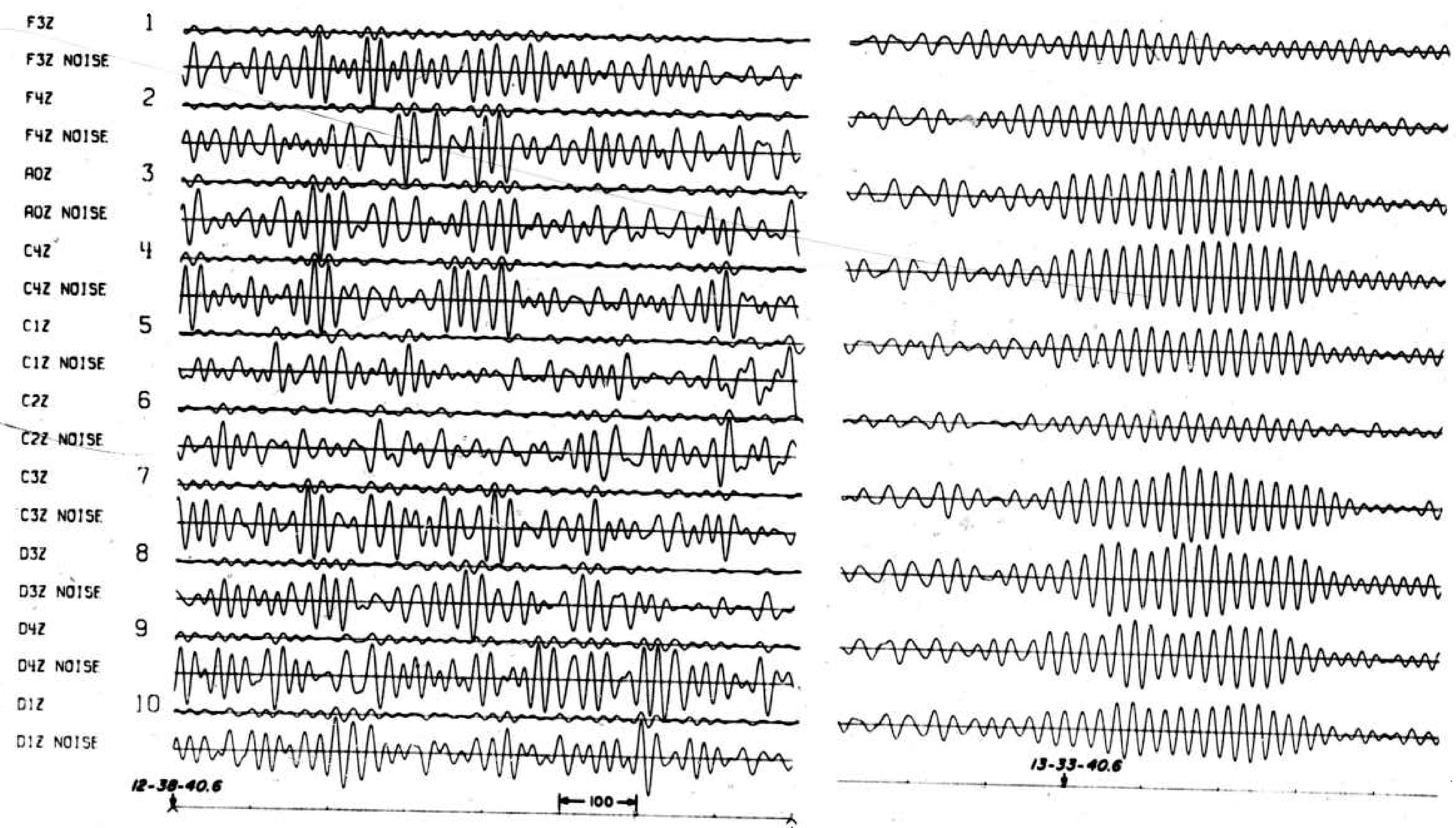

Figure 67a. Band pass filtered noise and signal traces with unphased and phased sums for an event in East New Guinea recorded at LASA.

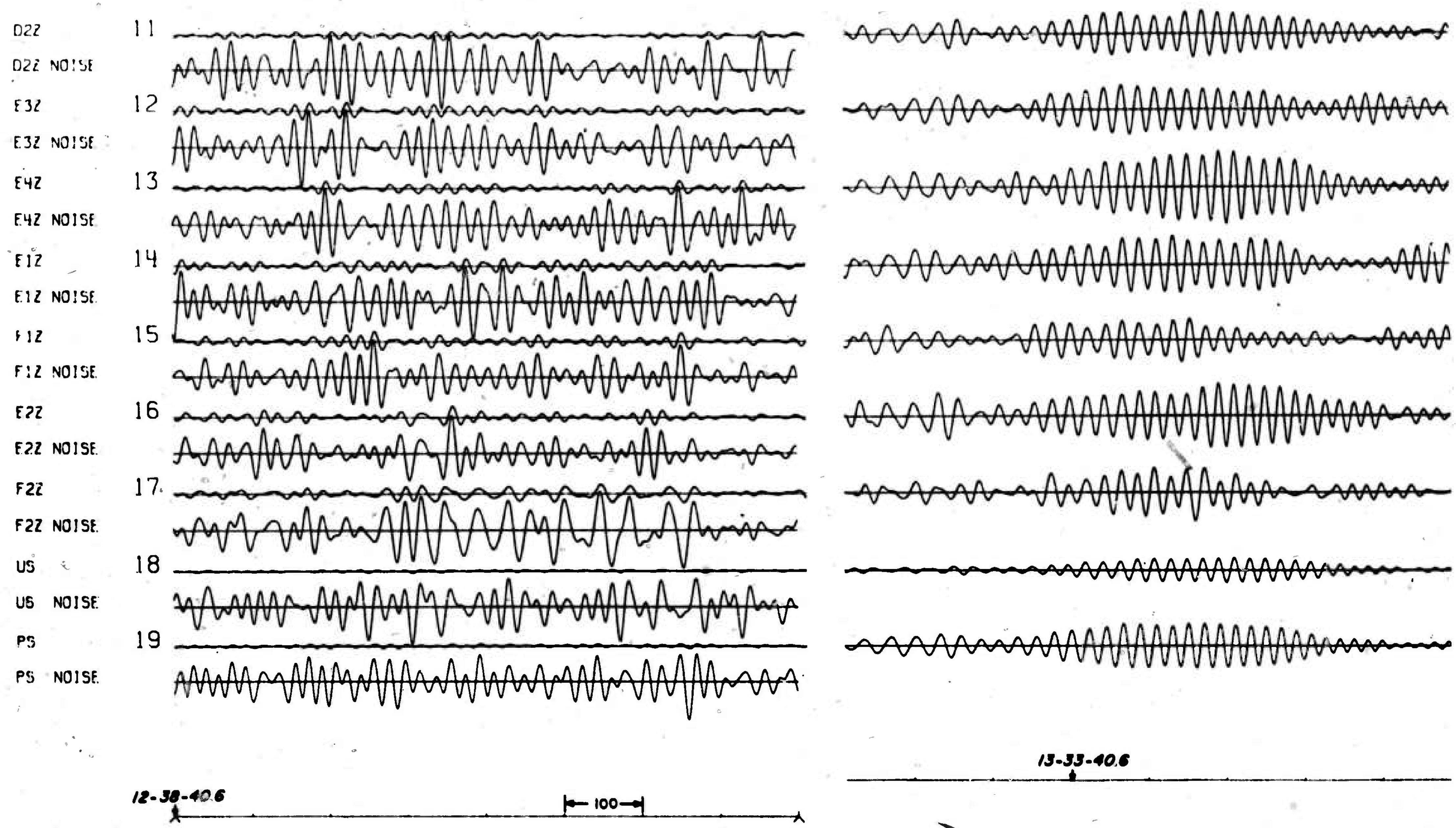

Figure 67b. Band pass filtered noise and signal traces with unphased and phased sums for an event in East New Guinea recorded at LASA.

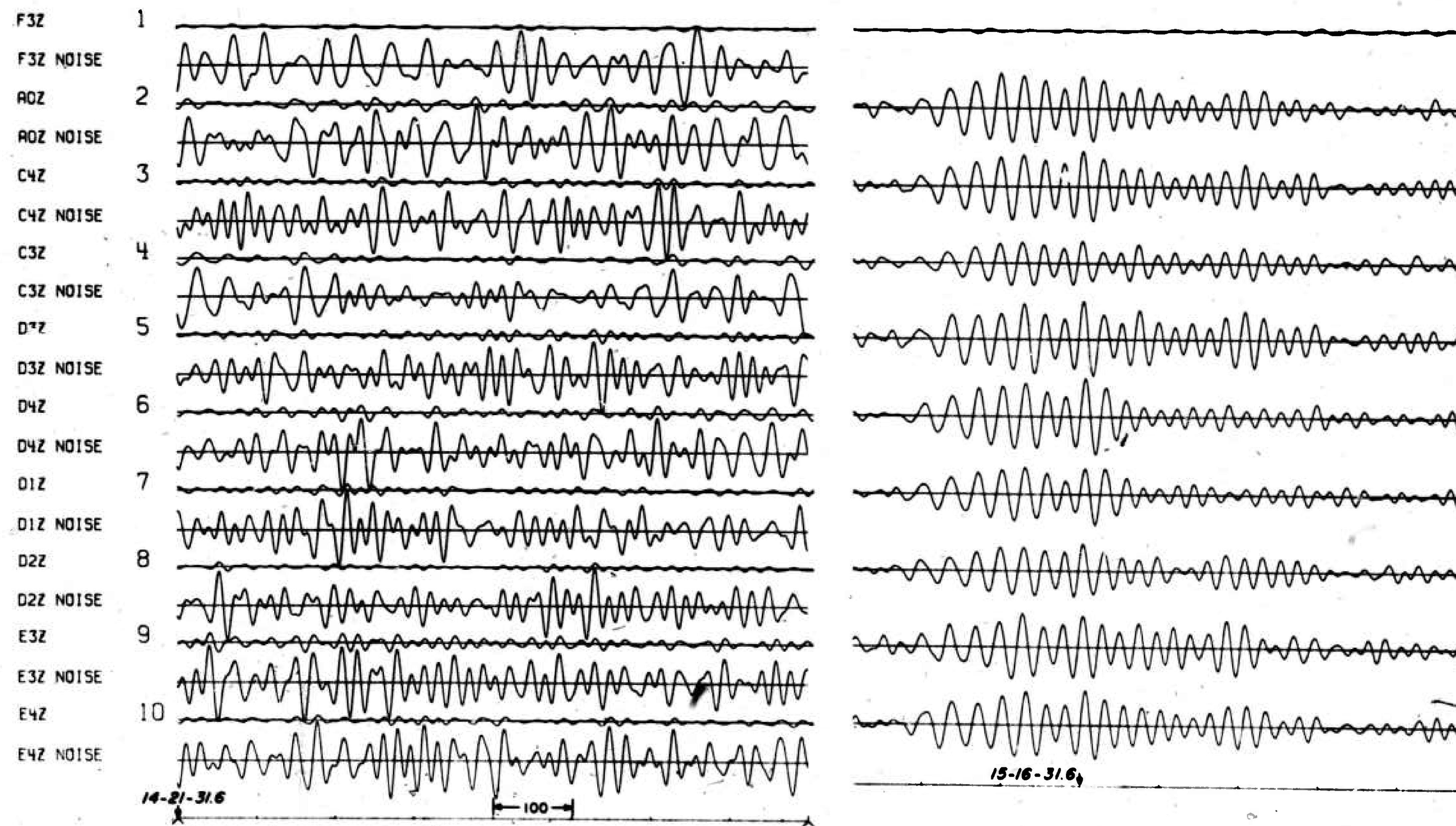

Figure 68a. Band pass filtered noise and signal traces with unphased and phased sums for an event in the Philippine Islands recorded at LASA.

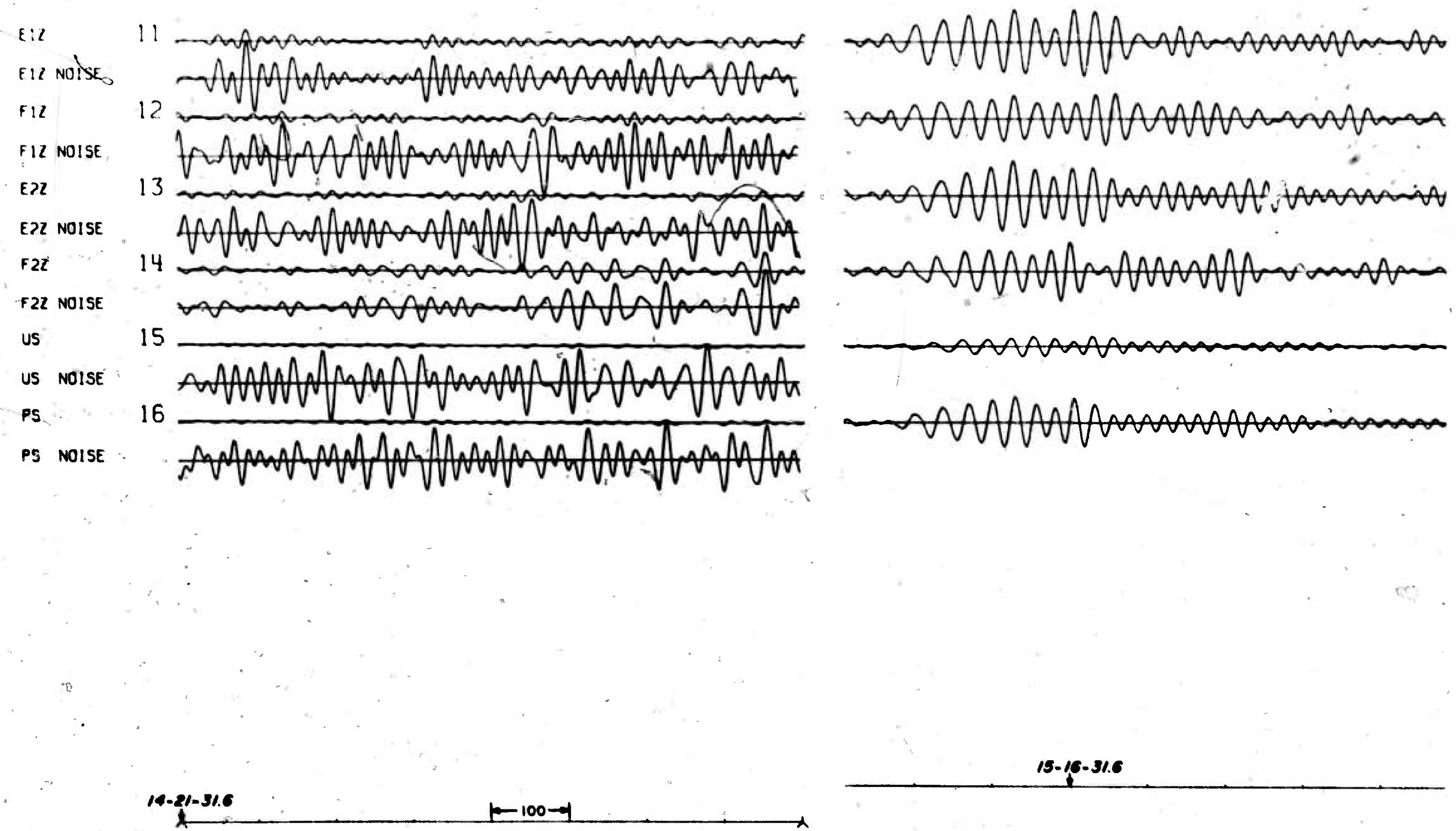

Figure 68b. Band pass filtered noise and signal traces with unphased and phased sums for an event in the Philippine Islands recorded at LASA.

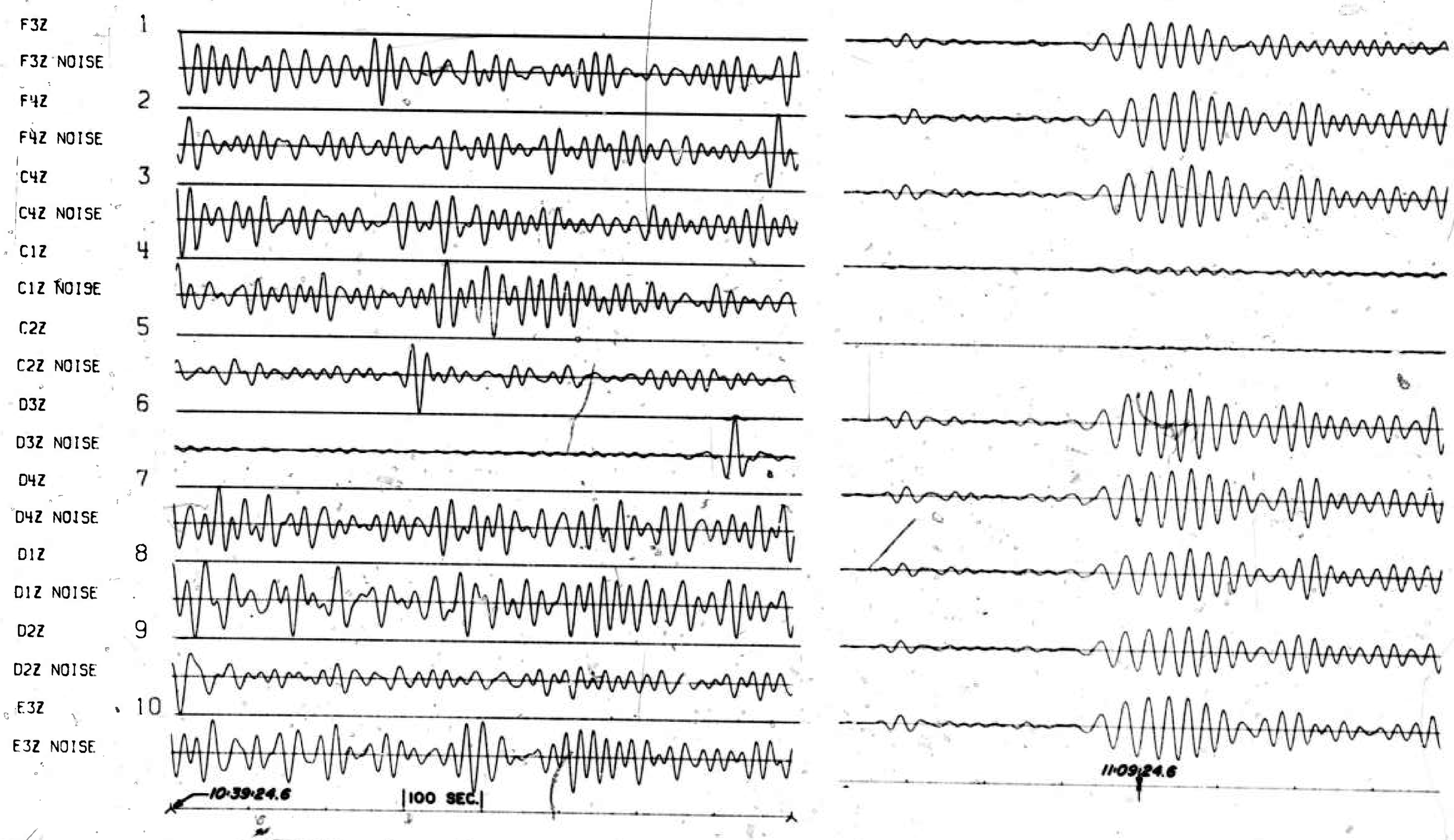

Figure 69a. Band pass filtered noise and signal traces with unphased and phased sums for an event in the Rat Islands recorded at LASA.

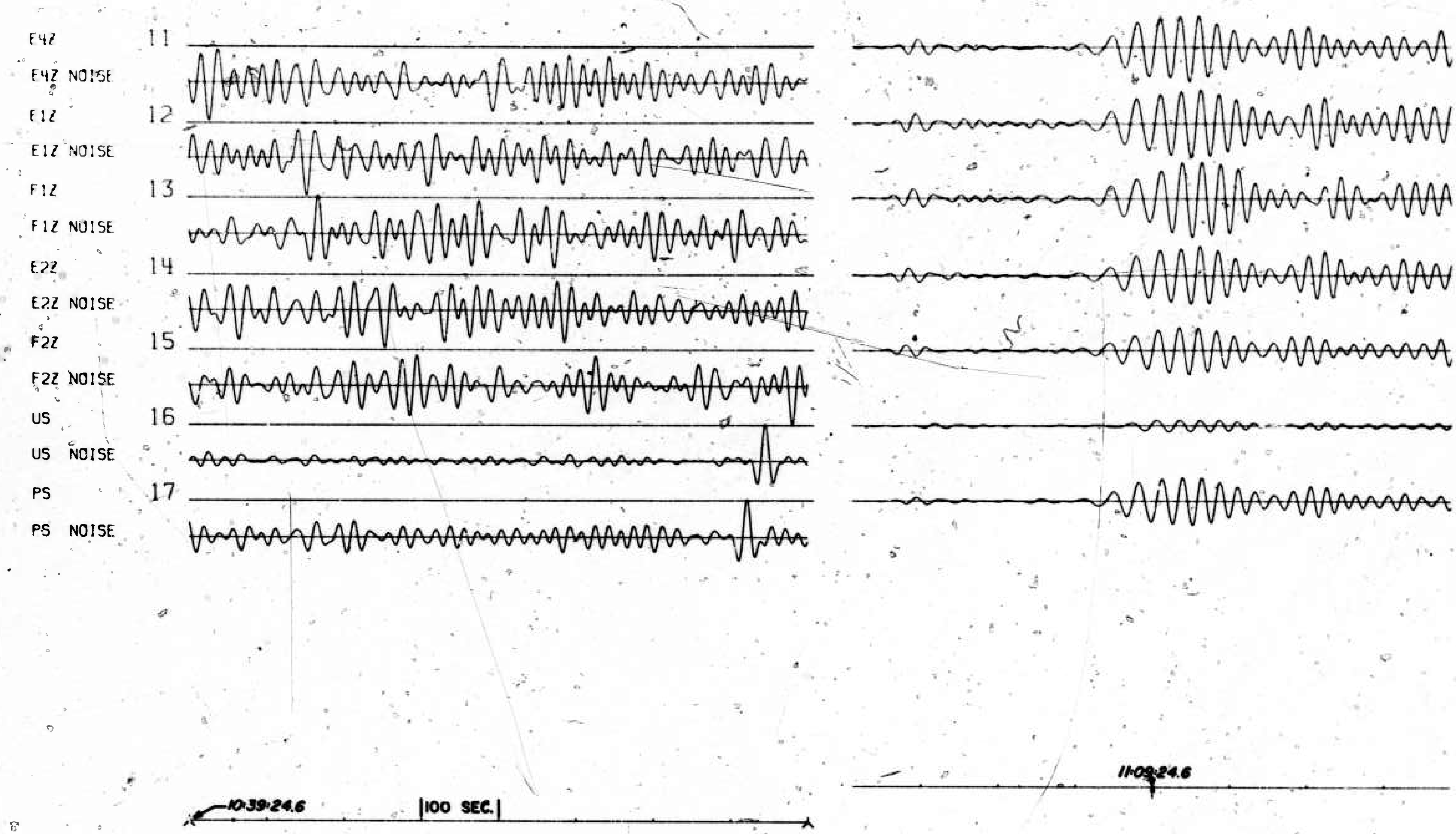

Figure 69b. Band pass filtered noise and signal traces with unphased and phased sums for an event in the Rat Islands recorded at LASA.

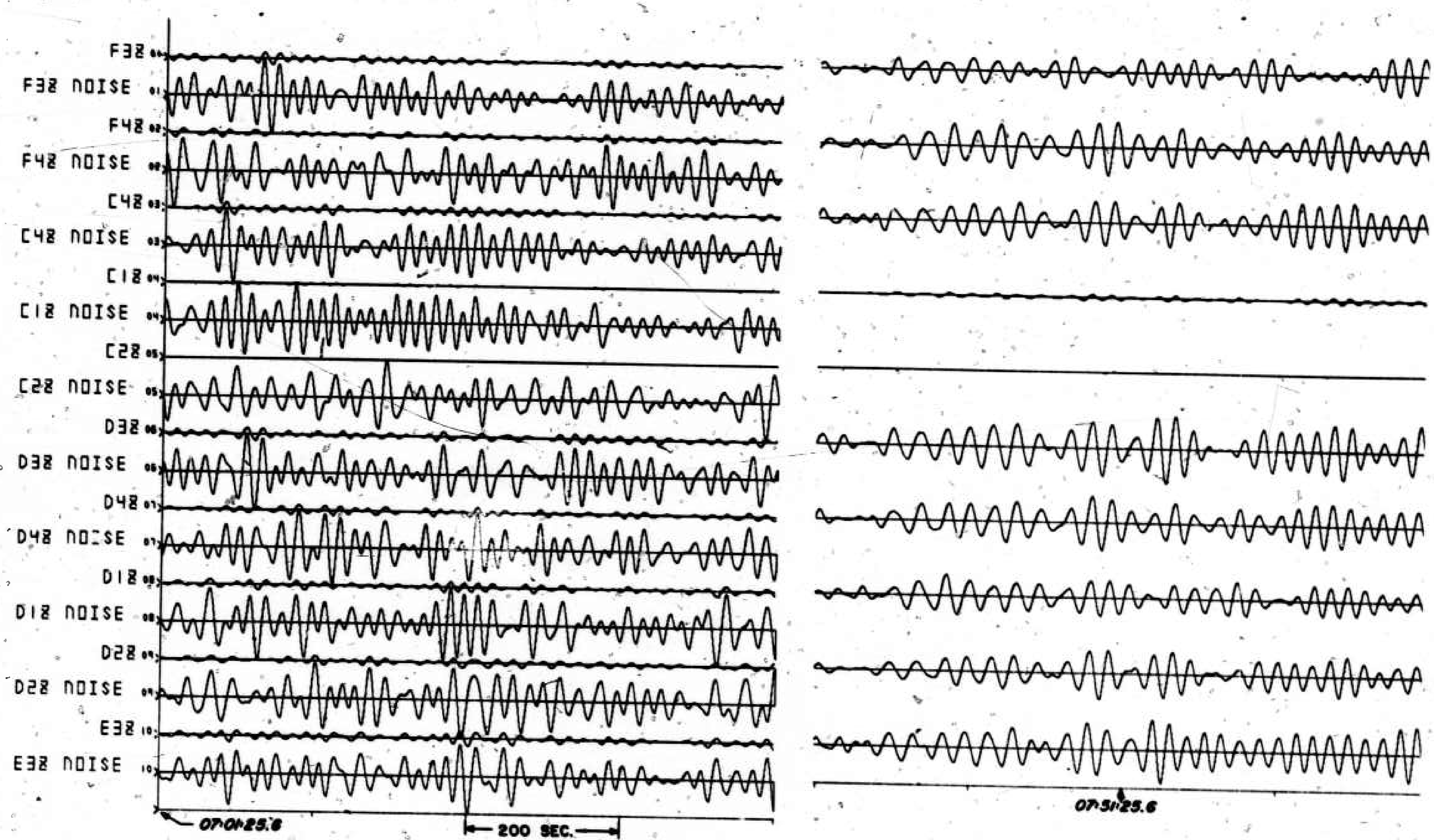

Figure 70a. Band pass filtered noise and signal traces with unphased and phased sums for an event in the Ryukyu Islands recorded at LASA.

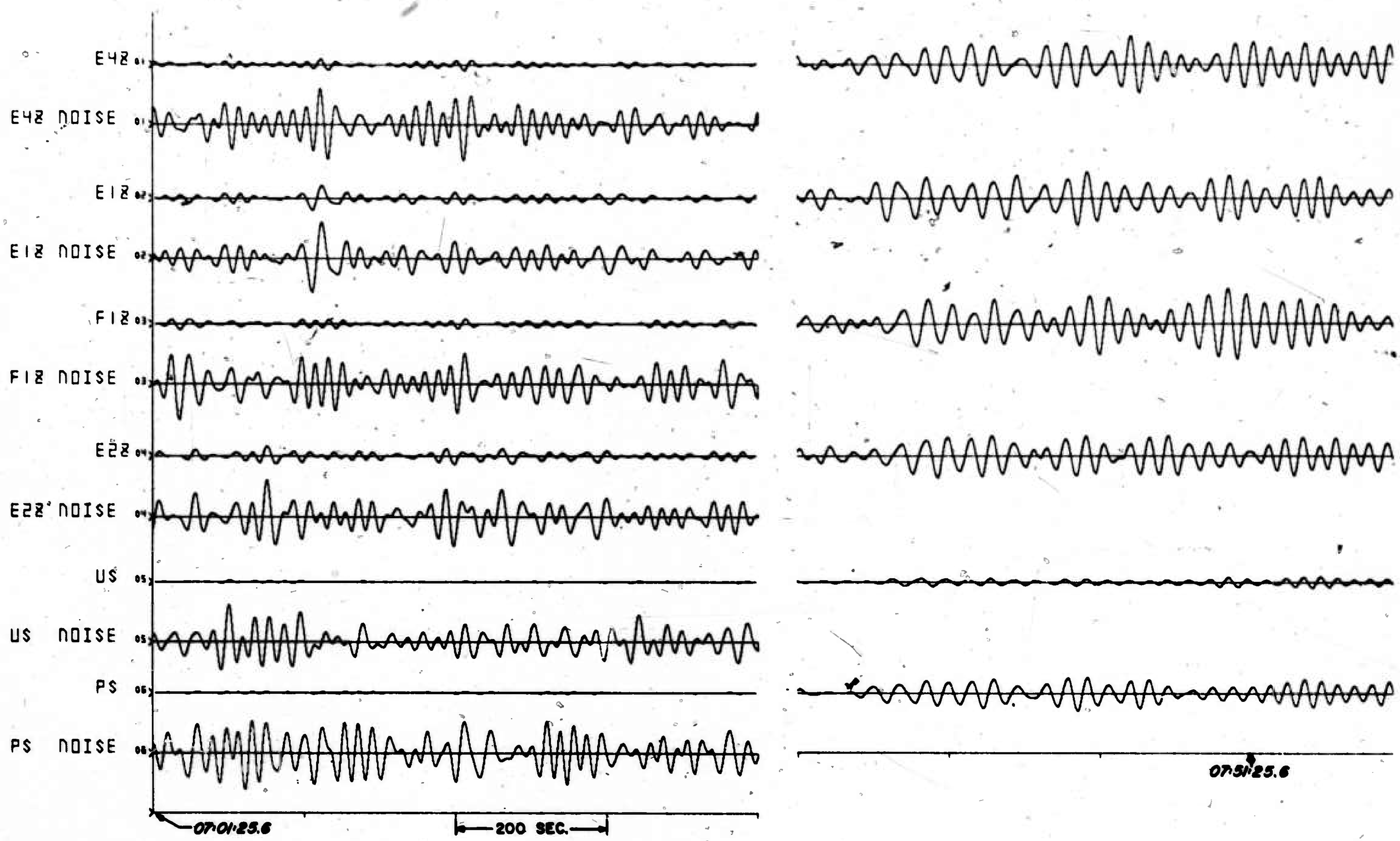

Figure 70b. Band pass filtered noise and signal traces with unphased and phased sums for an event in the Ryukyu Islands recorded at LASA.

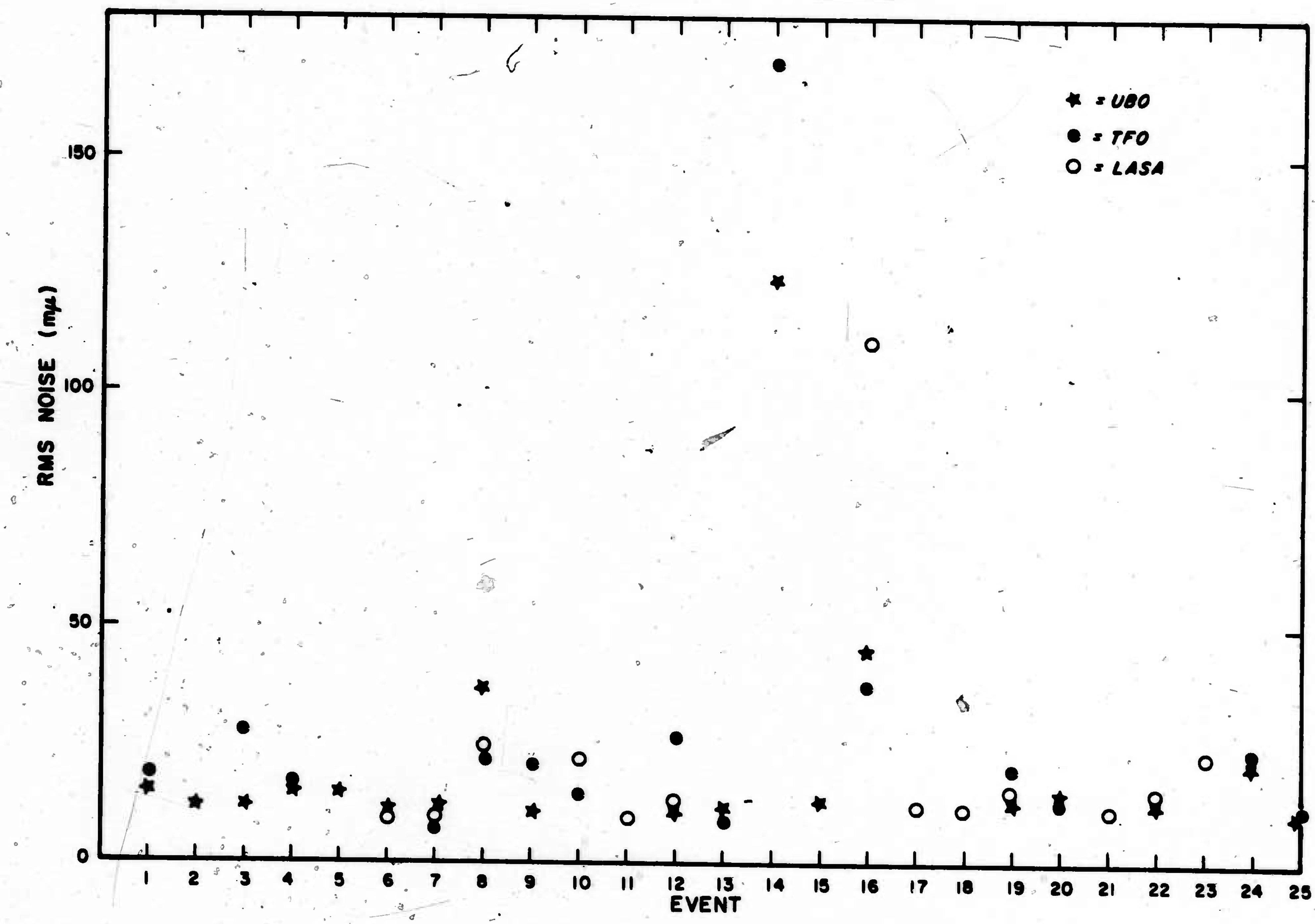

Figure 71. Long-period RMS noise levels at UBO, TFO and LASA.

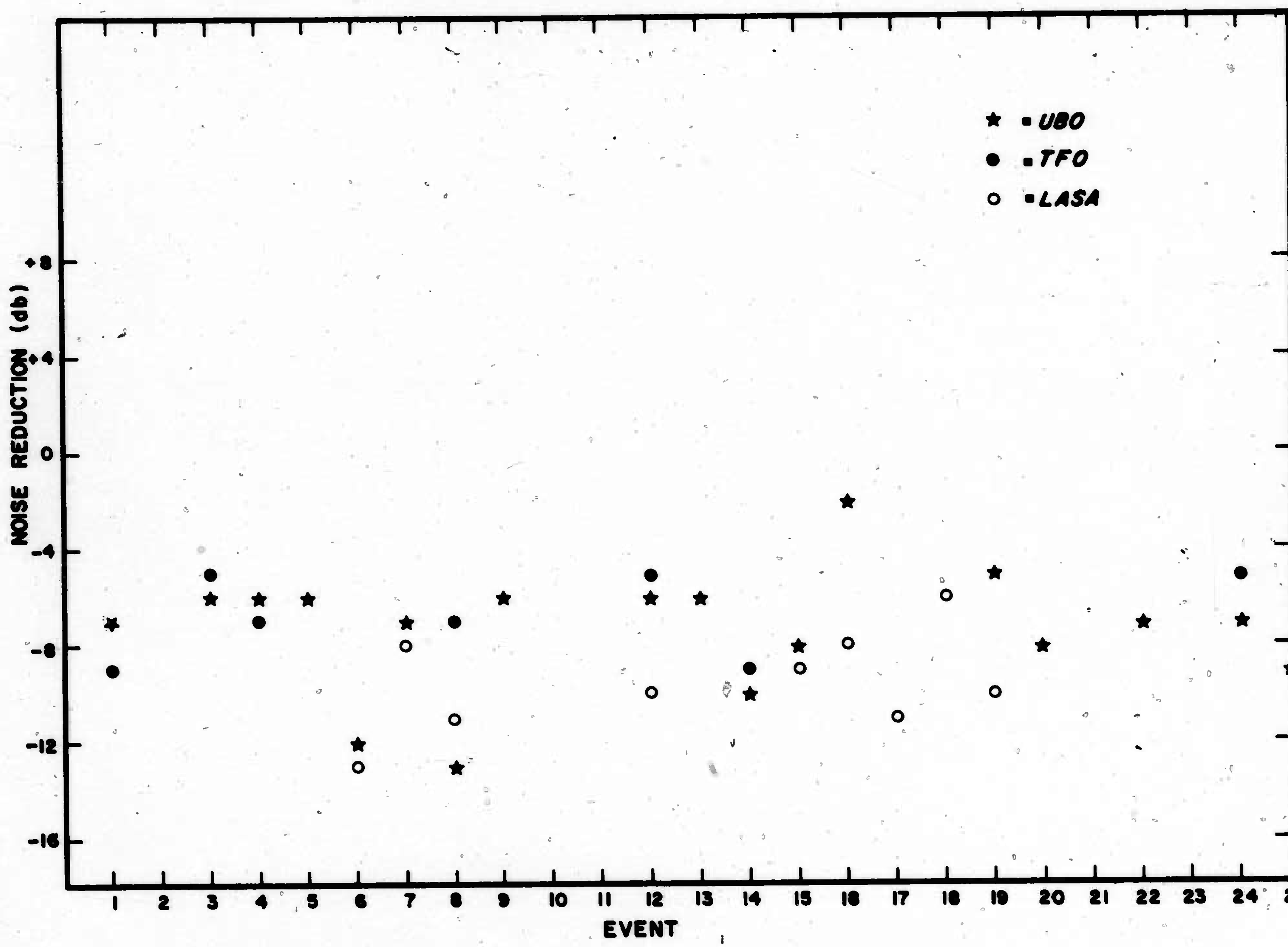

Figure 72. Noise reduction of long period beams of UBO, TFO and LASA.

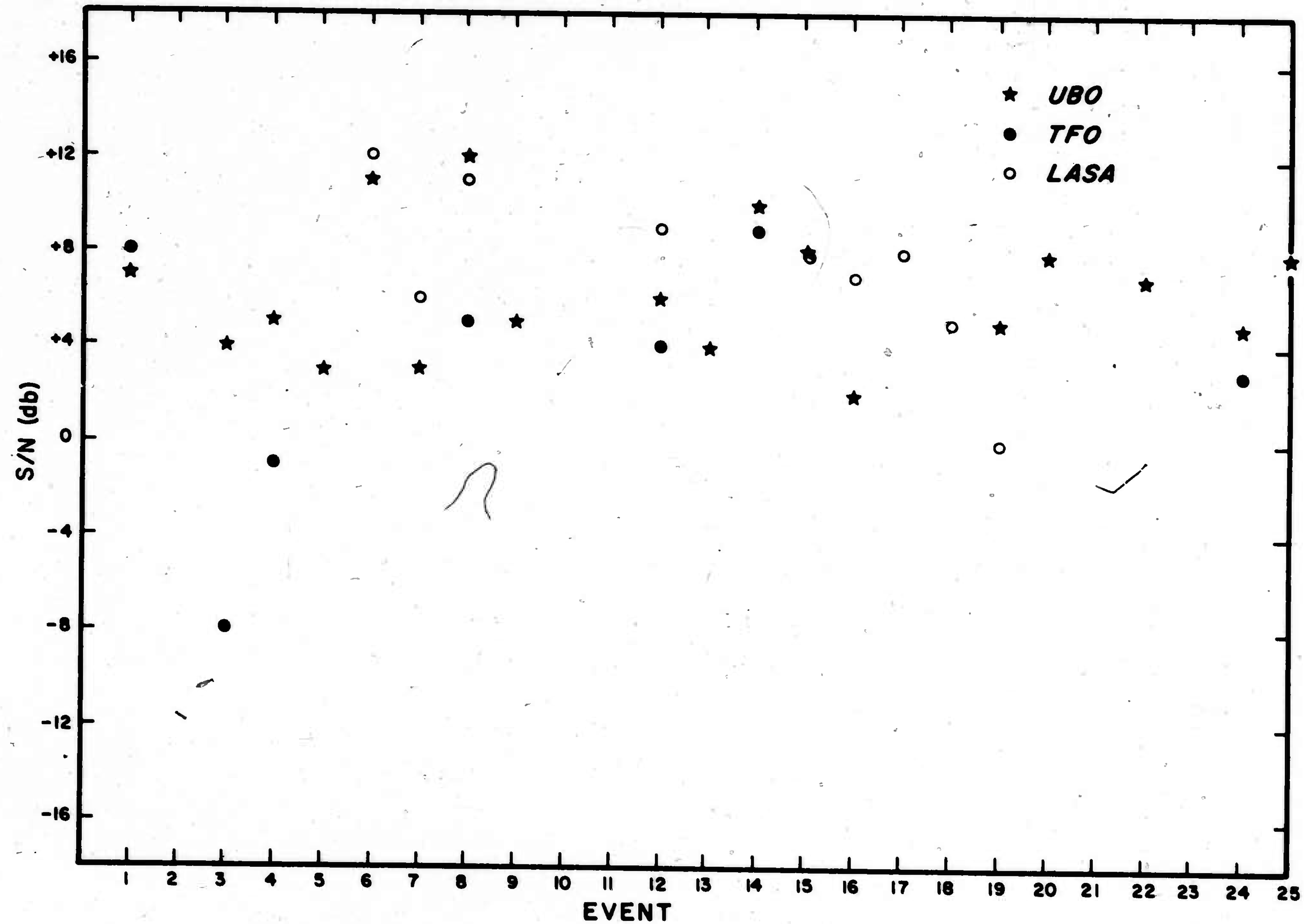

Figure 73. S/N improvement of long period beams of UBO, TFO and LASA.

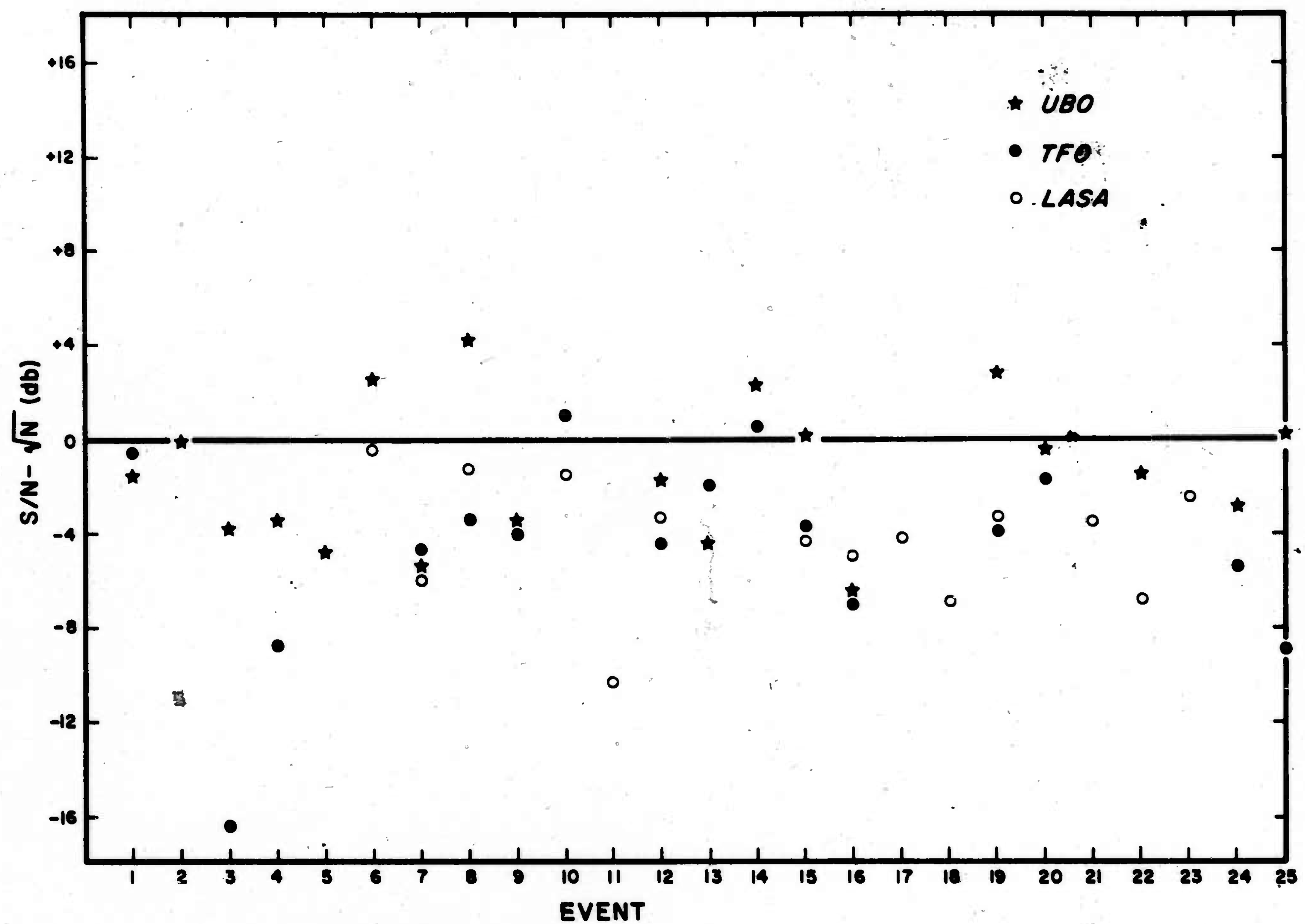

Figure 74. Actual S/N improvement of long period UBO, TFO and LASA beams minus $N^{\frac{1}{2}}$.

TABLE I

Source Parameters of Events and the Specific Recording Instruments of the Arrays used in Computation of Group Velocity Dispersion

EVENT	DATE	ORIGIN	LOCATION Lat.	Long.	UBO DISTANCE Km	UBO INSTRUMENT	TFO DISTANCE Km	TFO INSTRUMENT	LASA DISTANCE Km	LASA INSTRUMENT
Albania	26 Aug 69	02 15 38.8	41.8N	20.1E	9583	LPZ1	10220	LPZ1	8853	D3Z
N. Atlantic	06 Sep 69	14 30 39.5	36.9N	11.9W	-	-	8535	LPZ1	-	-
N. Atlantic Ridge	30 Oct 69	08 37 38.4	45.5N	27.5W	6370	LPZ2	-	-	5751	F3Z
Balleny Islands	29 Jun 69	17 09 13.9	62.8S	166.3E	-	-	-	-	14376	F4Z
Costa Rica	04 Jul 69	11 16 01.0	7.4N	82.7W	4538	LPZ1	4186	LPZ1	4925	F3Z
El Salvador	28 Jun 69	04 34 42.6	12.8N	89.2W	3632	LPZ1	3256	LPZ2	4067	F4Z
Galapagos	26 Jun 69	02 30 58.4	2.0N	90.5W	4636	LPZ1	4145	LPZ1	-	-
Hindu Kush	08 Aug 69	06 30 57.1	36.4N	70.9E	-	-	12236	LPZ1	10859	F3Z
Hokkaido	27 Jun 69	02 15 46.3	42.4N	142.9E	8339	LPZ1	8683	LPZ2	-	-
Kermadec Islands	28 Aug 69	16 49 56.8	31.8S	177.8W	10653	LPZ1	10121	LPZ1	-	-
Kodiac Islands	28 Jul 69	06 29 53.9	57.5N	153.9W	3675	LPZ1	4077	LPZ1	-	-
Kurile Islands	22 Jun 69	02 33 52.8	49.2N	158.5E	6936	LPZ1	-	-	6671	F3Z
Kurile Islands	14 Aug 69	14 19 01.6	43.1N	147.5E	7951	LPZ1	-	-	-	-
W. New Guinea	05 Jul 69	01 44 01.1	3.8S	131.5E	-	-	12702	LPZ2	-	-
Nicaragua	24 Jun 69	00 35 05.5	11.7N	85.7W	3989	LPZ1	3636	LPZ2	-	-
Rat Islands	22 Jun 69	10 45 24.5	51.5N	179.9W	5404	LPZ1	5711	LPZ1	5212	F3Z
Sinkiang	14 Sep 69	16 15 24.8	3[illegible].7N	74.9E	11113	LPZ1	11760	LPZ1	-	-
Soloman Islands	14 Jun 69	03 22 56.8	07.9S	159.0E	10697	LPZ1	10478	LPZ2	11012	F3Z
Unimak Islands	20 Jun 69	02 37 51.5	53.2N	162.4W	-	-	4488	LPZ2	3949	F3Z
Yugoslavia	26 Oct 69	15 36 51.8	44.9N	17.3E	9260	LPZ1	-	-	-	-

TABLE II

Source Parameters of Events Analyzed by Beam Formation

EVENT	DATE	ORIGIN TIME	LOCATION LAT.	LOCATION LONG.
Albania	26 Aug 69	02 15 38.8	41.8N	20.1E
Argentina	25 Jul 69	06 06 42.4	25.6S	63.3W
N. Atlantic	29 Jul 69	00 40 42.5	19.9N	64.1W
N. Atlantic Ridge	30 Oct 69	08 37 38.4	45.5N	27.5W
Coast of Chile	22 Oct 69	10 21 52.1	18.1S	71.5W
Costa Rica	04 Jul 69	11 16 01.0	7.4N	82.7W
El Salvador	28 Jun 69	04 34 42.6	12.8N	89.2W
Fox Is.	24 Oct 69	00 46 14.6	52.5N	168.6W
Galapagos	26 Jun 69	02 30 58.4	2.0N	90.5W
Greece-Albania	12 Oct 69	13 34 15.8	39.7N	20.4E
Gulf of Alaska	02 Jun 69	09 47 59.4	59.5N	144.7W
Hindu Kush	08 Aug 69	06 30 57.1	36.4N	70.9E
Hakkaido	27 Jun 69	02 15 46.3	42.4N	142.9E
Kermadec Is.	28 Aug 69	16 49 56.8	31.8S	177.8W
Kodiac Is.	28 Jul 69	06 29 53.9	57.5N	153.9W
Kurile Is.	22 Jun 69	02 33 52.8	49.2N	158.5E
Mexico	10 Sep 69	17 41 25.0	18.0N	103.4W
Near Is.	18 Oct 69	08 44 00.0	52.5N	173.5E
E. New Guinea	24 Aug 69	12 39 30.1	7.3S	148.1E
Nicaragua	24 Jun 69	00 35 05.5	11.7N	85.7W
Philippine Is.	28 Jun 69	14 22 15.0	6.7N	126.6E
Rat Is.	22 Jun 69	10 45 24.5	51.5N	179.9W
Ryukyu Is.	19 Jun 69	07 03 04.9	28.1N	130.0E
Sinkiang	14 Sep 69	16 15 24.8	39.7N	74.9E
Volcano Is.	28 Jul 69	15 37 56.2	24.1N	142.7E

TABLE III

Amplitude Data for Vertical Compone[...]
Beams with Individual Traces B[...]

EVENT NO.	EVENT	UBO n	UBO SIGNAL mμ MEAN	UBO SIGNAL mμ Σ	UBO SIGNAL db Σ/MEAN	UBO NOISE mμ rms	UBO NOISE mμ Σ	UBO NOISE db Σ/RMS	UBO S/N MEAN	UBO S/N Σ	UBO S/N db Σ/MEAN	UBO db √n	n	SIGNAL mμ MEAN	SIGNAL mμ Σ	SIGNAL db Σ/MEAN	mμ rms
1	Albania	7	133	119	-1	15	6	-7	9	19	7	6.5	7	215	201	-1	19
2	Argentina	5	720	562	-2	12	4	-9	50	137	7	7.0					
3	S. Atlantic	6	184	169	-1	12	6	-6	10	29	4	7.6	7	161	50	-9	26
4	N. Atlantic Ridge	7	746	721	0	16	8	-6	49	91	5	6.5	6	878	359	-6	16
5	Coast of Chile	6	930	708	-2	15	7	-6	64	96	3	7.6					
6	Costa Rica	7	1101	1068	0	11	3	-12	100	393	11	8.5					
7	El Salvador	7	1939	1309	-3	12	5	-7	100	249	3	6.5	3	1579	1095	-3	8
8	Fox Is.	6	650	685	-1	37	9	-13	18	78	12	7.6	7	310	250	-2	22
9	Galapagos	7	7671	7326	0	11	5	-6	729	1372	5	6.5	4	381	306	-2	21
10	Greece - Albania												4	107	163	0	15
11	Gulf of Alaska																
12	Hindu Kush	6	1276	1268	0	12	6	-6	163	215	6	7.8	7	645	799	6	27
13	Hokkaido	7	646	587	-1	12	6	-6	61	102	4	6.5	4	97	88	-1	9
14	Kermadec Is.	6	1344	1226	-1	124	38	-10	11	32	10	7.8	7	616	682	6	178
15	Kodiac Is.	6	1709	1761	0	14	5	-8	120	313	8	7.6	3	652	754	-1	12
16	Kurile Is.	7	481	469	0	45	35	-2	11	13	2	8.5	4	288	261	-1	38
17	Mexico																
18	Near Is.																
19	E. New Guinea	6	166	161	0	14	8	-5	12	20	5	7.6	5	216	193	-1	20
20	Nicaragua	6	691	675	0	14	6	-8	49	121	6	7.6	3	609	688	0	13
21	Philippine Is.																
22	Rat Is.	7	6000	5999	0	13	6	-7	464	1012	7	8.5					
23	Ryukyu Is.																
24	Sinkiang	6	706	594	-2	23	11	-7	31	55	5	7.8	7	1135	884	-2	23
25	Volcano Is.	6	163	89	-1	11	4	-9	16	24	6	7.6	4	59	29	-6	11

A

TABLE III

Amplitude Data for Vertical Component Long Period Array Beams with Individual Traces Band Pass Filtered

TFO											LASA										
	SIGNAL			NOISE			S/N					SIGNAL			NOISE			S/N			
n	mμ MEAN	mμ Σ	db Σ/MEAN	mμ rms	mμ Σ	db Σ/RMS	MEAN	Σ	db Σ/MEAN	db $\sqrt{n}$	n	mμ MEAN	mμ Σ	db Σ/MEAN	mμ rms	mμ Σ	db Σ/RMS	MEAN	Σ	db Σ/MEAN	db $\sqrt{n}$
7	215	281	-1	19	7	-9	11	20	0	8.5											
7	161	58	-9	28	16	-5	9	4	-8	8.5											
6	878	359	-8	16	7	-7	57	53	-1	7.8											
											17	1086	966	-1	10	2	-13	107	434	12	12.3
3	1579	1095	-3	8	6	-3	208	199	0	4.8	16	1615	1289	-2	10	4	-8	164	320	6	12.8
7	310	256	-2	22	10	-7	14	26	5	8.5	17	974	934	0	25	7	-11	39	131	11	12.3
4	301	306	-2	21	11	-5	21	28	2	6.0											
4	107	103	0	15	6	-8	3	2	7	6.0	14	303	255	-2	22	6	-12	14	45	10	11.5
											11	325	128	-8	10	4	-8	34	34	8	10.4
7	845	799	0	27	15	-5	32	52	4	8.5	17	1043	892	-1	14	4	-10	75	285	9	12.3
4	97	88	-1	9	5	-6	12	19	4	6.0											
7	616	602	0	178	61	-9	4	10	9	8.5											
3	852	754	-1	12	8	-3	77	90	1	4.8	17	2232	1859	-2	14	5	-9	149	377	8	12.3
4	200	261	-1	38	35	-1	8	7	-1	6.0	16	1047	900	-1	111	42	-8	18	21	7	12.8
											17	466	372	-2	12	3	-11	42	107	8	12.3
											16	1217	998	-2	12	5	-6	102	100	5	12.8
5	216	193	-1	28	11	-5	13	18	3	7.0	17	151	126	-2	15	4	-10	10	28	9	12.3
1	609	608	0	13	8	-5	61	86	3	4.8											
											14	134	113	-1	11	4	-9	12	30	8	11.5
											15	4838	4242	-1	14	7	-6	378	636	5	11.8
											14	250	193	-2	22	6	-11	11	31	9	11.5
7	1135	884	-2	23	11	-5	50	59	3	8.5											
4	59	29	-6	11	7	-4	6	4	-3	6.0											

B

TABLE IV

Amplitude Data for Vertical Component Long Period Array Beams using LASA C or F Ring Instruments with Individual Traces Band Pass Filtered

EVENT NO.	EVENT	INSTRUMENTS	GROUP VEL. OF BEAM	N	SIGNAL			NOISE			S/N		
					mμ MEAN	mμ Σ	db Σ/MEAN	mμ rms	mμ Σ	db Σrms	MEAN	Σ	db Σ/MEAN
6	Costa Rica	AOZ and C-ring	3.0 km/sec	5	750	722	-.3	7	4	-5.2	96	194	6.1
6	Costa Rica	AOZ and C-ring	3.8 km/sec	5	750	727	-.3	7	4	-4.4	96	178	5.3
6	Costa Rica	AOZ and F-ring	3.0 km/sec	5	1124	608	-5.3	11	5	-7.3	96	124	2.2
6	Costa Rica	AOZ and F-ring	3.8 km/sec	5	1124	952	-1.4	11	5	-6.3	96	174	5.2

TABLE V

Amplitude Data for Vertical Component Long

Beams with Individual Traces Low Pass F

		UBO												TFO					
			SIGNAL			NOISE			S/N					SIGNAL			NOISE		
EVENT NO	EVENT	N	mu MEAN	mu Σ	db Σ/MEAN	mu rms	mu Σ	db Σ/RMS	MEAN	Σ	db Σ/MEAN	db $N^{½}$	N	mu MEAN	mu Σ	db Σ/MEAN	mu rms	mu Σ	
9	Galapagus	7	7630	7280	0	14	7	-6	606	1063	5	8.5	7	--					
13	Hokkaido	7	660	597	-1	13	6	-8	55	93	4.5	8.5	4	99	92	-1	58	41	
16	Kurile Is.	7	484	473	0	46	37	-2	11	14	2	8.5							
23	Ryukyu Is.																		
25	Volcano Is.	6	103	89	-1	12	4	-9	9	21	7	7.8	4	61	33	-5	32	17	

TABLE V

Amplitude Data for Vertical Component Long Period Beams with Individual Traces Low Pass Filtered

TFO											LASA										
	SIGNAL			NOISE			S/N					SIGNAL			NOISE			S/N			
N	mμ MEAN	mμ Σ	db Σ/MEAN	mμ rms	mμ Σ	db Σ/RMS	MEAN	Σ	db Σ/MEAN	db $N^{1/2}$	N	mμ MEAN	mμ Σ	db Σ/MEAN	mμ rms	mμ Σ	db Σ/RMS	MEAN	Σ	db Σ/MEAN	db $N^{1/2}$
4	99	92	-1	58	41	-3	3	2	-2	6.0											
											16	1040	893	-1	111	42	-8	6	21	7	12.0
											14	247	191	-2	23	7	-11	10	29	9	11.5
4	61	33	-5	32	17	-6	2	2	-1	6.0											

B

TABLE VI

Amplitude Data for Horizontal Component Long Period Array Beams with Individual Traces Band Pass Filtered

		UBO								TFO							
		NOISE N-S				NOISE E-W				NOISE N-S				NOISE E-W			
EVENT NO.	EVENT	N	mμ rms	m Σ	db Σ/rms	N	mμ rms	mμ Σ	db Σ/rms	N	mμ rms	mμ Σ	db Σ/rms	N	mμ rms	mμ Σ	db Σ/rms
3	N. Atlantic	7	35	20	-5	6	29	15	-6								
14	Kermadec Is.	7	96	29	-10	6	138	50	-9	7	104	33	-10	7	122	37	-10
16	Kurile Is.	6	76	33	-7	6	69	34	-6	5	80	54	-3	4	87	55	-4
24	Sinkiang									5	21	12	-5	5	50	28	-5

Unclassified

Security Classification

DOCUMENT CONTROL DATA - R&D

(Security classification of title, body of abstract and indexing annotation must be entered when the overall report is classified)

1. ORIGINATING ACTIVITY (Corporate author) TELEDYNE GEOTECH ALEXANDRIA, VIRGINIA	2a. REPORT SECURITY CLASSIFICATION Unclassified 2b. GROUP

3. REPORT TITLE

ANALYSIS OF LONG PERIOD SEISMIC SIGNALS AND NOISE RECORDED AT LASA, TFO AND UBO

4. DESCRIPTIVE NOTES (Type of report and inclusive dates)

Scientific

5. AUTHOR(S) (Last name, first name, initial)

Massé, R.P.; Clark, D.M.; Mecklenburg, H.J.

6. REPORT DATE	7a. TOTAL NO. OF PAGES	7b. NO. OF REFS
19 June 1970	116	3

8a. CONTRACT OR GRANT NO. F33657-70-C-0941 b. PROJECT NO. VELA T/0706 c. ARPA Order No. 624 d. ARPA Program Code No.:	9a. ORIGINATOR'S REPORT NUMBER(S) 254 9b. OTHER REPORT NO(S) (Any other numbers that may be assigned this report)

10. AVAILABILITY/LIMITATION NOTICES

This document is subject to special export controls and each transmittal to foreign governments or foreign nationals may be made only with prior approval of Chief, AFTAC.

11. SUPPLEMENTARY NOTES	12. SPONSORING MILITARY ACTIVITY
	ADVANCED RESEARCH PROJECTS AGENCY NUCLEAR MONITORING RESEARCH OFFICE WASHINGTON, D. C.

13. ABSTRACT

Long period signals recorded at the seismic arrays UBO, TFO and LASA were analyzed to determine the fundamental mode Rayleigh wave dispersion curves for paths from different source areas to each of the arrays. These paths are mixed continental and oceanic, and the dispersion curves calculated fall within the range between the average dispersion for a pure continental path and that for a pure oceanic path. Analysis of the long period noise (15 to 50 seconds) recorded at each array shows the rms value to be in the 8 to 20 mμ range. Simple beamforming gives approximately $N^{\frac{1}{2}}$db reduction in noise at all arrays. Using a group velocity of 3.5 km/sec results in signal loss for some events in the LASA beams.

14. KEY WORDS

Long period signals
UBO, TFO and LASA
Rayleigh wave dispersion
Beamforming
rms

Unclassified

Security Classification